

Ingrid J. Paulsen, Veronika Konevega

# Fading of Minor Elements in Aluminium (V, Ni, Sr & Bi)

Bachelor's thesis in Chemical Engineering

Supervisor: Robert Fritzsich

May 2022



Ingrid J. Paulsen, Veronika Konevega

# **Fading of Minor Elements in Aluminium (V, Ni, Sr & Bi)**

Bachelor's thesis in Chemical Engineering  
Supervisor: Robert Fritzsch  
May 2022

Norwegian University of Science and Technology  
Faculty of Natural Sciences  
Department of Materials Science and Engineering





DEPARTMENT OF MATERIALS SCIENCE AND  
ENGINEERING

TKJE3001 - BACHELOR THESIS CHEMISTRY (40 ECTS)

---

**Fading of Minor Elements in Aluminium**

(V, Ni, Sr & Bi)

**Fading av mindre elementer i aluminium**

(V, Ni, Sr & Bi)

---

*Author:*

Ingrid Johanne Paulsen

Veronika Konevega

Project number: IMA-B-3-2022

Submission date: 20. May 2022

Grading: Open

Internal supervisor: Robert Fritsch

Client: NTNU/Hösch Metallurgy

Contact person: I. J. Paulsen, [ijpauls00@gmail.com](mailto:ijpauls00@gmail.com)

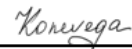
---

## Statutory Declaration

I declare that I have developed and written the enclosed thesis entirely by myself and in collaboration with the group signed onto this work, and have not used sources or means without declaration in the text. Any thoughts or quotations, which were inferred from these sources, are clearly marked as such.

This report was not submitted in the same or in a substantially similar version, not even partially, to any other authority to achieve an academic grading and was not published elsewhere.

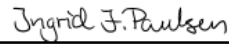
**Trondheim, May 2022**



---

**Veronika Konevega**

**Trondheim, May 2022**



---

**Ingrid Johanne Paulsen**

---

## Acknowledgment

«Fading of Minor Elements in Aluminium (V, Ni, Sr & Bi)» is a project developed by Dr. Robert Fritzsich at the Department of Materials Science and Engineering (NTNU) and Dr. V. Ohm from Hösch Metallurgy, Germany. The goal of the thesis is to provide fundamental research of whether the minor elements in aluminium fades, or stays in the melt.

The project was chosen because of its relevance concerning the recycling of aluminium, in addition to it being an interesting field of study in relation to our chemistry background.

We would like to start by thanking our supervisor Dr. Robert Fritzsich for the guidance given through all stages of the project.

We would also like to thank: Sergey Khromov for the development of the GD-OES method, and for training and guidance regarding the GD-OES and GD-MS, Hösch Metallurgy for the analysis of samples by ICP-OES, Dr. Volker Ohm for source material, Dr. Lars Arnberg for discussion regarding interpretation of the results, Dmitry Slizovskiy for lab training and tour of the premises, and Pål C. Skaret for access to experimental materials.

---

## Abstract

The recycling of aluminium (Al), called secondary Al, has become a major part of the total value of all Al produced. The growth of secondary Al usage in many different industries is driven by the low energy consumption, requiring only approx. 5% of the total energy in comparison to the production of the primary Al. The growth of secondary Al production has led to the discovery of new challenges, such as accumulation or fading of elements in the recycled metal, which can, over time accumulate to such amounts that affect the quality, composition and properties of the end-product.

This study has focused on four elements: V, Ni, Sr and Bi, and their interactions with molten Al of commercially purity (99,7%), and its alloy, here tested with AlSi7. The interactions between the elements, which have been added with a concentration of approx. 200 ppm, and molten Al were analysed over intervals of 1h, 2h and 20h. The elements were added to the molten aluminium in liquid state, the temperature was continuously kept at  $730^{\circ}\text{C} \pm 5^{\circ}\text{C}$ , ambient pressure and atmosphere in Boron Nitride (BN) coated crucibles. Samples were taken after dedicated stirring actions, at a decided interval by pouring melt out of the crucible, avoiding contaminating the melt.

The samples were then analysed using GD-OES and GD-MS, while some samples were sent to Hösch Metallurgy, Germany, to be analysed using ICP-OES.

FactSage was used to generate the required binary phase diagrams. The phase diagrams were used to theoretically determine possible interactions between the elements and Al.

The results suggest that V, Ni and Bi are stable in both the pure Al and the AlSi7-alloy for a 20 hour time period, showing no sign of fading. Sr in contrast, is the only element in this study that fades out of the melt, where it appears to fade to concentrations of  $< 1$  ppm after 6 hours.

Further work should include the study of further major alloying elements. Experimental trials at an industrial scale may also be considered.



---

## Sammendrag

Resirkuleringen av aluminium (Al), kalt sekundær Al, har blitt en stor del av den totale omsetningen av produsert Al. Veksten i bruk av sekundær Al i industrien er drevet av det lave energiforbruket, hvor det kun kreves ca. 5% av den totale energien ved produksjon av primær Al. Veksten i produksjon av sekundær Al har ført til oppdagelsen av nye utfordringer, som akkumulering eller fading av elementer i det resirkulerte metallet, som over tid kan akkumulere til mengder som påvirker kvaliteten, sammensetningen og egenskapene til sluttproduktet.

Denne studien har fokusert på fire elementer: V, Ni, Sr og Bi, og deres interaksjoner med smeltet aluminium med kommersiell renhet (99,7%), og dens legering, her testet med AlSi7. Interaksjonene mellom elementene, som er tilsatt en konsentrasjon på ca. 200 ppm, og det smeltede Al ble analysert over intervaller på 1 time, 2 timer og 20 timer. Elementene ble tilsatt det smeltede aluminiumet i flytende tilstand, temperaturen ble kontinuerlig holdt på  $730^{\circ}\text{C} \pm 5^{\circ}\text{C}$ , med omgivelig trykk og atmosfære i Boron Nitride (BN) belagte digler. Prøver ble tatt etter bestemt røring, med et gitt intervall, ved å helle smelten ut av digelen, samt ved å unngå kontaminering i smelten.

Prøvene ble deretter analysert ved GD-OES og GD-MS, mens noen prøver ble sendt til Hösch Metallurgy, Tyskland, for analyseres ved ICP-OES.

FactSage ble brukt til å generere de nødvendige binære fasediagrammene. Fasediagrammene ble brukt til å teoretisk bestemme mulige interaksjoner mellom elementene og Al.

Resultatene antyder at V, Ni og Bi er stabile i både ren Al og AlSi7-legering, for en tidsperiode på 20 timer, og viser ingen tegn til fading. Sr derimot, er det eneste elementet i denne studien som fader ut av aluminiumet, hvor elementet etter 6 timer viser antydninger til å ha fadet til konsentrasjoner på  $< 1$  ppm.

Videre arbeid bør inkludere flere viktige legeringselementer. Eksperimentelle forsøk i industriell skala kan også vurderes.

---

# Contents

<b>Statutory Declaration</b>	<b>i</b>
<b>Acknowledgment</b>	<b>ii</b>
<b>Abstract</b>	<b>iii</b>
<b>Sammendrag</b>	<b>iv</b>
<b>List of Figures</b>	<b>viii</b>
<b>List of Tables</b>	<b>xii</b>
<b>1 Introduction</b>	<b>1</b>
<b>2 Theory</b>	<b>3</b>
2.1 Aluminium . . . . .	3
2.1.1 Al life-cycle . . . . .	3
2.1.2 Physical properties . . . . .	4
2.1.3 Alloys of aluminium . . . . .	5
2.1.4 Grain Boundaries . . . . .	6
2.1.5 Melting process of Aluminium . . . . .	6
2.2 Phase Diagram . . . . .	7
2.2.1 Vanadium . . . . .	7
2.2.2 Nickel . . . . .	7
2.2.3 Strontium . . . . .	8
2.2.4 Bismuth . . . . .	8
2.3 GD-OES . . . . .	9
2.3.1 Quantification in GD-OES . . . . .	10
2.3.2 Identifying elements & calibration . . . . .	11
2.4 GD-MS . . . . .	12
2.4.1 System set-up . . . . .	12
2.4.2 Data processing . . . . .	13
2.5 ICP-OES . . . . .	14
<b>3 Material and Methodology</b>	<b>15</b>
3.1 Equipment and Material . . . . .	15
3.2 Method . . . . .	16

---

3.2.1	Cutting of materials . . . . .	16
3.2.2	Weighing of Al and alloying element . . . . .	17
3.2.3	Reference trials . . . . .	18
3.2.4	Trial structure . . . . .	18
3.2.5	Casting of samples . . . . .	19
3.2.6	Metallographic Sample Preparations . . . . .	20
3.2.7	GD-OES . . . . .	20
3.2.8	GD-MS . . . . .	21
3.2.9	ICP-OES . . . . .	21
3.2.10	FactSage . . . . .	21
<b>4</b>	<b>Results and Discussion</b>	<b>22</b>
4.1	Sources of Error and Limitations . . . . .	22
4.1.1	Deviation in temperature . . . . .	22
4.1.2	Contamination in the samples . . . . .	22
4.1.3	Loss of the liquid metal . . . . .	23
4.1.4	Addition of the elements to the aluminium . . . . .	23
4.1.5	Master alloys . . . . .	23
4.1.6	Hydrogen solubility . . . . .	24
4.1.7	Samples . . . . .	24
4.2	GD-OES data and its interpretation . . . . .	25
4.2.1	GD-OES-data from 1h V-trial . . . . .	25
4.2.2	GD-OES-data from 2h V-trial . . . . .	29
4.2.3	GD-OES-data from 22h V-trial . . . . .	33
4.2.4	GD-OES-data from V-trial with AlSi7-alloy . . . . .	35
4.2.5	GD-OES-data from 1h Ni-trial . . . . .	38
4.2.6	GD-OES-data from 2h Ni-trial . . . . .	41
4.2.7	GD-OES-data from 20h Ni-trial . . . . .	46
4.2.8	GD-OES-data from Ni-trial with AlSi7-alloy . . . . .	48
4.2.9	GD-OES-data from 1h Sr-trial . . . . .	50
4.2.10	GD-OES-data from 2h Sr-trial . . . . .	54
4.2.11	GD-OES-data from 20h Sr-trial . . . . .	59
4.2.12	GD-OES-data from Sr-trial with AlSi7-alloy . . . . .	63
4.2.13	GD-OES-data from 1h Bi-trial . . . . .	65
4.2.14	GD-OES-data from 2h Bi-trial . . . . .	68

---

---

4.3	Average measurements from GD-MS . . . . .	69
4.4	Average measurements from ICP-OES . . . . .	70
4.5	Summary of the results . . . . .	72
4.5.1	Vanadium . . . . .	72
4.5.2	Nickel . . . . .	76
4.5.3	Strontium . . . . .	80
4.5.4	Bismuth . . . . .	84
<b>5</b>	<b>Conclusion</b>	<b>85</b>
<b>6</b>	<b>Future Work</b>	<b>87</b>
	<b>References</b>	<b>88</b>
<b>A</b>	<b>H/P-phrases for BN-coating</b>	<b>i</b>

---

## List of Figures

1	The 2019 global production of aluminium [2]. . . . .	1
2	Shredded metal scraps [8]. . . . .	2
3	Contamination found in the recycling facility [8]. . . . .	2
4	Aluminium life cycle [12]. . . . .	3
5	Major alloying elements in the wrought aluminium alloy system. . . . .	5
6	Grains in Al. [15] . . . . .	6
7	Heat-exchange in crucible. . . . .	6
8	Phase diagram of Al-V. . . . .	7
9	Phase diagram of Al-Ni. . . . .	7
10	Phase diagram of Al-Sr. . . . .	8
11	Phase diagram of Al-Bi. . . . .	8
12	Distribution of light [18] . . . . .	9
13	GD-qualification [17] . . . . .	10
14	Nu Astrum GD-MS instrument [20]. . . . .	12
15	GD-MS loading of samples[19]. . . . .	12
16	Electrical Grade Al, Commercial Grade Al, AlSi7 (from left to right). . . . .	16
17	Aluminium (1kg) and element (200 ppm). . . . .	16
18	Cutting machine. . . . .	16
19	Bandsaw. . . . .	16
20	Weighing of element, element in foil, and Al. . . . .	17
21	RSD-tool. . . . .	18
22	Crucible and rod. . . . .	18
23	Nabertherm Furnace. . . . .	19
24	Measuring of temperature. . . . .	19
25	Casting-tools. . . . .	19
26	Sample handling. . . . .	19
27	Polishing machine. . . . .	20
28	Sample after polishing. . . . .	20
29	GD-OES. . . . .	20
30	Sample after GD-OES. . . . .	20
31	GD-MS. . . . .	21
32	Sample after GD-MS. . . . .	21
33	Samples sent to ICP-OES analysis. . . . .	21

---

34	Reference Al-sample before addition of V. . . . .	25
35	Al-sample with V at 5 min. . . . .	25
36	Al-sample with V at 10 min. . . . .	26
37	Al-sample with V at 20 min. . . . .	26
38	Al-sample with V at 30 min. . . . .	27
39	Al-sample with V at 40 min. . . . .	27
40	Al-sample with V at 50 min. . . . .	28
41	Al-sample with V at 60 min. . . . .	28
42	Reference Al-sample before addition of V. . . . .	29
43	Sample of V after 10 min. . . . .	29
44	Sample of V after 20 min. . . . .	30
45	Sample of V after 40 min. . . . .	30
46	Sample of V after 60 min. . . . .	31
47	Sample of V after 80 min. . . . .	31
48	Sample of V after 100 min. . . . .	32
49	Sample of V after 120 min. . . . .	32
50	Reference Al-sample before addition of V. . . . .	33
51	Sample of V after 360 min. . . . .	33
52	Sample of V after 1160 min. . . . .	34
53	Sample of V after 1320 min. . . . .	34
54	Reference AlSi7-sample before addition of V. . . . .	35
55	Sample of V after 20 min. . . . .	35
56	Sample of V after 60 min. . . . .	36
57	Sample of V after 120 min. . . . .	36
58	Sample of V after 240 min. . . . .	37
59	Sample of Ni after 10 min. . . . .	38
60	Sample of Ni after 20 min. . . . .	38
61	Sample of Ni after 30 min. . . . .	39
62	Sample of Ni after 40 min. . . . .	39
63	Sample of Ni after 50 min. . . . .	40
64	Sample of Ni after 60 min. . . . .	40
65	Reference Al-sample before addition of Ni. . . . .	41
66	Sample of Ni after 5 min. . . . .	41
67	Sample of Ni after 10 min. . . . .	42
68	Sample of Ni after 20 min. . . . .	42

---

---

69	Sample of Ni after 40 min. . . . .	43
70	Sample of Ni after 60 min. . . . .	43
71	Sample of Ni after 80 min. . . . .	44
72	Sample of Ni after 100 min. . . . .	44
73	Sample of Ni after 120 min. . . . .	45
74	Reference Al-sample before addition of Ni. . . . .	46
75	Sample of Ni after 360 min. . . . .	46
76	Sample of Ni after 1080 min. . . . .	47
77	Sample of Ni after 1200 min. . . . .	47
78	Reference AlSi7-sample before addition of Ni. . . . .	48
79	Sample of Ni after 40 min. . . . .	48
80	Sample of Ni after 60 min. . . . .	49
81	Reference Al-sample before addition of Sr. . . . .	50
82	Sample of Sr after 10 min. . . . .	50
83	Sample of Sr after 20 min. . . . .	51
84	Sample of Sr after 30 min. . . . .	51
85	Sample of Sr after 40 min. . . . .	52
86	Sample of Sr after 50 min. . . . .	52
87	Sample of Sr after 60 min. . . . .	53
88	Reference Al-sample before addition of Sr. . . . .	54
89	Sample of Sr after 5 min. . . . .	54
90	Sample of Sr after 10 min. . . . .	55
91	Sample of Sr after 20 min. . . . .	55
92	Sample of Sr after 40 min. . . . .	56
93	Sample of Sr after 60 min. . . . .	56
94	Sample of Sr after 80 min. . . . .	57
95	Sample of Sr after 100 min. . . . .	57
96	Sample of Sr after 120 min. . . . .	58
97	Reference Al-sample before addition of Sr. . . . .	59
98	Sample of Sr after 10 min. . . . .	59
99	Sample of Sr after 130 min. . . . .	60
100	Sample of Sr after 240 min. . . . .	60
101	Sample of Sr after 360 min. . . . .	61
102	Sample of Sr after 1080 min. . . . .	61
103	Sample of Sr after 1200 min. . . . .	62

---

---

104	Reference AlSi7-sample before addition of Sr. . . . .	63
105	Sample of Sr after 40 min. . . . .	63
106	Sample of Sr after 120 min. . . . .	64
107	Sample of Sr after 240 min. . . . .	64
108	Sample of Bi after 10 min. . . . .	65
109	Sample of Bi after 20 min. . . . .	65
110	Sample of Bi after 30 min. . . . .	66
111	Sample of Bi after 40 min. . . . .	66
112	Sample of Bi after 50 min. . . . .	67
113	Sample of Bi after 60 min. . . . .	67
114	Reference Al-sample before addition of Bi. . . . .	68
115	Regression analysis of the 1h trial of V. . . . .	72
116	Box-plot of the 1h trial of V. . . . .	72
117	Regression analysis of the 2h trial of V. . . . .	73
118	Box-plot of the 2h trial of V. . . . .	73
119	Regression analysis of the 20h trial of V. . . . .	74
120	Box-plot of the 20h trial of V. . . . .	74
121	Regression analysis of the alloy-trial of V. . . . .	75
122	Box-plot of the alloy-trial of V. . . . .	75
123	Regression analysis of the 1h trial of Ni. . . . .	76
124	Box-plot of the 1h trial of Ni. . . . .	76
125	Regression analysis of the 2h trial of Ni. . . . .	77
126	Box-plot of the 2h trial of Ni. . . . .	77
127	Regression analysis of the 20h trial of Ni. . . . .	78
128	Box-plot of the 20h trial of Ni. . . . .	78
129	Regression analysis of the alloy-trial of Ni. . . . .	79
130	Box-plot of the alloy-trial of Ni. . . . .	79
131	Regression analysis of the 1h trial of Sr. . . . .	80
132	Box-plot of the 1h trial of Sr. . . . .	80
133	Regression analysis of the 2h trial of Sr. . . . .	81
134	Box-plot of the 2h trial of Sr. . . . .	81
135	Regression analysis of the 20h trial of Sr. . . . .	82
136	Box-plot of the 20h trial of Sr. . . . .	82
137	Regression analysis of the alloy-trial of Sr. . . . .	83
138	Box-plot of the alloy-trial of Sr. . . . .	83

---



---

## List of Tables

1	Overview of experimental material. . . . .	15
2	Summary of trials. . . . .	17
3	Results from the GD-MS-analysis . . . . .	69
4	Results from the analysis of minor elements in pure Aluminium, by ICP-OES at Hösch Metallurgy, Germany. . . . .	70
5	H/P-phrases for softcoat. . . . .	i
6	H/P-phrases for hardcoat. . . . .	ii

---

# 1 Introduction

Aluminium is a metal used in many industries, such as transport, electrical power transmission, electronics, food, and many more due to its high strength-to-weight ratio, good corrosion resistance and high formability. Aluminium does also not degrade and can be recycled theoretically unlimited [1]. In 2019 the global annual production of aluminium consisted of 32.7 Mt recycled aluminium and 63.7 Mt primary aluminium (Figure 1).

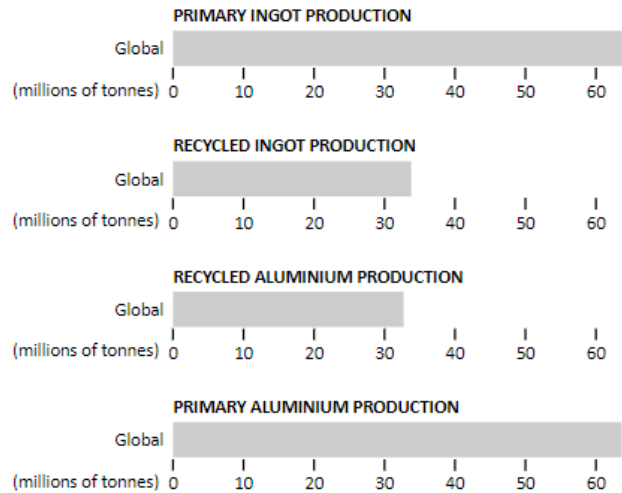


Figure 1: The 2019 global production of aluminium [2].

Recycling of aluminium is economically and environmentally friendly process, and it requires only 4.86% of the power that is needed to produce primary aluminium [3].

Perfect material separation during the end-of-life (EoL) phase is not possible in the shredder-based recycling practices, due to the complex product designs and the difficulty in separating different material types from their associated joining techniques [4]. This on the other hand leads to lower grades and qualities of recyclable material retrieved, due to the presence of impurities and unwanted elements. This is then leading to "cascade" recycling [5] and the loss of the material. This is particularly the case for recycling Al scrap that has more limitations during metallurgical recycling in comparison to other metals such as iron and copper [6].

A logical reason is the melting point of Al, which makes it difficult to remove impurities or tramp elements/contaminants, which will affect the quality of the final product. These contamination are not added on purpose during the secondary Al melting and refining processes, resulting in undesired alloys and properties. The most common strategies used to address this challenge are either dilution using primary Al or down-cycling to lower grade Al alloys that are associated to additional environmental burden [7], [5].

---

As an example, a study of shredded metal scraps in an European recycling facility (Figure 2) found mechanical fasteners to be the main source of contamination [8]. A selection of the scraps found is shown in Figure 3.

Since 1980, the production of the secondary aluminium has significantly increased [1].



Figure 2: Shredded metal scraps [8].

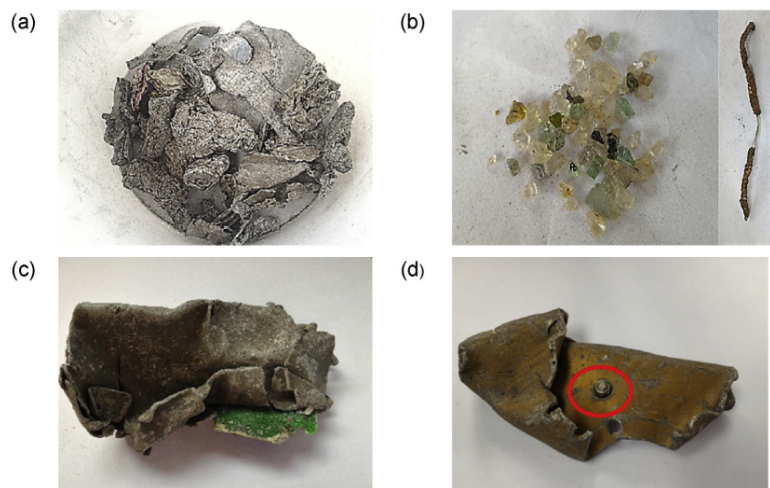


Figure 3: Contamination found in the recycling facility [8].

---

## 2 Theory

### 2.1 Aluminium

Aluminium is a low-density, non-ferrous metal widely used in a number of various industries, such as transportation, food processing, electrical industry, chemical industry, etc.. Aluminium is the third most abundant element in earth's crust. However, it does not occur in an elemental state; it is always combined in a chemical compound, such as oxides and silicates [9].

The potential for aluminium alloys as engineering materials has been recognized before aluminium was acknowledged as an industrial metal [9]. Aluminium can be categorized into two types: primary- and secondary aluminium. Primary aluminium is produced from raw materials, while secondary aluminium is produced with recycled materials.

#### 2.1.1 Al life-cycle

Aluminium's life-cycle starts from the alumina refining, through Bayer's process, where aluminium oxide is extracted from bauxite in a refinery. The alumina is used to produce the primary metal. The primary method produces aluminium through electrolysis, which is an energy intensive process that requires a lot of electricity. Primary aluminium is produced in a variety of grades, ranging from 99.0% purity to 99.999% [10]. Aluminium is classified into different purity grades depending on the amount of the impurities. For the commercial purity aluminium the requirement is at 99.5%, and the ultra purity is over 99.999%, according to the USA Standard [11].

After the primary production, Al is extruded, rolled or cast, depending on the industry requirement. After the aluminium product is used, it reaches the end of its life-cycle, and then goes through the recycling process. The schematic life-cycle of aluminium is shown in Figure 4.

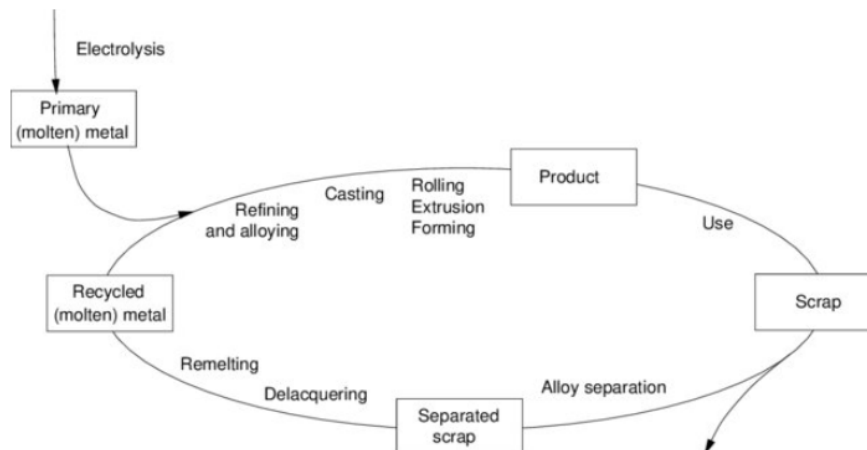


Figure 4: Aluminium life cycle [12].

---

Secondary Al is produced by remelting Al scrap, end of life products or any recycled/secondary sourced Al, and is usually recovered in the forms of the alloys [10]. Even if the high-quality Al scrap is remelted, the secondary Al will be less pure than primary sourced metal due to the contamination with other materials. An industrial standard to get secondary Al to its alloying specifications and concentration limits, is to dilute the melt with primary metal, adjusting the chemical composition to the demanded purity.

Aluminium secondary metallurgy consists of two processes: the melting of scraps and the processing of the white dross. White dross is a superficial oxidation layer that occurs during the melting process and is formed on the top of the bath. The white dross is recycled through salt refluxes. The dross layer protects the liquid metal against further oxidation, and is removed at the end of the melting. When the dross is extracted from the bath, some Al will be extracted along [11].

Melting of scraps occurs in rotary furnaces at an industrial scale, but at smaller foundries, melting can forego in crucibles or reverberatory furnaces. After the aluminium is molten, it is transferred to teeming or holding furnaces. The collected white dross is kept in a steel container. The range of these melting processes are from 700-800°C [11].

Before Al scraps are recycled, there is often a need for primary handling. Primary handling involves possible removal of the contaminants from the scrap. The removal of impurities can be done manually, however, at industrial scale there is a need for a automated primary handling of the scrap [11]. A visualisation of common scrap is shown in Figure 3.

### 2.1.2 Physical properties

Aluminium's atomic number is 13, and accented value for the atomic weight of Al is 26.9815 u based on the  $^{12}\text{C}$  standard. The main isotope of aluminium is  $^{27}\text{Al}$ . This isotope is stable, unlike most of the other Al-isotopes, which have short half-lives, and therefore can be neglected [10].

The properties of aluminium depend, to some extend, on its purity. Aluminium is silver-white in appearance, has a low density, and high potential for electrical and thermal conductivity. It is also very resistant to oxygen corrosion, due to the formation of an oxide film, that protects the metal against further oxidation [11].

Aluminium has the face-centered cubic (fcc) crystal structure with the coordination number of 12. This is the most packed cubic lattice, and it remains stable over the whole temperature up to the melting point.

---

### 2.1.3 Alloys of aluminium

Aluminium in its pure form has a low mechanical strength, and cannot be used in industries where resistance to deformations and fractures is of high interest. That leads to the introduction of other elements into the aluminium, which are then called alloys. The introduction of other elements is equipping the aluminium alloys with different adjustable physical properties. The properties of the aluminium alloys depend on the interactions of the added chemical elements, their compositions and the resulting micro-structural features developed during thermal treatment, solidification, and in some cases, deformation processes.

Aluminium is classified in different alloy classes, where the major groups are wrought (approx. 85% of all Al used) and casting alloys. Cast aluminium alloys often contain larger amounts of alloying elements comparing to wrought alloys. Figure 5 shows an overview of different aluminium wrought alloys, based on their major alloying element. The wrought alloy designation system consists of four digits, where the first digit indicates the principle alloying element.

<b>Alloy</b>	<b>Major alloying elements</b>
<i>1xxx</i>	Mostly pure aluminium; no major alloying additions
<i>2xxx</i>	Copper
<i>3xxx</i>	Manganese
<i>4xxx</i>	Silicon
<i>5xxx</i>	Magnesium
<i>6xxx</i>	Magnesium and silicon
<i>7xxx</i>	Zinc
<i>8xxx</i>	Other elements (e.g., iron and silicon)
<i>9xxx</i>	Unassigned

Figure 5: Major alloying elements in the wrought aluminium alloy system.

The second digit is the variation of that alloy. When the second digit is 0, it indicates presence of the naturally pure aluminium making up the bulk of the alloy. When the second digit varies from 1 to 9, it indicates control over the impurity levels.

The third and the fourth digits indicate the purity level of the alloy, and can be interpreted as 99.XX% purity of the aluminium used to make the alloy [13].

---

### 2.1.4 Grain Boundaries

Most metals in commercial use are polycrystalline, which means that the metal as a whole is made up of a large number of small interlocking crystals, that are also called grains. Grains are joined to its neighbors at all points by a grain boundary, the shape of which does not correspond to the internal structure of the crystal. The packing of the boundaries is almost as compact as within the grains themselves [14]. Figure 6 show an example of the grain structure in aluminium.

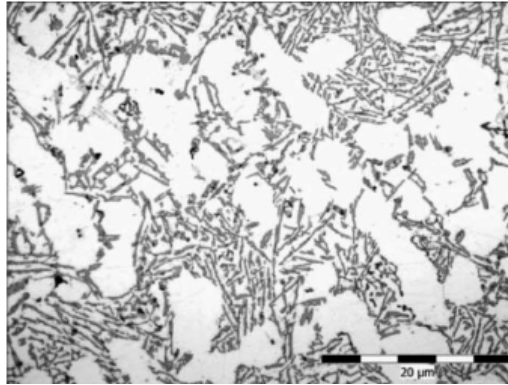


Figure 6: Grains in Al. [15]

### 2.1.5 Melting process of Aluminium

When melting Al in a crucible the heat will travel from the bottom and upwards the center of the crucible, then in loops downwards the sides of the inner walls, as shown in Figure 7. At the beginning of the melting the solid aluminium is placed inside a furnace in a crucible. Heat is then added to the system, and the melting starts when the melting point ( $660^{\circ}\text{C}$ ) of the aluminium is reached. The impact different elements have on the melting of aluminium can be visualised in a phase diagram.

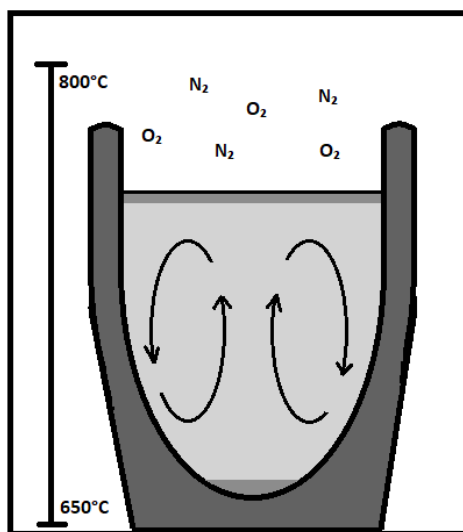


Figure 7: Heat-exchange in crucible.

---

## 2.2 Phase Diagram

Phase diagrams visualizes the calculations from thermodynamic equilibrium systems giving the solid-, liquid- and vapour phase of a compound material, depending on the composition concentration. Phase diagrams for the alloying elements of interest are shown in Figure 8-11 [16].

### 2.2.1 Vanadium

Figure 8 show the phase diagram of the system containing aluminium and vanadium, where the zoomed inn figure is the area of interest. The melt is heated to approx. 650°C, where the melting/solidification line is met, and the metal liquefies into an eutectic system.

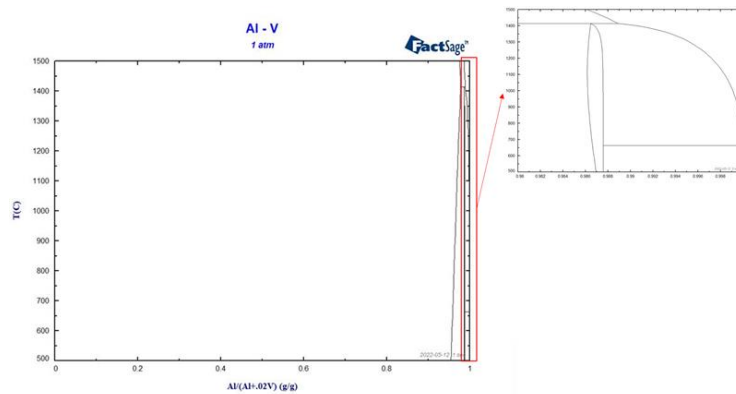


Figure 8: Phase diagram of Al-V.

### 2.2.2 Nickel

Figure 9 show the phase diagram of the system containing aluminium and nickel. The system reaches the melting line at approx. 640°C, where it becomes a monotectic system for Al (99.998 wt%) and Ni (200 ppm).

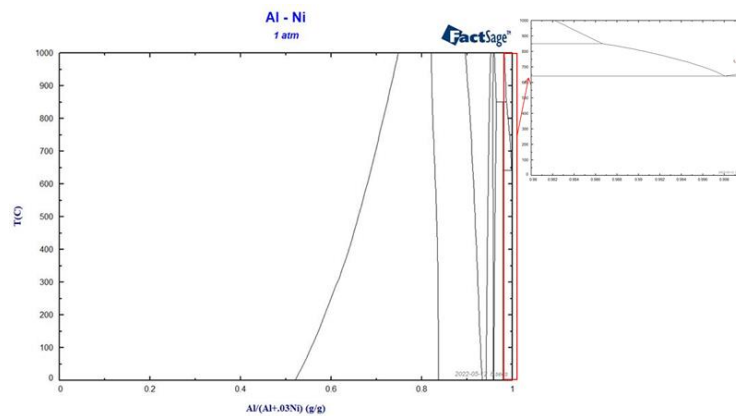


Figure 9: Phase diagram of Al-Ni.



---

### 2.2.3 Strontium

Figure 10 show the phase diagram of the system containing aluminium and strontium, where the zoomed inn figure is the area of interest. The melt is heated to 400°C, where the melting/solidification line is met, and the metal liquefies into an eutectic system.

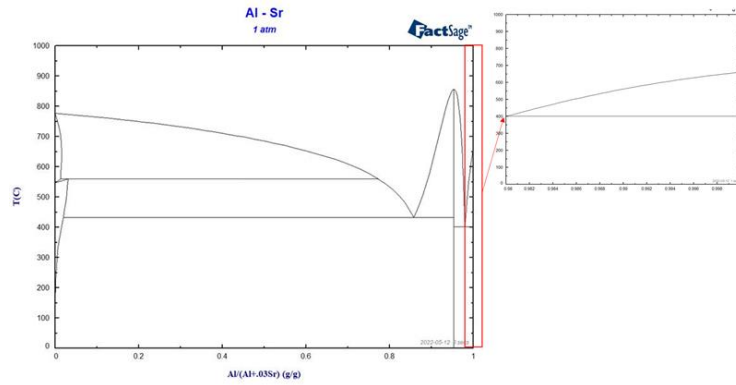


Figure 10: Phase diagram of Al-Sr.

### 2.2.4 Bismuth

Figure 11 show the phase diagram of the system containing aluminium and bismuth, where the zoomed inn figure is the area of interest. The melt is heated to 660°C, where the melting/solidification line is met. For concentrations higher than approx. 80 ppm Bi the metal liquefies into an eutectic system, while it liquefies to a monotectic system for lower concentrations.

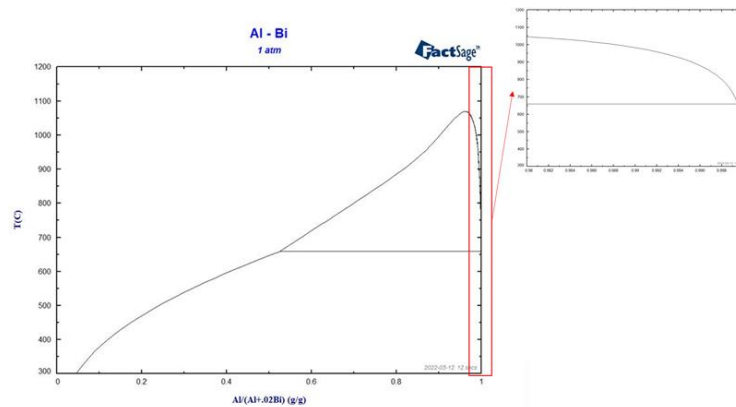


Figure 11: Phase diagram of Al-Bi.

---

## 2.3 GD-OES

Glow Discharge Optical Emission Spectroscopy (GD-OES) works on the premises that any given atom has a large number of possible energy levels. An emission spectrum is a result of an electronic transition from a higher level energy to a lower one. Those transitions are given by the rules of quantum mechanics [17].

A certain amount of energy is transferred to an atom when it collides with another particle. The atom then becomes excited, and displaces an electron from its external layer to a higher excitation level. Following this excitation, the electron then return to its original energy level.

The atomic emission technique measures the energy lost by an atom when it goes from a high excitement state to a lower state. This energy is released in the form of photons, that yield spectral lines. The atomic emission spectrum is thus made up of discrete spectral lines, and the number of photons emitted is proportional to the number of atoms of the element being analyzed [17].

In order for the sample to get excited, it must be atomized, which means that the sample must be dissociated into free atoms or ions.

Excitation of elements by glow discharge involves phenomena of passage of an electrical current through a low-pressure gas. The plasma in the instrument is induced by an electric field. However, the glow is not uniform along the axis between the electrodes, as shown in figure 12.

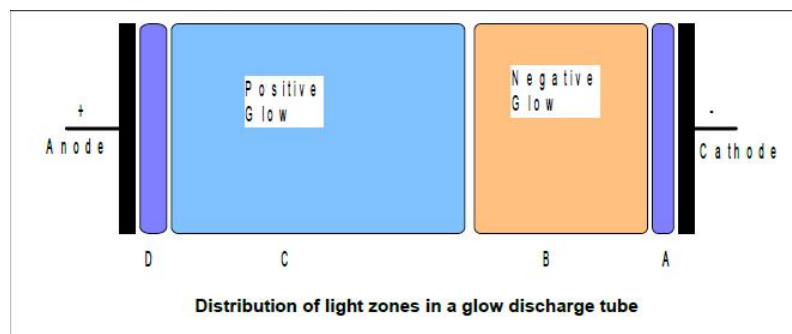


Figure 12: Distribution of light [18]

For the GD analysis, the negative glow (B) and the cathode dark region (A) are of importance. In the negative glow region, there is absence of an electrical field and a relatively high charge density. At the cathode dark space, the charge is relatively low [17].

Electrons flow from the cathode, through the plasma, to the anode. During the time the electrons travel, they will occasionally collide with the gas atoms, forming positively charged atoms. Those positively charged atoms are then attracted to the cathode, where they impact with sufficient energy to knock atoms off the surface of the electrode.

This way, they result in the emission by the cathode of secondary electrons, that are then accelerated to the anode through the negative glow. Those secondary electrons cause formation of new electrons and that establishes the self-maintenance of the discharge [17].

---

The sputtered atoms then enter the plasma where they get excited by collisions with more energetic electrons or by the collisions with excited gas atoms.

The excited atoms then are de-excited by optical emission, which causes the glow. De-exciting atoms emit photons that have characteristic wavelengths. By measuring the signals of those wavelengths, the amount of atoms of each types can then identified.

Mostly positive electrode (anode) for the GD-OES is a hollow metal tube, made of Cu with a hole in the centre opposite to the sample. The diameter of the tube can vary from 1-8 mm. The sample surface is positioned against a ceramic body close to the tip of the tube. The precision of the ceramic/tube distance is crucial, as it ensures that the anode will end into the dark region of the plasma and so the sputtering only occurs in the area of the sample opposite to the tube [18].

RF power is applied to the back of the sample, also assuring the cooling of the sample.

### 2.3.1 Quantification in GD-OES

The instrument used for the analysis is the GD-Profilier 2. This instrument is a spectrometer, which is a comparative instrument. In order to obtain the quantitative information, the instrument will need to be calibrated [18].

GD is capable of providing composition and depth information at the same time, even for multilayered samples.

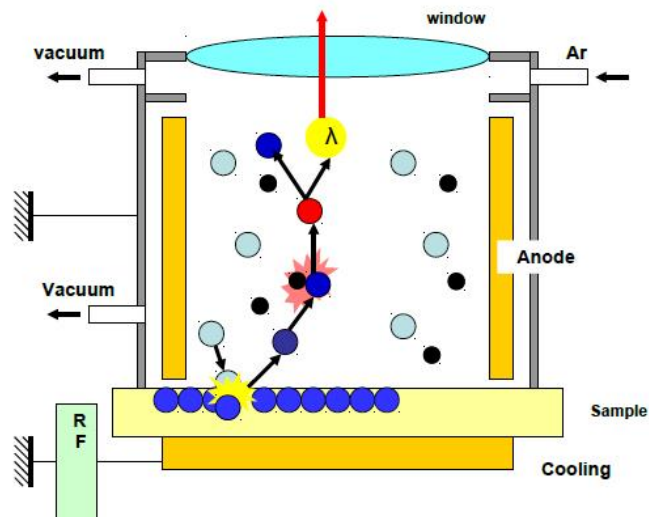


Figure 13: GD-quantification [17]

Figure 13 shows a quantification principle for GD-OES. There are three primary processes that are involved in the process, and are assumed to be independent: 1) the supply of sputtered atoms, 2) excitation followed by de-excitation, and 3) detection.

---

The supply of atoms is dependent on sputtering efficiency, and the sputtering takes place at the sample surface facing the anode, and the incident Ar ions collide with this sample surface. The sputtering efficiency changes depending on the material, its structure and its morphology.

Once the sputtering occurs, the atoms become independent. As the excitation and de-excitation take place in the negative glow region, this process is linked to only plasma parameters [17].

The detection is then dependent on the spectrometer.

The software used (Quantum) is able to convert qualitative information, intensities vs time, into quantitative information, which is concentration vs depth [17].

### **2.3.2 Identifying elements & calibration**

The calibration procedure is crucial for a precise and accurate quantification in bulk and composition depth profiles, and the most important aspect of the process is the selection of appropriate samples.

For the bulk analysis, the selection is more straightforward as the calibrations are done for a specific alloy or group of alloys.

For CDP (Compositional Depth Profiles), the samples that are analysed are usually multilayered, and so either similar multilayered samples must be used as reference, or bulk samples of different materials have to be used.

The quantification procedure is based on the direct link between the measured intensities, and the effective concentrations. It is important that the complete range of the effective concentrations is covered by the calibration curve.

---

## 2.4 GD-MS

### 2.4.1 System set-up

The glow discharge mass spectrometer (GD-MS) provides an elemental analysis of conducting samples, providing the concentrations of the trace elements. This is achieved by combining features of mass spectrometer and ionization source. The detection system, along with mass spectrometer, provide required wide linearity, whilst the glow discharge serves to deliver high ion yields [19].

The instrument used for the analysis of the samples for this thesis is the Nu Astrum glow discharge mass spectrometer, and a schematic picture of the instrument is shown in Figure 14.

The schematic representation of the sample loading chamber is shown in Figure 15. It is used to load and unload the samples. This is the only part of the instrument that is vented to atmospheric pressure. The pressure in the chamber is monitored by a Pirani gauge [19].

A slide valve is separating the sample loading chamber from the GD-chamber. After the sample is loaded, the sample chamber is evacuated by a turbo-molecular and rotary pumps. When the needed vacuum is achieved in the chamber, the slide valve can be opened, and the vacuum in both chambers is equal [19].

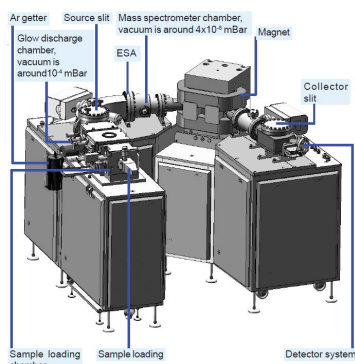


Figure 14: Nu Astrum GD-MS instrument [20].

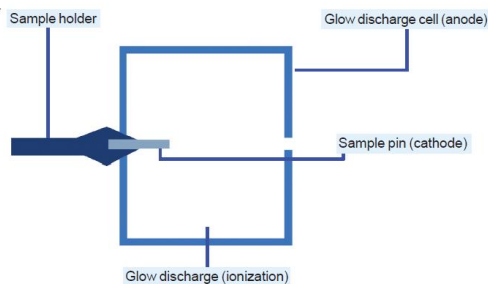


Figure 15: GD-MS loading of samples[19].

The GD-ionization source delivers high ion yields from conducting samples. The GD-chamber is evacuated using a turbo-molecular pump, and backed by a rotary pump. Pressure is also monitored by a Pirani gauge [19].

In the GD-chamber the ions are generated for the subsequent analysis by the MS. As with GD-OES, the glow discharge require low pressure, high purity, argon atmosphere. Any atmospheric components that are left in the sample chamber after load, are removed from the argon by cryogenic cooling of the cell region [19].

---

Atoms of all elements will be able to enter the ionization region of the chamber equally easily and in proportion to their concentration. Thus, the sensitivity of analysis for a particular element will be similar. This sensitivity is determined primarily by the first ionization energy of the element, which answers to the extent of how easily the atoms of that element are ionized in GD-plasma [19].

This key feature of the GD-source allows to establish a relative sensitivity factor (RSF) for each element. The RSF can be applied across a wide range of sample types, and provides a high accuracy to the analysis [20].

After the sample loading chamber is evacuated, and the slide valve between the sample loading chamber and GD-chamber is open, the sample can then be inserted into the GD-chamber. Initiation of the glow discharge is controlled by the software, in which the GD-current and voltage are defined [19].

Pure argon gas is supplied to the GD-chamber to initiate and sustain the discharge. The cell is then cooled cryogenically. The vacuum is then achieved by implementation of the rotary and turbo-molecular pumps.

The ions exit the glow discharge cell with an accelerating voltage of about 6 kV, and the extractor lens extracts the ions from the GD-cell. The ions then enter the transfer lens stack, in the transfer region.

There are two options for the measurement of the ion beam. If the signal is intense ( $> 1\%$ ), it will be measured on the Faraday cup. Signals of low intensity will be measured on the secondary electron multiplier [19].

The deflector lens directs the beam to either of those detectors. The voltage can be changed manually, according to the concentration of the elements of interest [20].

#### **2.4.2 Data processing**

The software collects the raw data, which can then be processed by using "Data Acquisition". The quantitative data is obtained by applying Relative Sensitivity factors. If standards are available, the calibration graphs can be established, from which the RSF factors are calculated [20].

After the desired parameters are chosen, the data can be exported to an Excel sheet, where the data can be used for the chart or to create a graph.

---

## 2.5 ICP-OES

Inductively Coupled Plasma (ICP) is a method of OES, in which the plasma energy is given to a sample from outside. When the plasma is introduced the atoms get excited, and de-excite, when returned to low energy position [21].

As with GD-OES, the atoms release emission rays when they de-excite, and the element type is determined based on the position of photon rays.

The Ar gas is supplied to torch coil in order to generate plasma, and the high frequency electric current is applied to the work coil and the tip of the torch tube. The electromagnetic field is then created in the torch tube, which ionizes argon gas and creates plasma. Solution samples are then introduced into the plasma in an atomized state through the narrow tube in the center of the torch tube [21].

ICP-OES allows for simultaneous, sequential analysis of multiple elements, and it also has few chemical or ionization interferences. ICP-OES is also stable, highly sensitive and has a high number of measurable elements [21].

---

### 3 Material and Methodology

#### 3.1 Equipment and Material

An overview of the experimental equipment and materials are found in Table 1. The equipment and materials were provided by the Department of Materials Science and Engineering (NTNU) at Berg (Gløshaugen). For the analysis with ICP-OES, Hösch Metallurgy has been of assistance.

<b>Equipment</b>	<b>Material</b>
Furnace: Nabertherm K1/K2.1/K2.2	Commercial Grade Al (99.7%)
Horiba Profiler-GD/OES	Electrical Grade Al (99.999999%)
Nu Instruments-Astrum-GD/MS	Al-alloy, AlSi7
Labotrom-5 Cutting Machine	Bismuth, Bi (pure)
ATM Saphir 330, Struers RotoPol-21 (Manual grinding machines)	Al-11%Ni
Thermocouple	Al-10V (Master Alloy)
Rapid Solidified Disc sampling device	Al-10Sr (Master Alloy)
FactSage	BN Lubriccoat-Blue ZV
	BN Hardcoat

Table 1: Overview of experimental material.

For more information about the handling of the coatings see Attachment A H/P-phrases for BN-coating.



---

## 3.2 Method

### 3.2.1 Cutting of materials

The experimental method included the cutting of the pure metal, AlSi7-alloy and the alloying elements for every cast. The different Al used in this thesis is shown in Figure 16. For every trial it was aimed to add 200 ppm of the investigated element. The amount of element compared to aluminium, is shown in Figure 17.

The aluminium were cut into pieces of approx. Al (200 g). The aluminium ingot and AlSi7-alloy were cut with the Labotrom-5 cutting machine using a 10S25-disc, for soft, non-ferrous metals (Figure 18). Pure aluminum was cut with the bandsaw (Figure 19).

The master alloys and Al-11%Ni were first cut with the Labotrom-5 cutting machine, then adjusted to pieces containing alloying element (200 ppm) with a handsaw. The bismuth was broken into pieces (200 ppm) with a hammer.



Figure 16: Electrical Grade Al, Commercial Grade Al, AlSi7 (from left to right).



Figure 17: Aluminium (1kg) and element (200 ppm).



Figure 18: Cutting machine.



Figure 19: Bandsaw.

---

### 3.2.2 Weighing of Al and alloying element

Before each trial the amount of aluminium, added to the crucible, was weighed. The alloying element of interest for its respective trial, was weighed, packed in aluminium foil, and weighed again. An example of the weighing is shown in Figure 20.



Figure 20: Weighing of element, element in foil, and Al.

Table 2 gives an overview of all the performed trials with the amount of metal and alloying element, and at which temperature the addition has taken place.

<b>Trial</b>	<b>Al-ingot [g]</b>	<b>Element [g]</b>	<b>Element/foil [g]</b>	<b>Initial Temp. [°C]</b>
Pure Al	920.4	-	-	730
Ni 1h	930.1	1.7	2.8	729.7
Ni 2h	1004.21	2.17	2.99	726.2
Ni 20h	1000.12	1.97	2.45	733.6
V 1h	984.2	2.2	2.4	731.1
V 2h	1026.04	2.15	2.98	732.4
V 22h	1095.40	2.53	3.05	728.8
Sr 1h	950.3	1.7	2.7	727.2
Sr 2h	987.51	1.77	2.20	726.2
Sr 20h	980.83	2.12	2.58	725.5
Bi 1h	951.7	0.2	0.3	726.5
Bi 2h	970.49	0.21	0.52	733.3
Bi 22h	1024.1	0.19	0.24	727.6
Alloy, Ni 4h	1055.2	1.8	2.7	725.1
Alloy, V 24h	1072.9	2.1	2.6	726.8
Alloy, Sr 21h	1023.7	1.9	2.5	725.6
Alloy, Bi 20h	987.2	0.21	0.28	731.5

Table 2: Summary of trials.

---

### 3.2.3 Reference trials

At first, the initial trials of pure aluminium ingot were performed to generate reference samples. The aluminium was molten and heated to 730°C, at which temperature two samples were cast into the Rapid Solidified Disc.

The Rapid Solidified Disc (RSD) sampling device used for this thesis, shown in Figure 21, gives circular samples of approx. aluminium (40 g), with a diameter of approx. 40 mm.

The existing master alloys and the pure Al-ingot were analysed by GD-OES before initial runs. All trials have been conducted in parallel to the ongoing analysis with the GD-OES.



Figure 21: RSD-tool.



Figure 22: Crucible and rod.

### 3.2.4 Trial structure

All trials were conducted in the same crucible types, where the crucibles have been coated with BN Lubriccoat after every cast. The coating hindered the interactions between the equipment and the aluminium. As a stirring device, carbon rods coated with BN Lubriccoat after every trial have been used. Both, the crucible and the rod, shown in Figure 22, were coated with the BN Hardcoat before the first appliance of the soft coat. The melting has been done in the Nabertherm furnace (Figure 23) without any artificial atmosphere. Before every casting the melt has been skimmed of dross and was well stirred.

Before the start of the trial, the temperature of the melt was measured as shown in Figure 24. The measurement was done by a thermocouple coated first with BN Hardcoat then with BN Lubriccoat. When the temperature was measured to approximately 730°C, the alloying element of interest was added.



Figure 23: Nabertherm Furnace.



Figure 24: Measuring of temperature.

### 3.2.5 Casting of samples

The sampling was done by two different methods: one with the casting tool operated by two people, and the other with the two thongs. The tools are shown in Figure 25.

In both methods the liquid metal was poured into the RSD sampling device. When the metal had solidified, the sampling device were hit against the ground to release the sample. The sample was then placed on foil to cool down, while the dross was stored beside (Figure 26).



Figure 25: Casting-tools.



Figure 26: Sample handling.

---

### 3.2.6 Metallographic Sample Preparations

The samples from all casting trials were sanded and polished using a TM Saphir 330 Struers RotoPol-21 (Figure 27), with SiC polishing paper with a grid from 80 - 800 and water. A grid of 500 is sufficient for GD analysis, while a fine surface was expected to reduce the deviation, hence a surface finish with a 800 grid paper was used. The surface of the sample after polishing is shown in Figure 28.



Figure 27: Polishing machine.

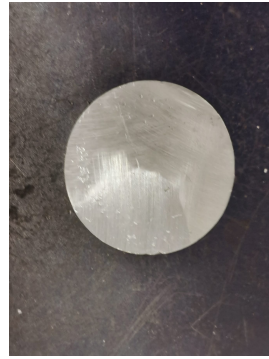


Figure 28: Sample after polishing.

### 3.2.7 GD-OES

The prepared samples were analysed using GD-OES (Figure 29). The sampling area of the GD-OES is a ring of 4 mm in diameter, allowing multiple GD samples on each RSD sample. One GD sample was taken in the middle, and (at least) three samples were taken among the outer rim for every RSD sample, as shown in Figure 30.



Figure 29: GD-OES.



Figure 30: Sample after GD-OES.

---

### 3.2.8 GD-MS

In addition the Bi-samples and the RSD samples with the alloy were analysed by GD-MS (Figure 31). The sampling area of the GD-MS is a ring of 10 mm in diameter. The RSD samples were analysed in the middle of the sample, as shown in Figure 32.



Figure 31: GD-MS.



Figure 32: Sample after GD-MS.

### 3.2.9 ICP-OES

The samples shown in Figure 33, was sent to Hösch Metallurgy in Germany for further analysis with ICP-OES.

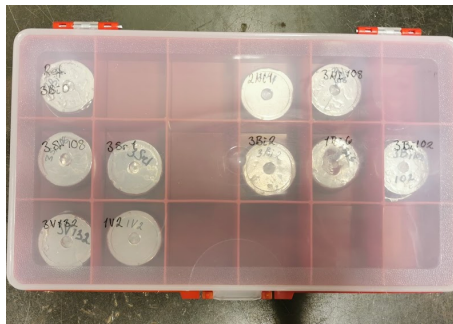


Figure 33: Samples sent to ICP-OES analysis.

### 3.2.10 FactSage

Phase diagrams generated by FactSage have been used to estimate impact and behaviour of the alloying elements in the different alloys.

---

## 4 Results and Discussion

### 4.1 Sources of Error and Limitations

#### 4.1.1 Deviation in temperature

Throughout the trials, there has been limitations regarding control and accuracy of the temperature of the molten aluminium. It is connected to the heat exchange in the crucible, mentioned in chapter 2.1.5, in addition to the temperature drop during the casting of the sample. The furnaces used may also display temperature values that deviate from those measured with a thermocouple. Deviation in temperature may lead to formation of unwanted phases in the mix, though it is unlikely, looking at the phase diagrams of the elements added, as mentioned in chapter 2.2. However, the results show no sign of the melt being affected to a large extent, as the results have been consistent.

The heat loss during casting of the samples, cannot be avoided, however it can be minimized by faster casting and immediate return of the crucible to the furnace. The temperature drops at a faster rate as the volume of the liquid metal decreases, which can lead to more rapid heat loss, which is harder to control and prevent. The temperature also drops when the liquid metal is stirred and the alumina layer is removed.

#### 4.1.2 Contamination in the samples

The mould that the samples are cast into, can be a source of the contamination of iron, however the contamination is on the surface, due to the rapid solidification. The crucibles can also provide contamination from the previous use of them. The contamination coming from crucible can be prevented by re-applying a thin layer of boron-nitrate coating between separate trials. Contamination from tongs that are used to move the crucible in and out of the furnace can also be prevented by re-applying the coating. However, it is harder to do so if several trials are running at the same time and tongs are continually used. This can lead to a different concentration of contamination in the samples from the same trial.

Some of the samples would also show contamination on the surface, however, the contamination would be polished away and not affect the results to a high extent.

Residual ingots showed some weird patterns and grains. The ingots would oxidize in a different way, differentiated based on the element introduced to the liquid aluminium. It may be due to the different elements oxidizing on the surface, and may also be contaminated by the iron that the RSD sampling device is made of.

---

### 4.1.3 Loss of the liquid metal

There is a certain amount of liquid metal that is lost throughout the trial, due to the formation of the aluminium oxide (dross), that is removed before each sample-taking. Some liquid metal also solidifies on the tongs, thus leaving the system. This can lead to the change of the concentration of the elements added to the system. The change in the concentration due to the volume of aluminium lost can be mistaken for the fading of the element, or can produce a higher concentration of an element in the samples, taken after some time.

As mentioned in the chapter 2.1.1, the loss of liquid aluminium also occurs during the formation of aluminium oxide level on top of the bath. This oxide is removed before the samples are taken, and may also include some of the elements added to the system. Although, the dross does not weigh much after each removal, the total mass after all the samples taken can be accumulated to a significant number, which can affect the concentrations of the elements in the melt, and change the liquid metal composition.

### 4.1.4 Addition of the elements to the aluminium

Throughout all the trials, the alloying elements have been covered in aluminium foil before being added to the liquid aluminium, to ensure consistent result. However, the element can either precipitate on the bottom, or oxidize, floating to the top and be removed as the dross. The risk of element not being introduced to the liquid metal can be minimized by sufficient stirring when element is first introduced and before each sample is taken.

The method has been efficient enough, and most elements were introduced to the liquid aluminium. However, bismuth has not been found in the systems during the trials with the industrial grade aluminium, but has been traced in the electrical grade aluminium.

### 4.1.5 Master alloys

The alloys with elements used are not uniform, which means that some parts of the ingots can contain more or less of the element than the theoretical value. Throughout the trials, the average weight percent of the elements in the master alloys have been used as the basis for the calculations, but the real wt% may differ. This is the case for all the elements, besides bismuth, which was added in its pure form.

The composition of master alloys may also result in a deviation from theoretically calculated values, which can be seen in the GD-OES/MS results. The desired concentration was in the range of around 200 ppm, and in some cases, the concentration would be significantly higher.



---

#### **4.1.6 Hydrogen solubility**

Some of the samples cast would have hydrogen bubbles under the surface, which could prove difficult to analyse with the GD-OES. For samples with vanadium introduced to the system, there has been a lot of hydrogen pores in the samples, which has caused it to be almost impossible to analyse with GD-MS, and caused issues with the analysis with GD-OES.

#### **4.1.7 Samples**

The industrial aluminium has had 0.15%-concentration of iron, which is known to be an issue in aluminium alloys, and can hinder the interactions between Al and the other alloying elements. However, the interactions of the iron in samples are not suspected to have a major impact, concerning the results derived from the samples.

---

## 4.2 GD-OES data and its interpretation

### 4.2.1 GD-OES-data from 1h V-trial

Figure 34 shows the results from the GD-OES-analysis of the Vanadium-sample taken at the start of the 1 hour trial. The sample was in total analysed six times for about 4 minutes each. The graph shows a stable signal between 0-0.02 wt% V, with peaks at 0, 0.3, 2.5 and 3,3 minutes.

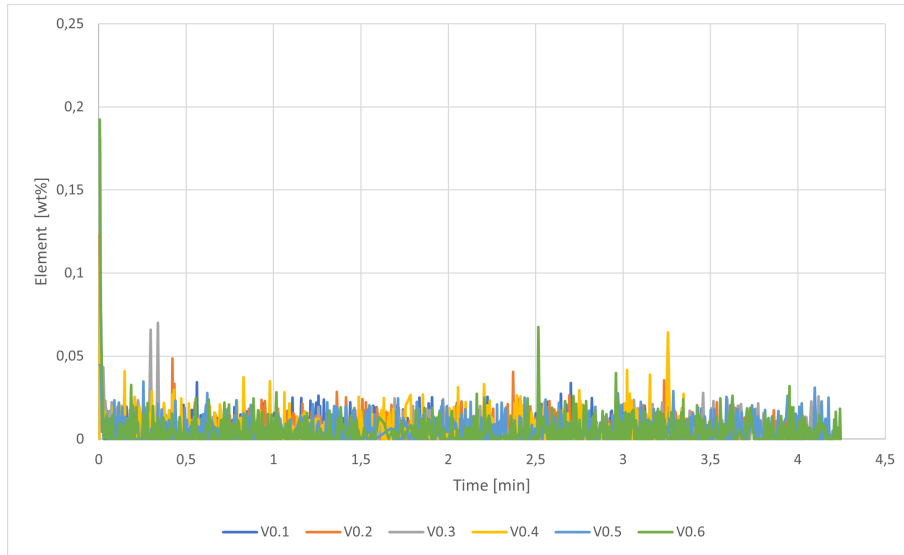


Figure 34: Reference Al-sample before addition of V.

The results from the Al-sample taken at 5 minutes are shown in Figure 35. The sample was analysed six times for 4 minutes. The graph shows a stable signal with values between 0-0.05 wt% V, with peaks at the beginning of the analysis and at 1.5 minutes.

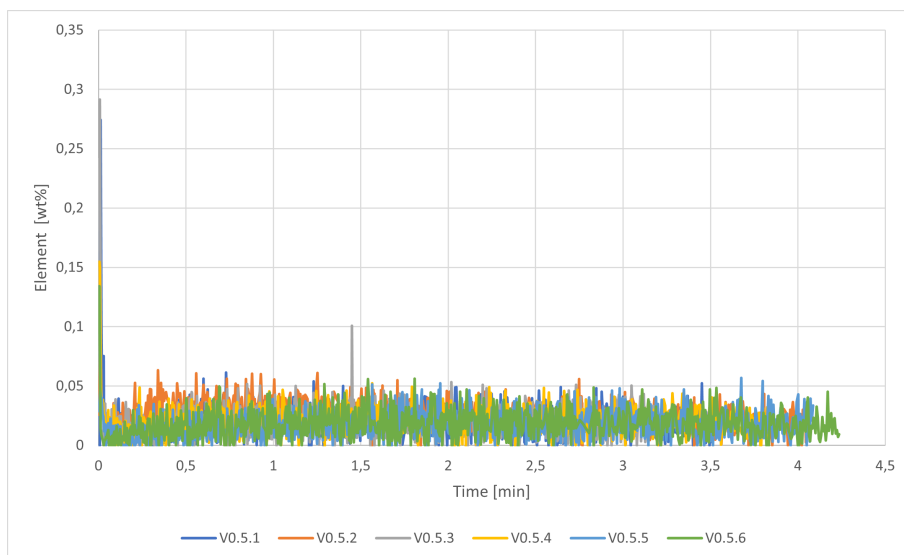


Figure 35: Al-sample with V at 5 min.

---

The results from the sample taken at 10 minutes are shown in Figure 36. The sample was analysed six times for 3-4 minutes. The graph shows a stable signal between 0-0.05 wt% V, with peaks at the beginning of the analysis.

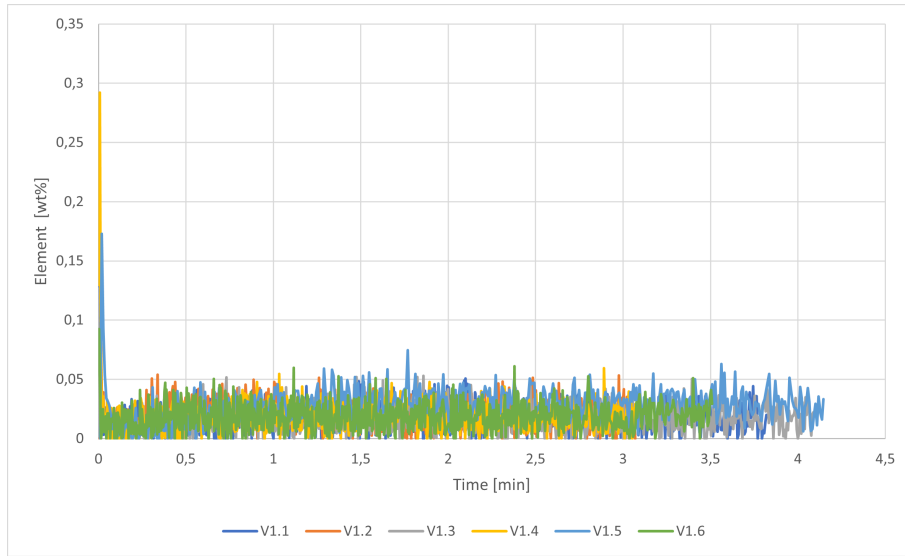


Figure 36: Al-sample with V at 10 min.

Figure 37 shows the results from the analysis of the Vanadium-sample taken at 20 minutes from the start of the trial. The sample was in total analysed six times for about 4 minutes. The graph shows a signal between 0-0.06 wt% V, with peaks at 0, 0.6, 1.5 and 2.5 minutes.

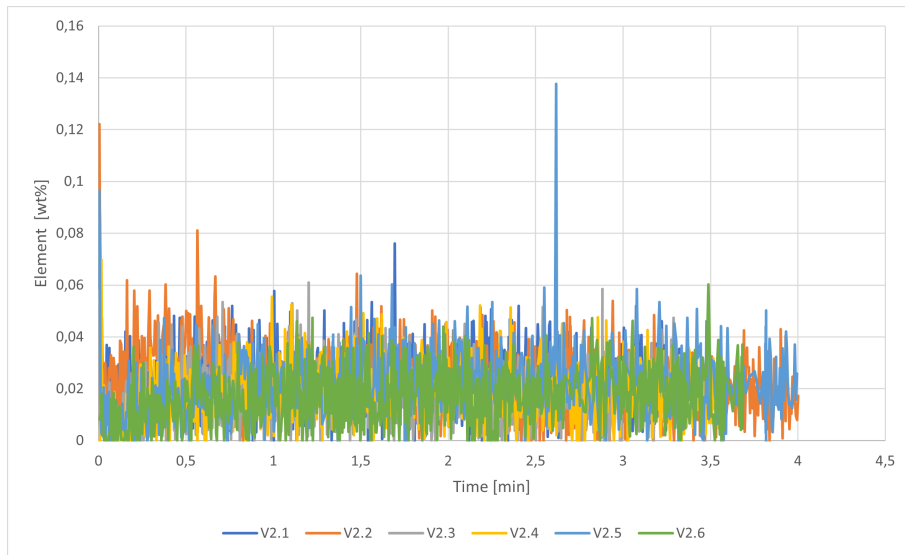


Figure 37: Al-sample with V at 20 min.

---

The results from the sample taken at 30 minutes are shown in Figure 38. The sample was analysed six times for between 2-4 minutes. The graph shows a stable signal between 0-0.05 wt% V, with peaks at the beginning of the analysis, and at 0.6, 1.4, 2.2 and 2.7 minutes.

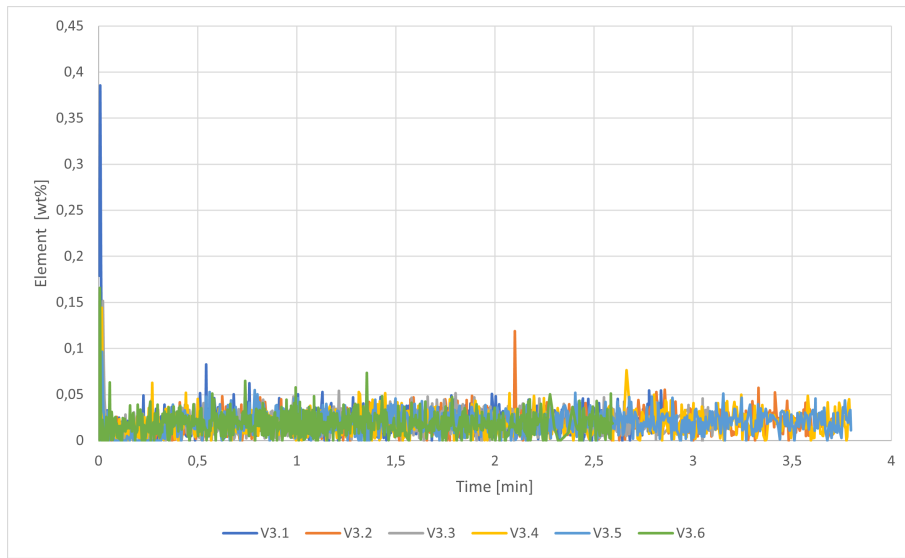


Figure 38: Al-sample with V at 30 min.

Figure 39 shows the GD-results from the analysis of the Vanadium-sample taken at 40 minutes. The sample was in total analysed six times for almost 4 minutes. The graph shows a varying signal between 0-0.04 wt% V, with the highest peaks at the beginning. The analysis marked as V4.2 shows an increased signal the first minute of the analysis, which then evens out in comparison to the other graphs. V4.1 differs from the rest of the parallels, and has a lower signal with less deviation.

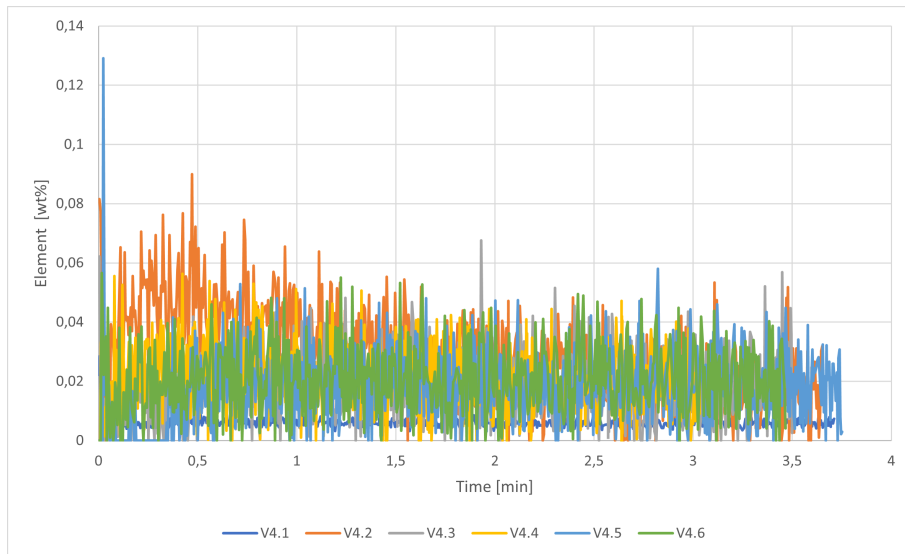


Figure 39: Al-sample with V at 40 min.

---

The results from the sample taken at 30 minutes are shown in Figure 40. The sample was analysed six times for 4 minutes. The graph shows a stable signal between 0-0.05 wt% V, with peaks at the beginning of the analysis and at 1.7 minutes.

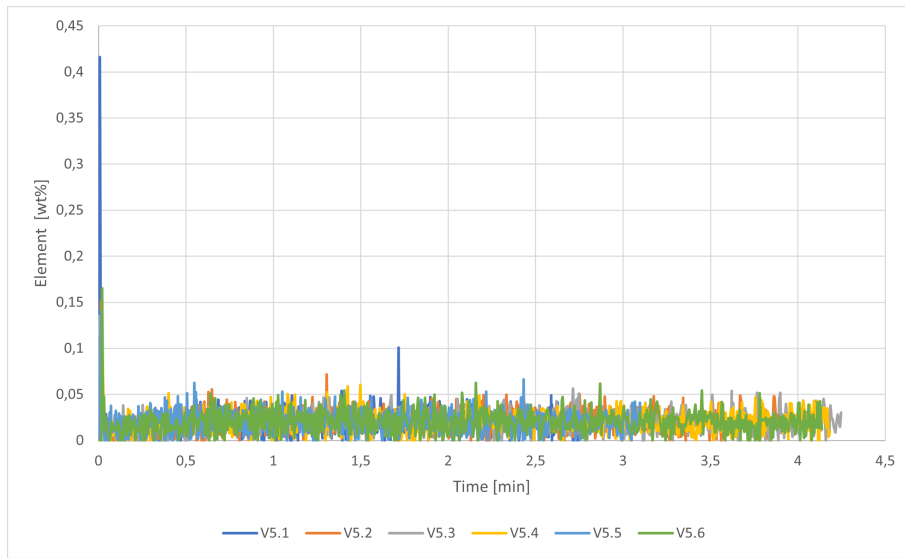


Figure 40: Al-sample with V at 50 min.

Figure 41 shows the results from the Vanadium-sample taken at the end of the 1 hour trial. The sample was in total analysed six times for about 3 minutes each. The graph shows a stable signal between 0-0.05 wt% V, with peaks at 0, 1.5 and 2.2 minutes.

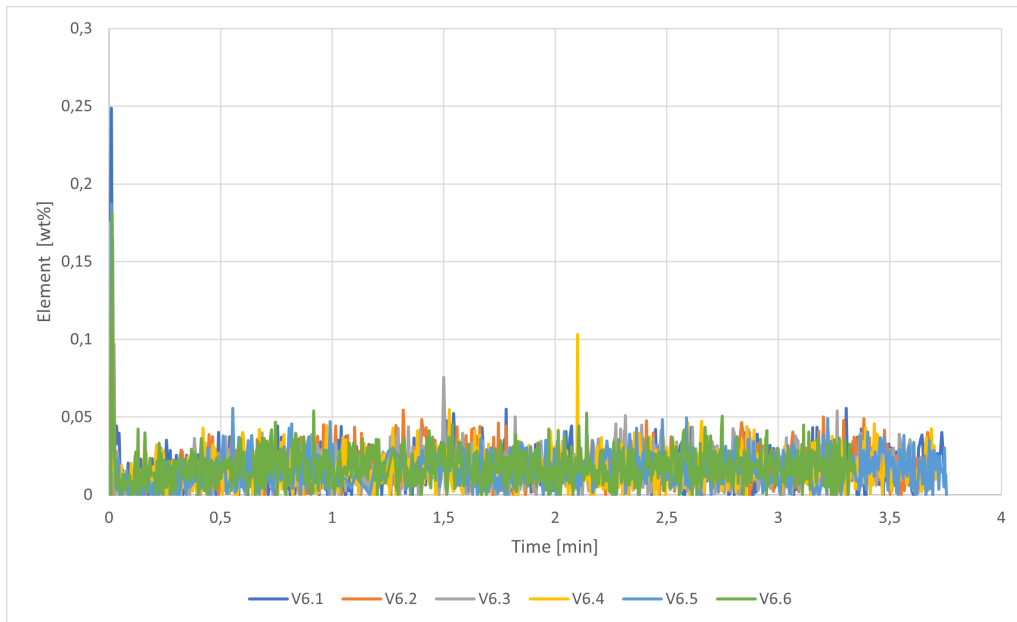


Figure 41: Al-sample with V at 60 min.

---

#### 4.2.2 GD-OES-data from 2h V-trial

Figure 42 shows the results from the Vanadium-sample, taken at the start of the trial. The sample was analysed four times for 3.5 minutes. The graphs shows a signal between 0-0.02 wt% V, with peaks at 0 minutes. V0.1 have a higher signal the first half minute, compared to the other graphs.

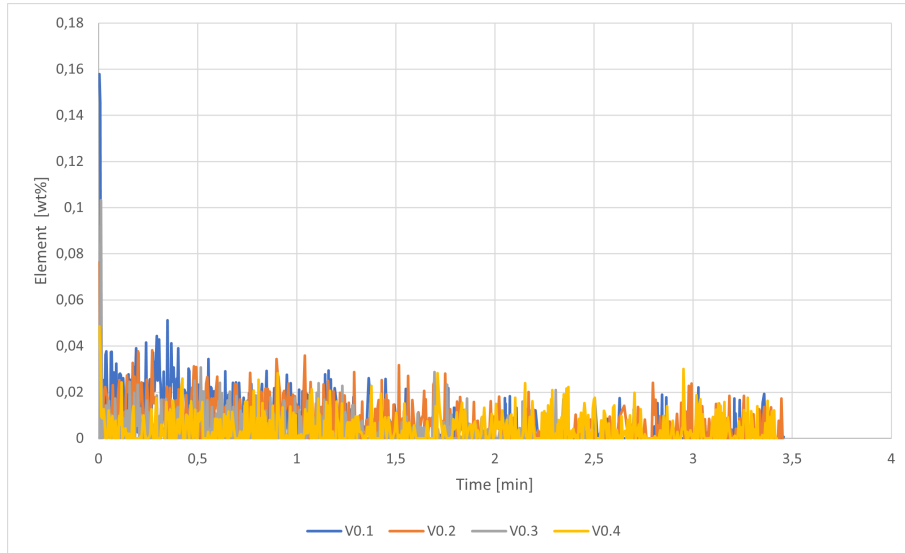


Figure 42: Reference Al-sample before addition of V.

The results from the Al-sample taken at 10 minutes are shown in Figure 43. The sample was analysed four times for 4 minutes. The graph shows a stable signal between 0-0.05 wt% V, with peaks at the beginning of the analysis.

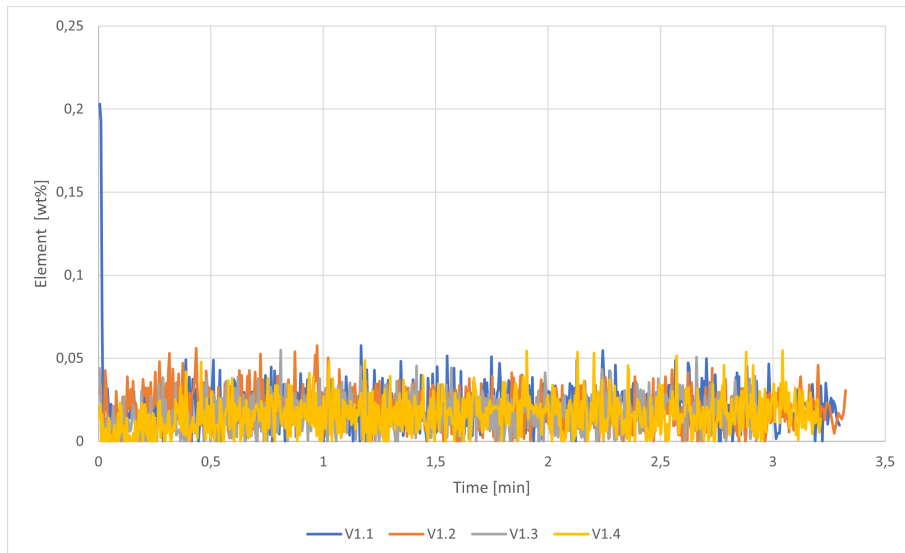


Figure 43: Sample of V after 10 min.

---

The results from the Al-sample taken at 20 minutes are shown in Figure 44. The sample was analysed four times for 3 minutes. The graph shows a stable signal between 0-0.05 wt% V, with peaks at the beginning of the analysis.

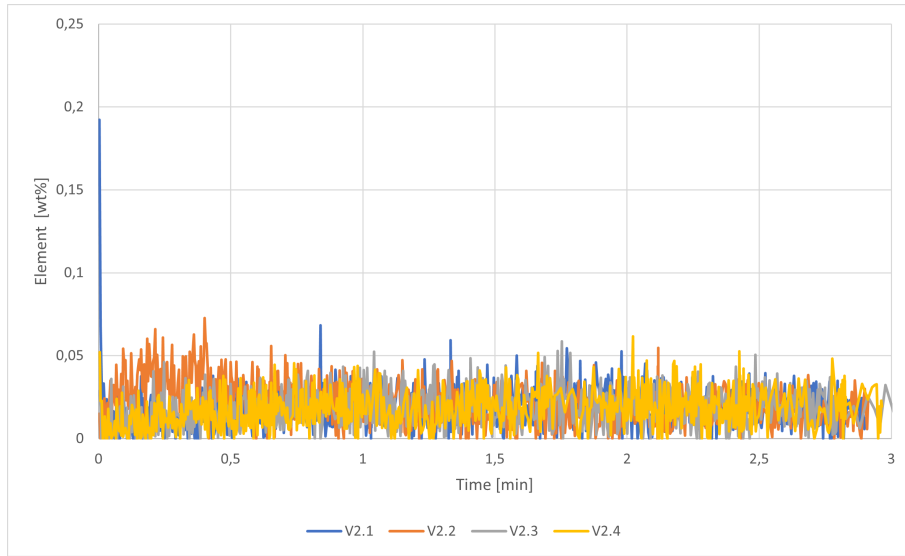


Figure 44: Sample of V after 20 min.

Figure 45 shows the results from the analysis of the Vanadium-sample taken at 40 minutes from the start of the trial. The sample was analysed four times for 2.5 minutes. The graph shows a stable signal between 0-0.06 wt% V.

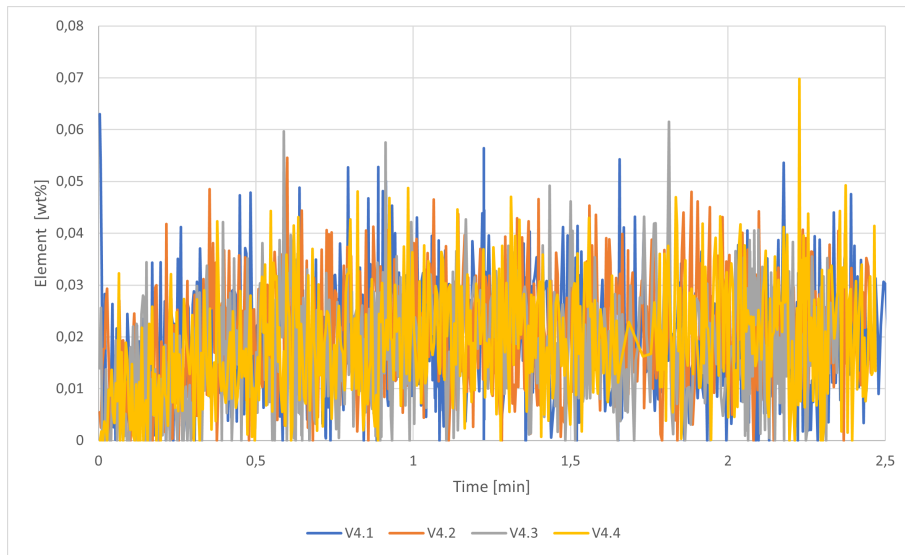


Figure 45: Sample of V after 40 min.

---

Figure 46 shows the results from the analysis of the Al-sample taken after 60 minutes. The figure shows a signal between 0-0.06 wt% V, with peaks at 0 minutes.

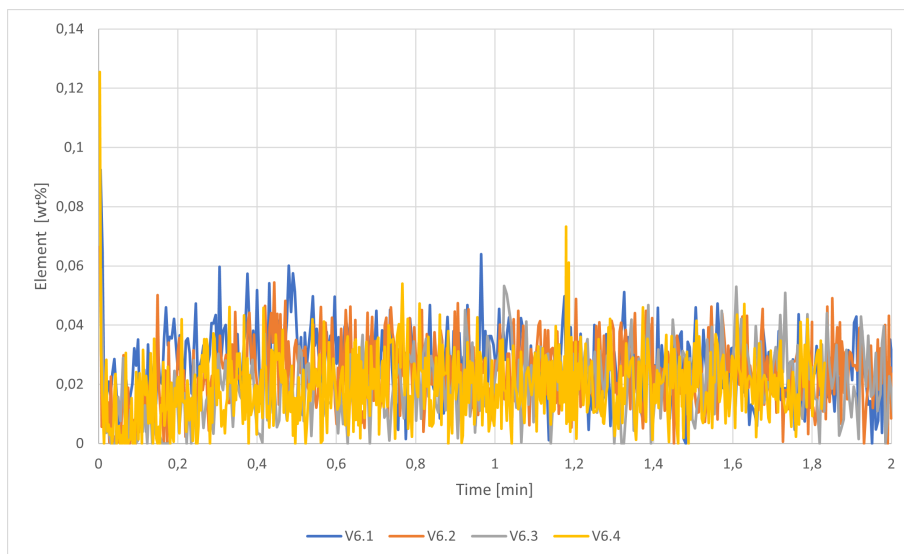


Figure 46: Sample of V after 60 min.

Figure 47 shows the results from the analysis of the Vanadium-sample taken after 80 minutes. The sample was analysed four times for 2.5 minutes. The graph shows a signal with values between 0-0.05 wt% V.

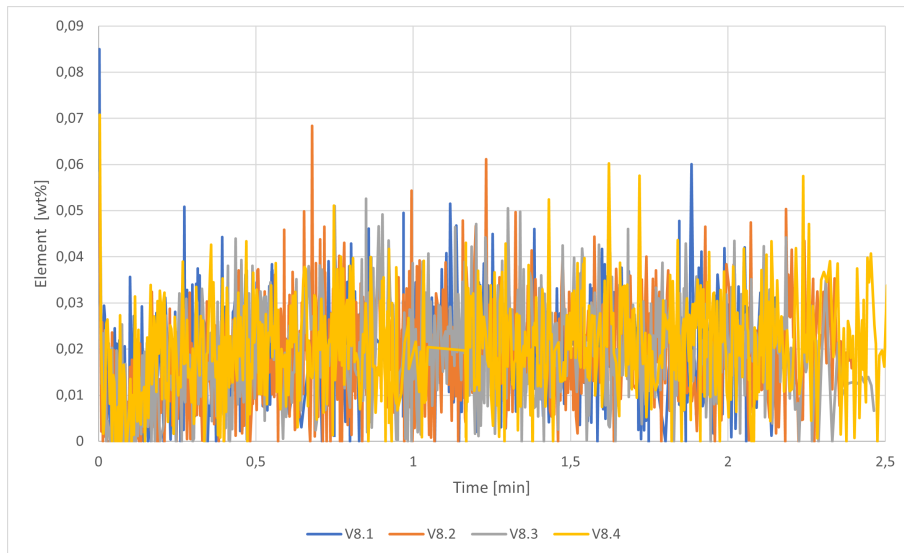


Figure 47: Sample of V after 80 min.



---

Figure 48 shows the results from the analysis of the sample taken after 100 minutes. The sample was analysed four times for 2 minutes. The analysis gave stable results between 0-0.04 wt% V, and its highest peaks at 0, 1 and 1.6 minutes.

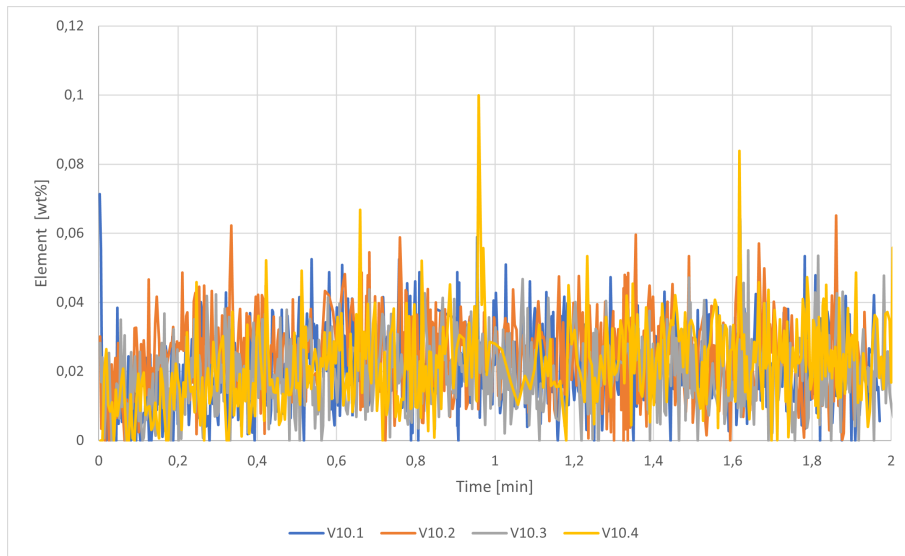


Figure 48: Sample of V after 100 min.

Figure 49 shows the data from the GD-OES-analysis of the Al-sample taken at 120 minutes. The sample was analysed four times for 2.5-3 minutes. The graph shows a stable signal with values between 0-0.05 wt% V.

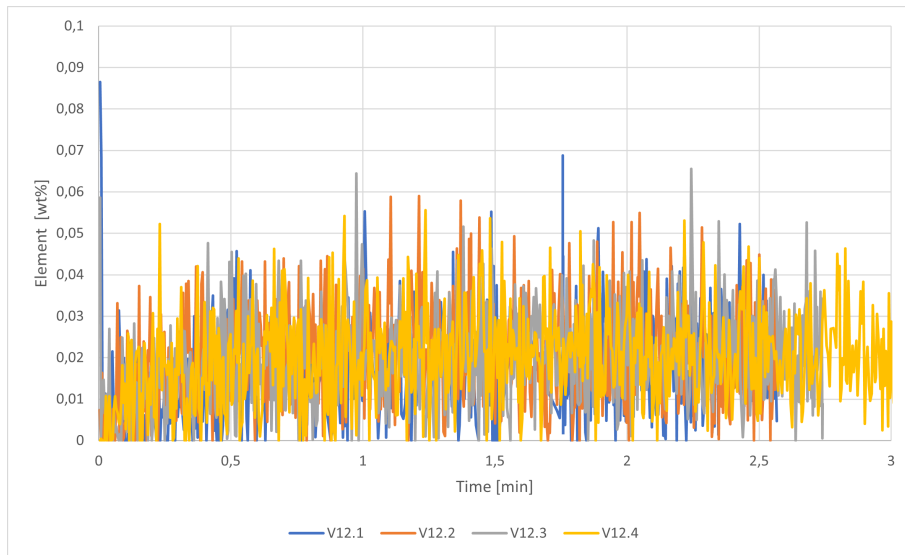


Figure 49: Sample of V after 120 min.

---

### 4.2.3 GD-OES-data from 22h V-trial

Figure 50 shows the data from the analysis of the Al-sample taken at the start of the trial. The sample was analysed three times for 3 minutes. The graph shows a stable signal between 0-0.02 wt% V. V0.1 peaks at 0 minutes.

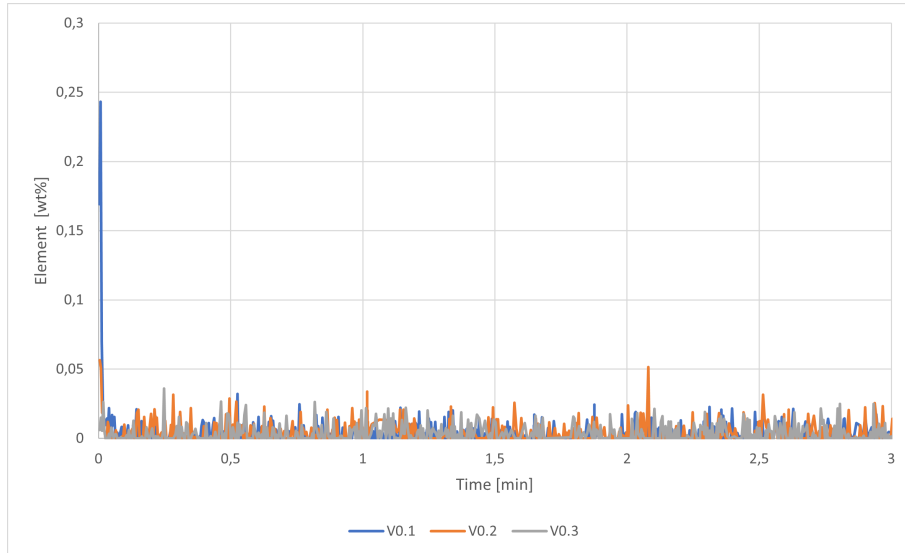


Figure 50: Reference Al-sample before addition of V.

Figure 51 shows the data from the analysis of the Al-sample taken after 6 hours. The sample was analysed three times for 2 minutes. The graph shows a stable signal between 0-0.05 wt% V, where V36.1 peaks at 0 minutes.

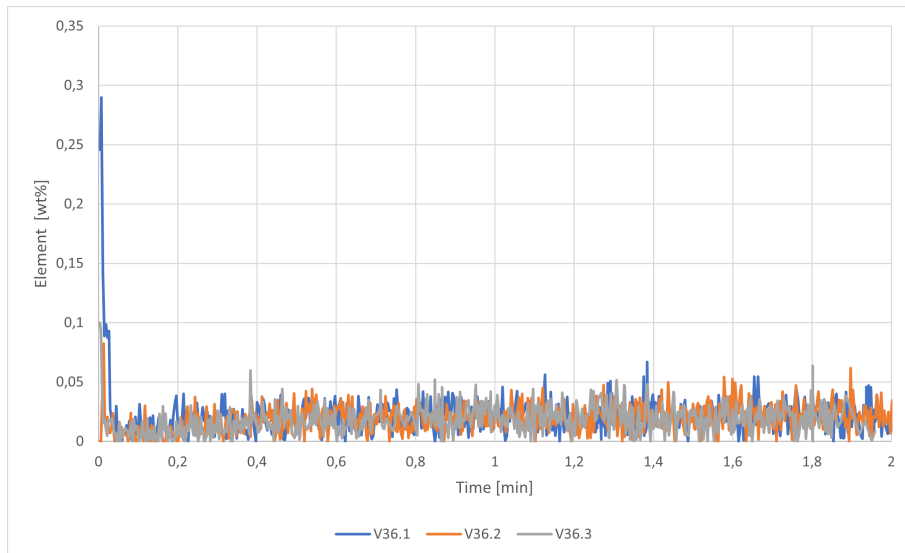


Figure 51: Sample of V after 360 min.

---

Figure 52 shows the data from the analysis of the Al-sample taken after 19 hours and 20 minutes. The sample was analysed three times for 3 minutes. The graph shows a signal between 0-0.05 wt% V.

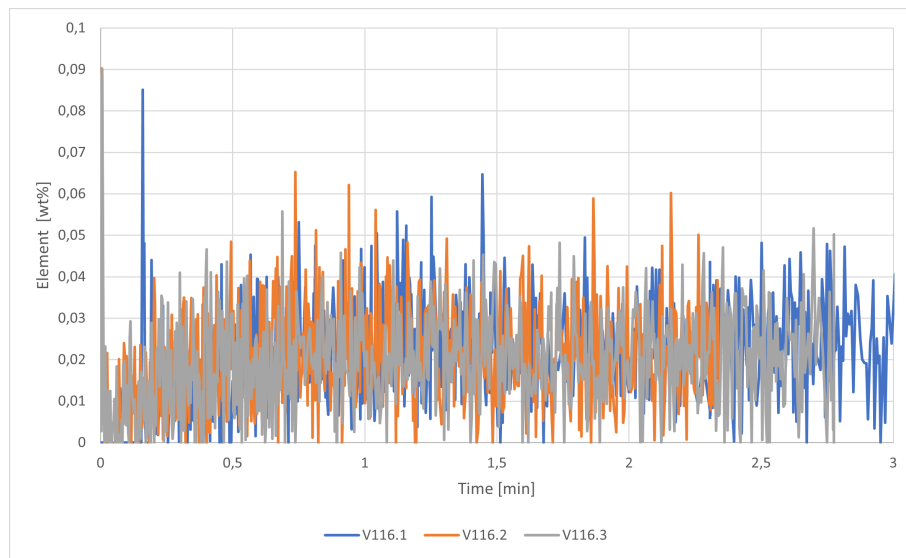


Figure 52: Sample of V after 1160 min.

Figure 53 shows the data from the analysis of the Al-sample taken after 22 hours. The sample was analysed four three for 3 minutes. The graph shows a stable signal between 0-0.05 wt% V, with peaks at 0 minutes. V132.1 shows a higher signal at 0-0.5 minutes in comparison to the other graphs.

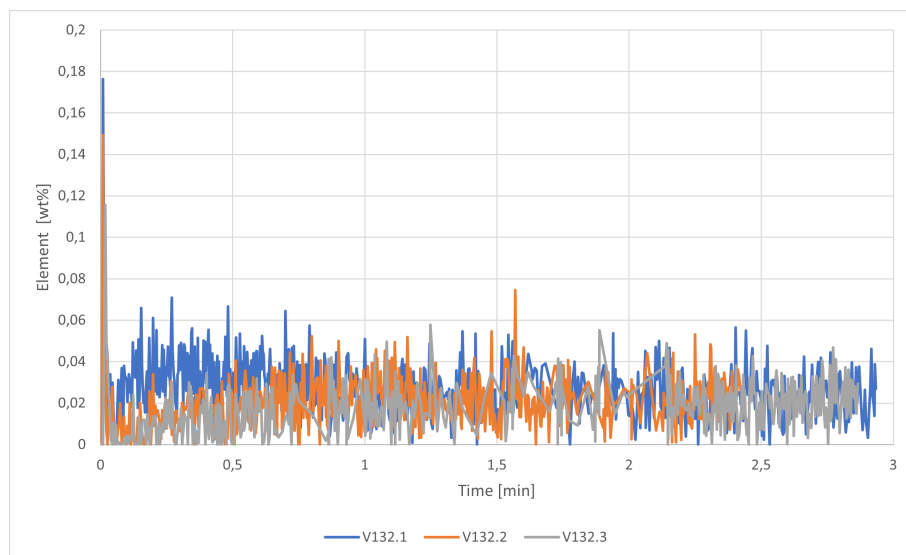


Figure 53: Sample of V after 1320 min.

---

#### 4.2.4 GD-OES-data from V-trial with AlSi7-alloy

Figure 54 shows the data from the analysis of the AlSi7-sample taken at the beginning of the trial. The sample was analysed four times for 3.5 minutes. The graph shows a signal between 0-0.04 wt% V. The graphs have a peak at 0 minutes.

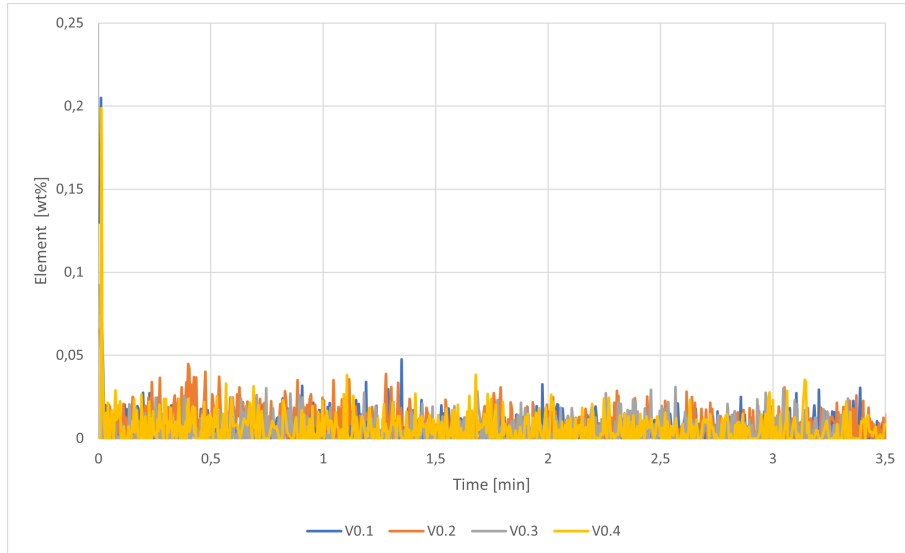


Figure 54: Reference AlSi7-sample before addition of V.

Figure 55 shows the data from the sample taken after 20 minutes. The sample was analysed three times for 4 minutes. The graph shows a signal between 0-0.05 wt% V. V2.1 have a peak at 0 minutes, and V2.2 have a peak at 2.7 minutes.

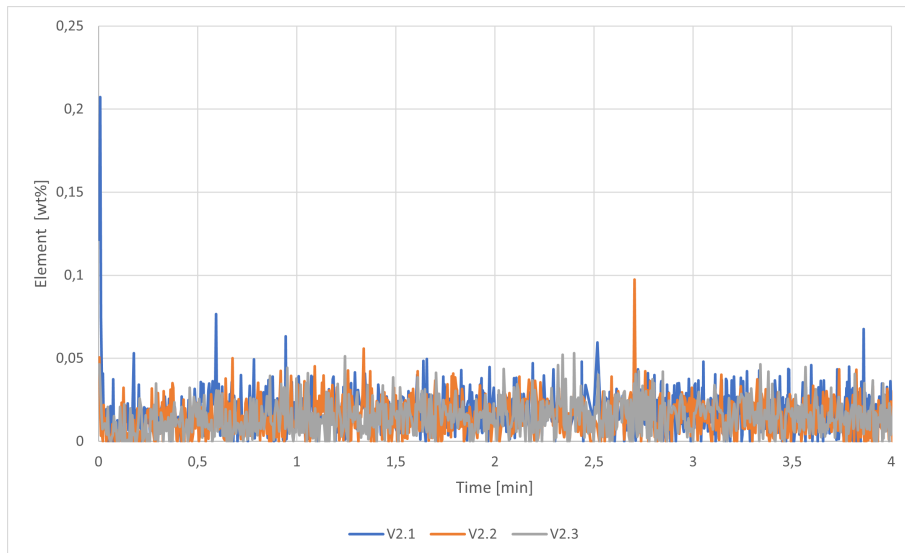


Figure 55: Sample of V after 20 min.

---

Figure 56 shows the data from the sample taken after 1 hour. The sample was analysed three times for 3.5 minutes. The graphs shows a signal between 0-0.05 wt% V, and have peaks at 0 minutes.

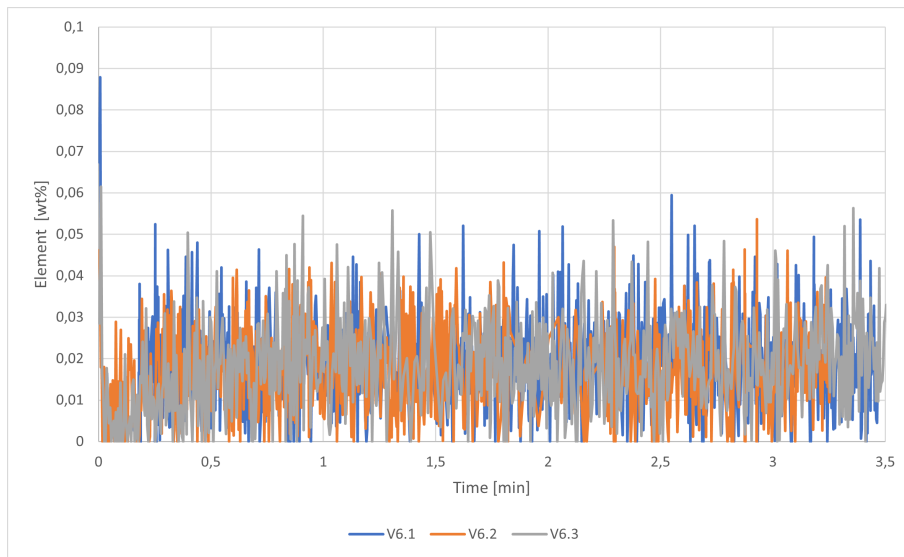


Figure 56: Sample of V after 60 min.

Figure 57 shows the data from the sample taken after 2 hours. The sample was analysed three times for 3.5 minutes. The graphs have peaks at the beginning, and shows a signal between 0-0.04 wt% V.

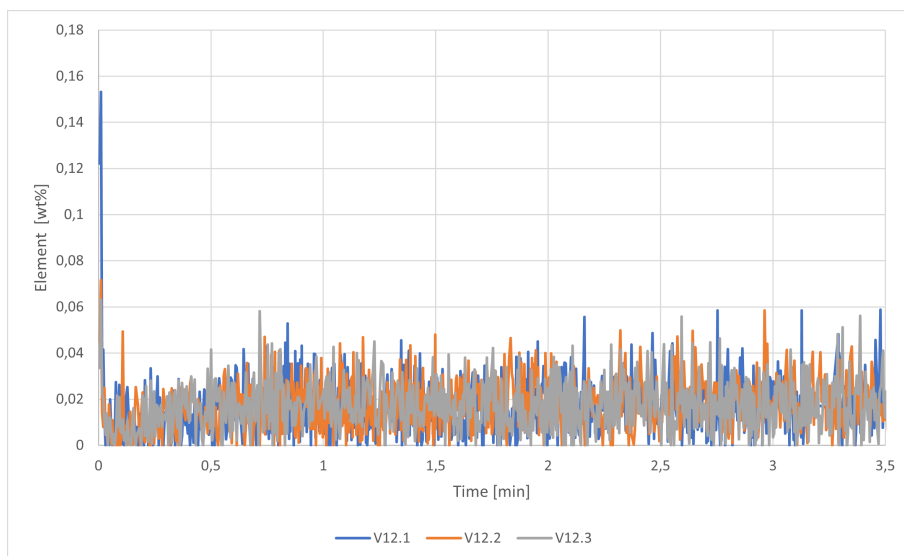


Figure 57: Sample of V after 120 min.

---

Figure 58 shows the data from the AlSi7-sample taken at 4 hours. The sample was analysed three times for 3.5 minutes. The graphs shows a signal between 0-0.04 wt% V, with peaks at 0 and 2.8 minutes.

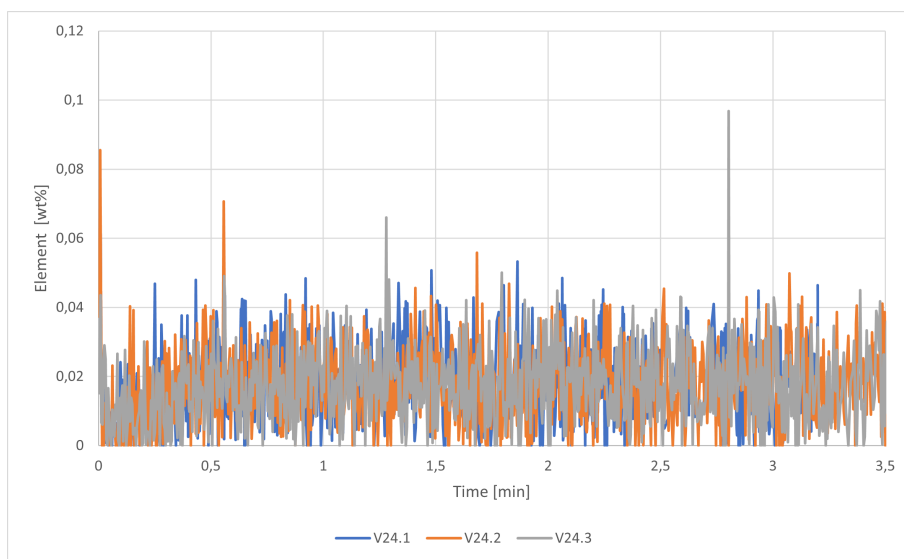


Figure 58: Sample of V after 240 min.

---

#### 4.2.5 GD-OES-data from 1h Ni-trial

Figure 59 is showing data from the GD-OES-analysis of the Al-sample taken at 10 minutes, for the 1h Ni-trial. The sample was analysed in four parallels, for 3-4 minutes. The graph show peaks at the beginning of the analysis, and a stabilization at 1.5-4 minutes.

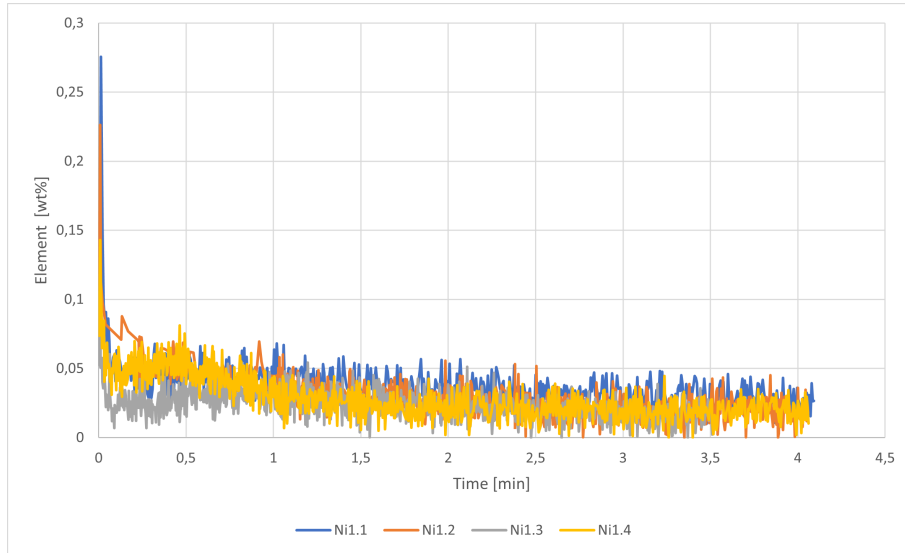


Figure 59: Sample of Ni after 10 min.

Figure 60 shows the data from the GD-OES-analysis of the Al-sample taken after 20 minutes. The sample was analysed four times for about 2 minutes. The graph show peaks at the beginning of the analysis, and a stabilization between 0-0.06 wt% Ni.

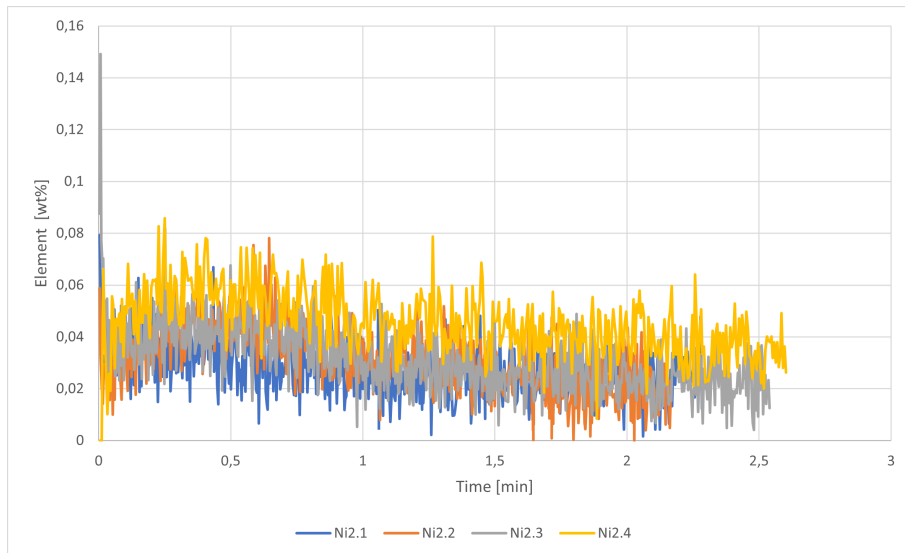


Figure 60: Sample of Ni after 20 min.

---

Figure 61 is showing data from the GD-OES-analysis of the Al-sample with Ni taken at 30 minutes. The sample was analysed in four parallels, for 4 minutes. The graph show peaks at the beginning of the analysis. The graph increases at the start of the analysis, decreases, and stabilizes at 1.5-4 minutes.

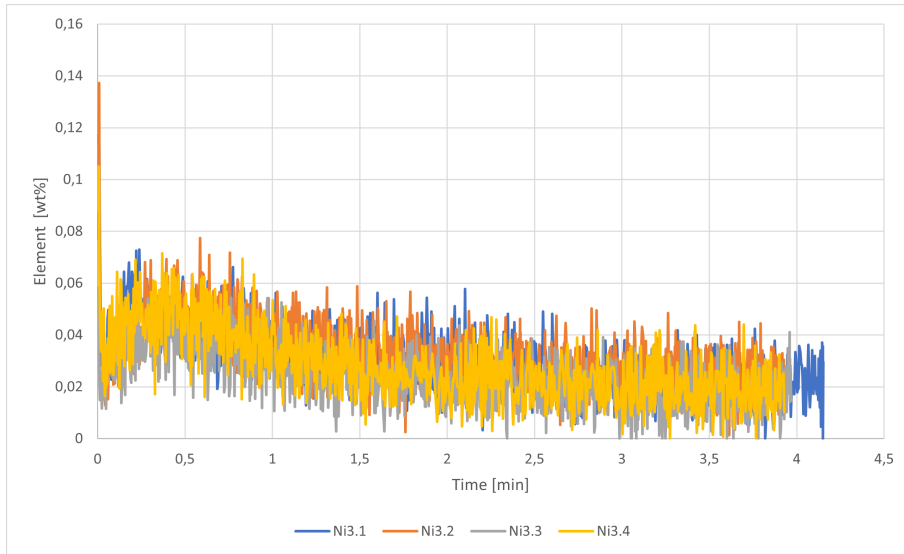


Figure 61: Sample of Ni after 30 min.

Figure 62 shows the results from the Nickel-sample taken 40 minutes into the 1 hour trial. The sample was in total analysed four times for about 4 minutes. The graph shows a stable signal between 0-0.06 wt% Ni, with peaks at the beginning of the graph.

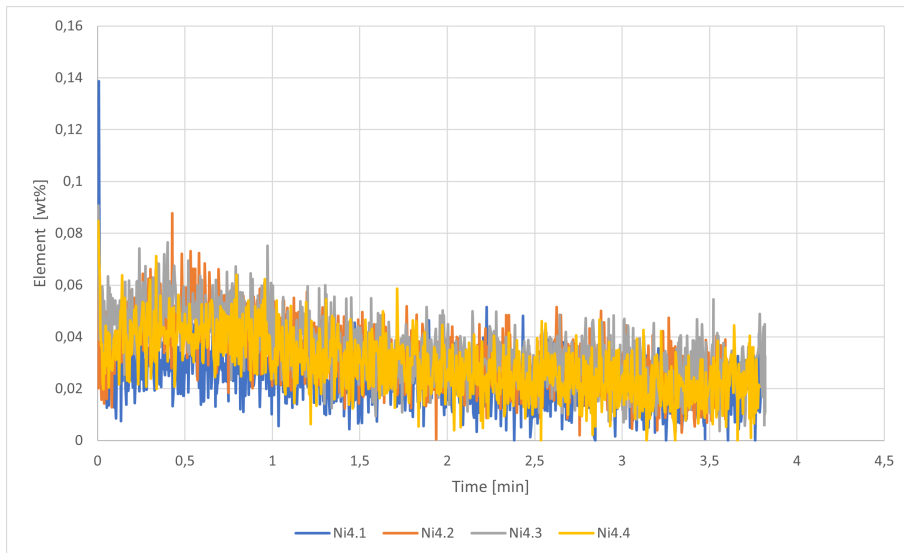


Figure 62: Sample of Ni after 40 min.



---

Figure 63 shows the data from the GD-OES-analysis of the Al-sample taken after 50 minutes. The sample was analysed three times for about 2.5 minutes. The graph show peaks at the beginning of the analysis. The graph increases at the start of the analysis, decreases, and stabilizes after 1.5 minutes, between 0-0.04 wt% Ni.

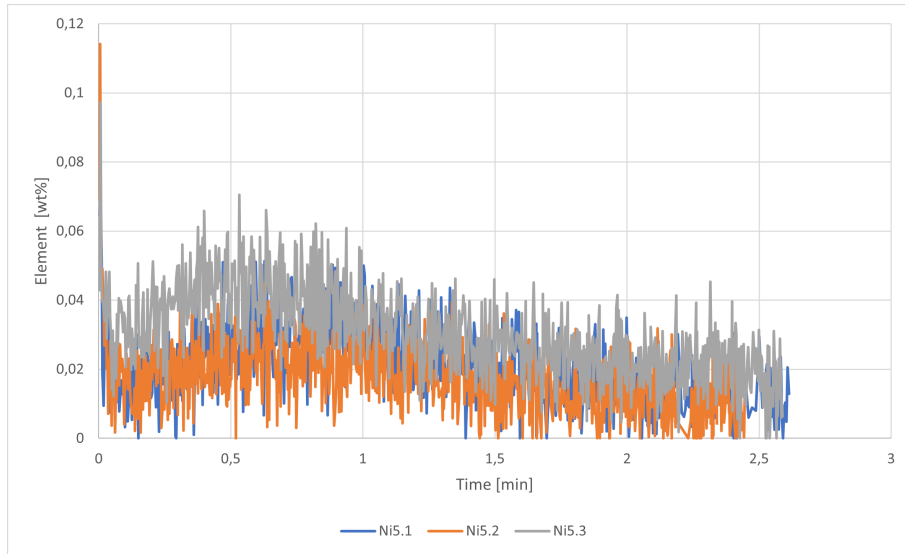


Figure 63: Sample of Ni after 50 min.

Figure 64 shows the results from the Nickel-sample taken at the end of the 1 hour trial. The sample was in total analysed four times for about 3 minutes. The graph shows a stable signal between 0-0.06 wt% Ni, with peaks at the beginning of the graph.

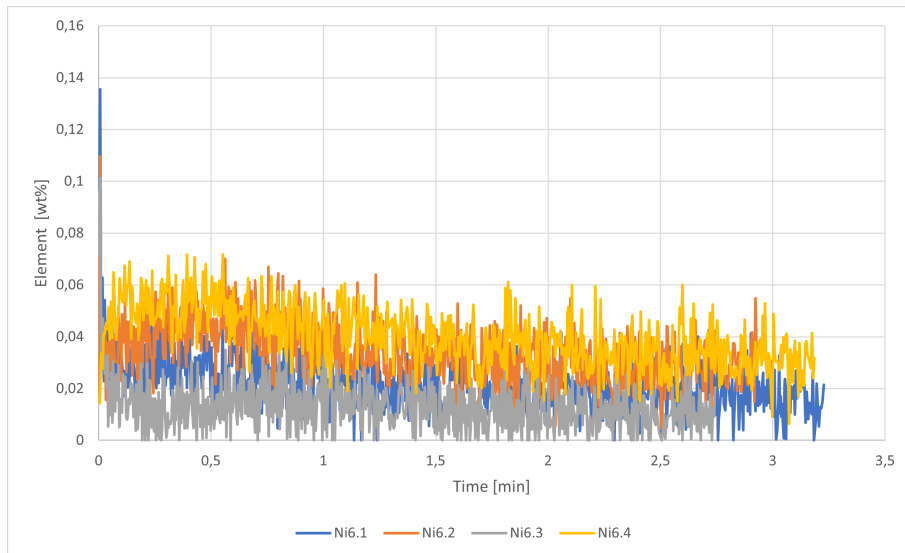


Figure 64: Sample of Ni after 60 min.

---

#### 4.2.6 GD-OES-data from 2h Ni-trial

Figure 65 shows the data from the analysis of the sample taken at the beginning of the 2h Ni-trial. The graph peaks at the beginning, and decreases to a signal around 0 wt% Ni. The sample was analysed three times for 2-3 minutes.

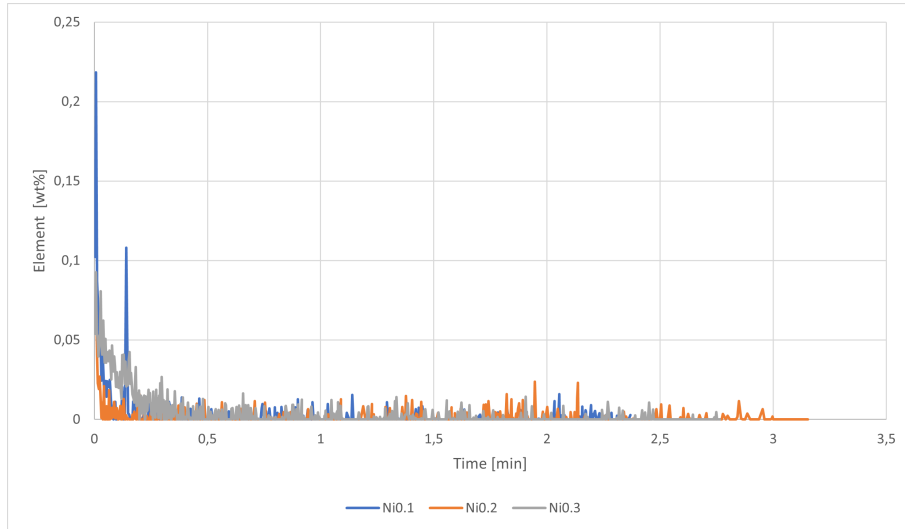


Figure 65: Reference Al-sample before addition of Ni.

Figure 66 shows the results from the analysis of the sample taken at 5 minutes. The sample was in total analysed four times for 2.5 minutes. The graph shows a signal between 0.01-0.06 wt% V, with peaks at the beginning. Ni0.5.4 gives the highest signal, followed by Ni0.5.1, Ni0.5.3 and Ni0.5.2.

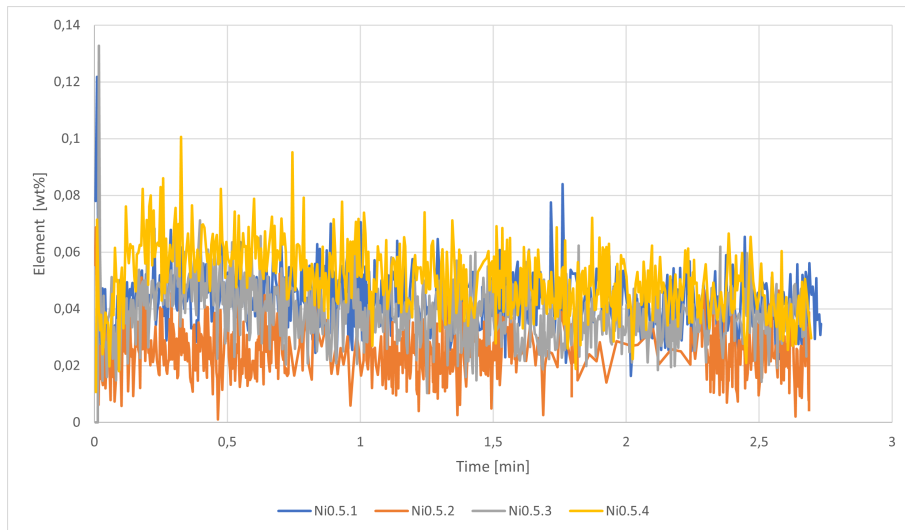


Figure 66: Sample of Ni after 5 min.

---

Figure 67 shows the results from the analysis of the Nickel-sample taken after 10 minutes. The sample was analysed four times for 3 minutes. The graph increases at the start of the analysis, decreases, and stabilizes at 1.5 minutes, with values between 0.02-0.06 wt% Ni. The graphs have peaks at 0 minutes.

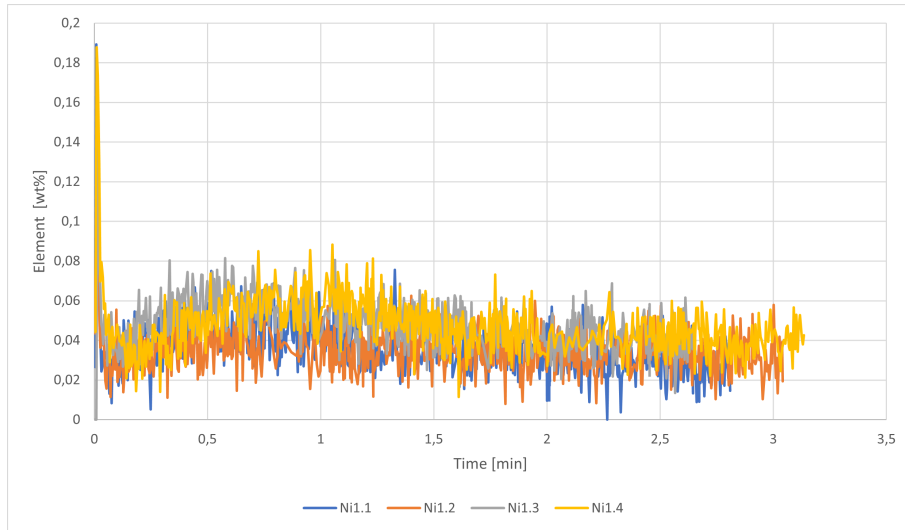


Figure 67: Sample of Ni after 10 min.

Figure 68 shows the data from the analysis of the sample taken at 20 minutes. The sample was analysed four times, for 3.5 minutes. The graph peaks at the start, and stabilizes after 2 minutes with a signal of 0.01-0.05 wt% Ni.

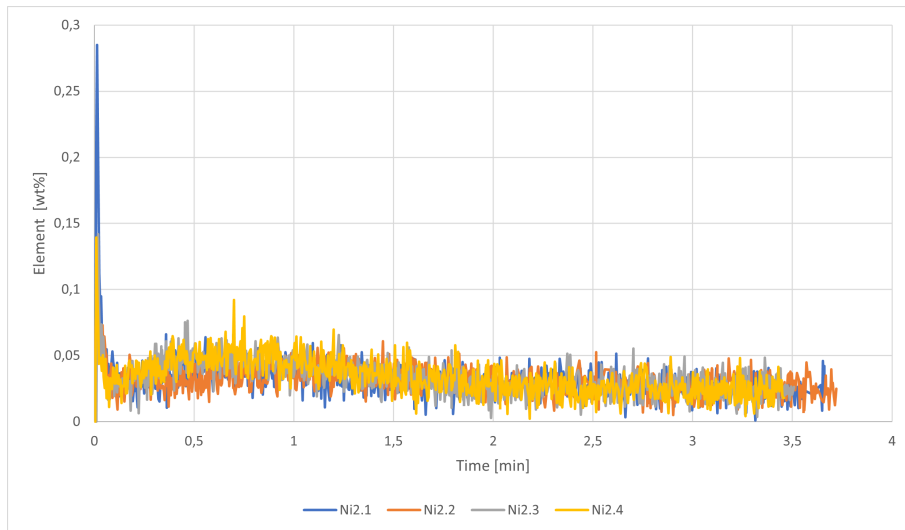


Figure 68: Sample of Ni after 20 min.

---

Figure 69 shows the data from the analysis of the sample taken 40 minutes into the trial. The graph peaks at the beginning, and stabilizes at 0.01-0.05 wt% Ni. The sample was analysed three times for 4 minutes.

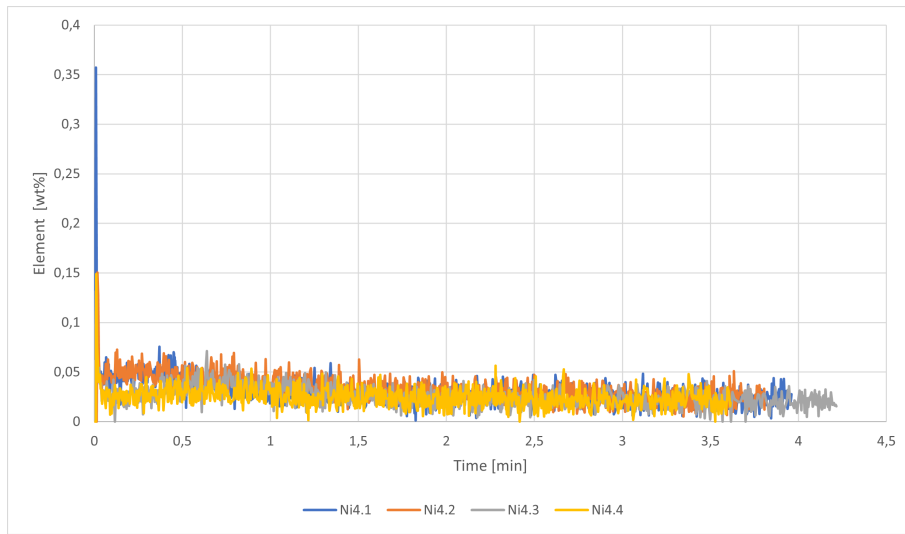


Figure 69: Sample of Ni after 40 min.

Figure 70 shows the results from the analysis of the sample taken at 1 hour. The sample was in total analysed four times for 2 minutes. The graph shows a signal between 0-0.08 wt% Ni, with peaks at the beginning. Ni6.1 gives the highest signal, followed by Ni6.2, Ni6.4 and Ni6.3.

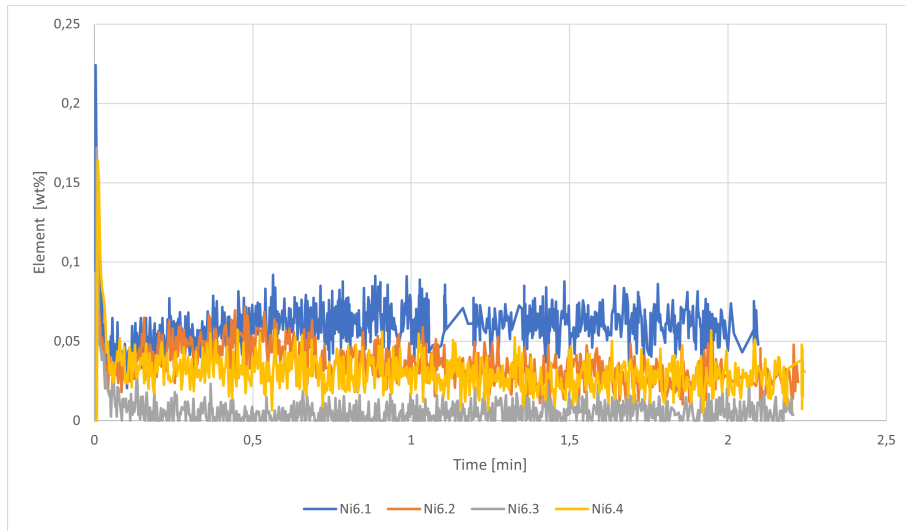


Figure 70: Sample of Ni after 60 min.

---

Figure 71 shows the results from the analysis of the sample taken at 80 minutes. The sample was in total analysed four times for 3 minutes. The graph shows a signal between 0-0.06 wt% Ni, with peaks at the beginning. Ni8.4 gives a slight higher signal in comparison to the other graphs.

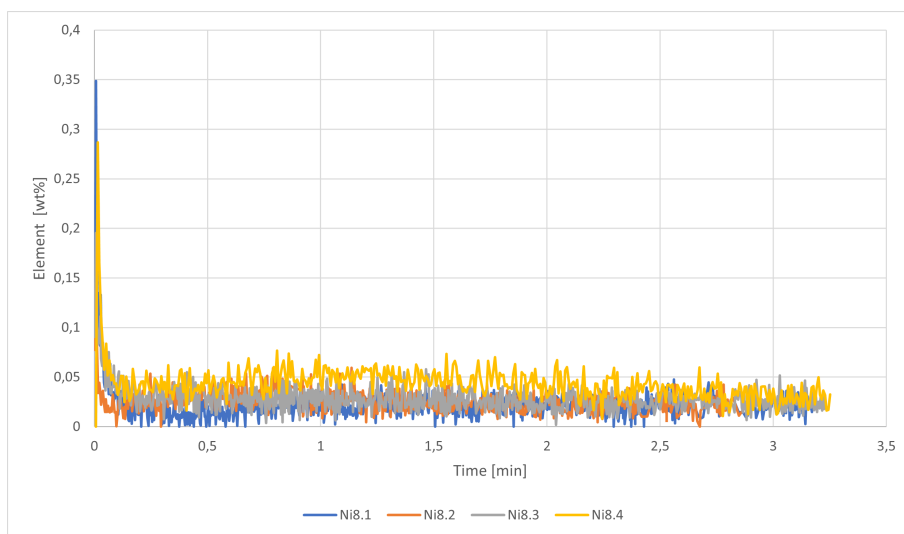


Figure 71: Sample of Ni after 80 min.

Figure 72 shows the results from the analysis of the sample taken after 100 minutes. The sample was in total analysed four times for 2 minutes. The graph shows a signal between 0-0.06 wt% Ni, with peaks at the beginning. Ni10.2 gives the highest signal, followed by Ni10.3, Ni10.1 and Ni10.4.

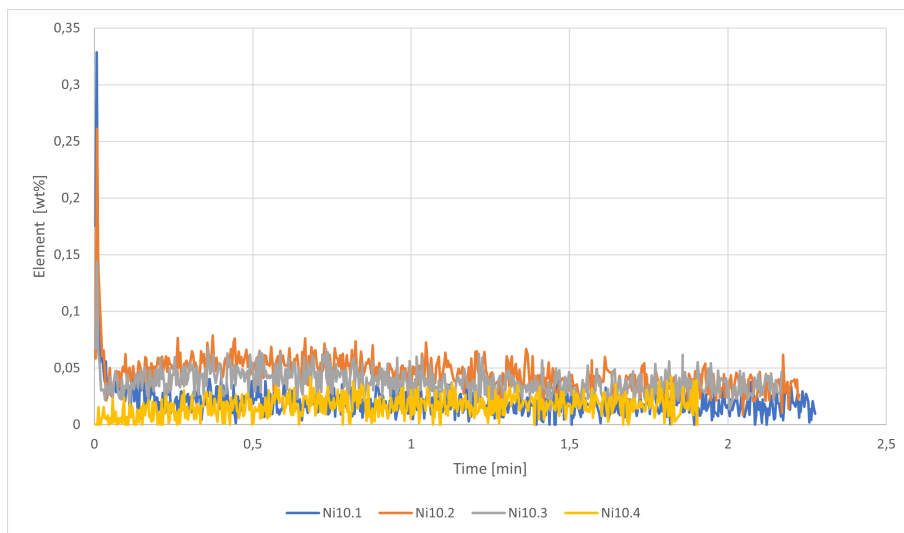


Figure 72: Sample of Ni after 100 min.

---

Figure 73 shows the results from the analysis of the sample taken at the end of the trial. The sample was in total analysed four times for 3.5 minutes. The graph shows a signal between 0-0.06 wt% Ni, with peaks at the beginning. The graph increases in the beginning, decreases, and stabilizes at 1 minute. Ni12.2 gives a lower signal in comparison to Ni12.1, Ni12.3 and Ni12.4.

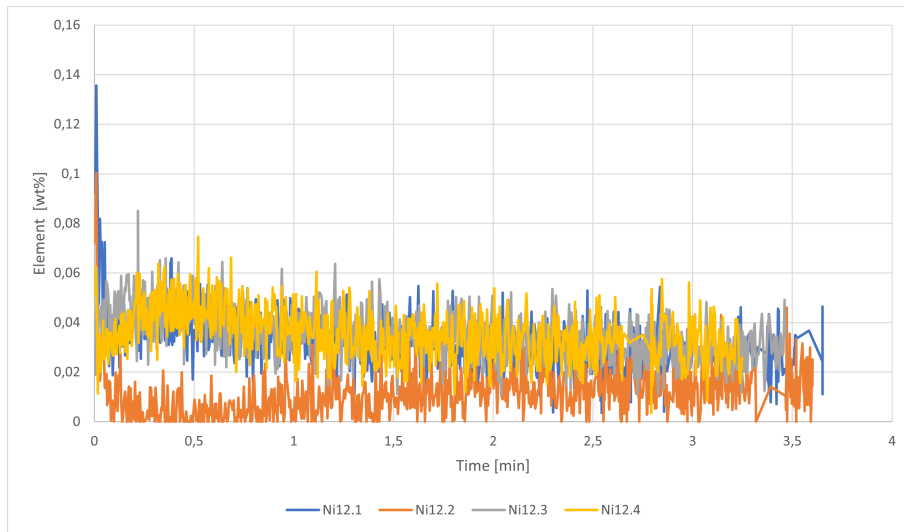


Figure 73: Sample of Ni after 120 min.

---

#### 4.2.7 GD-OES-data from 20h Ni-trial

Figure 74 shows the data from the analysis of the Al-sample taken at the start of the trial. The sample was analysed three times for 2.5 minutes. The graph shows a signal between 0-0.01 wt% Ni, with peaks at 0 minutes.

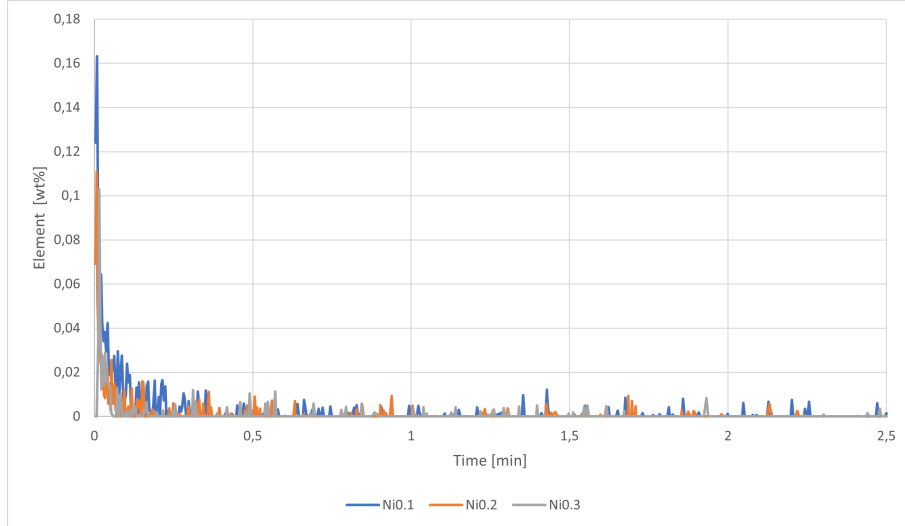


Figure 74: Reference Al-sample before addition of Ni.

Figure 75 shows the data from the analysis of the Al-sample taken after 6 hours. The sample was analysed three times for 2 minutes. The graph shows a stable signal between 0.01-0.05 wt% Ni, with peaks at 0 minutes.

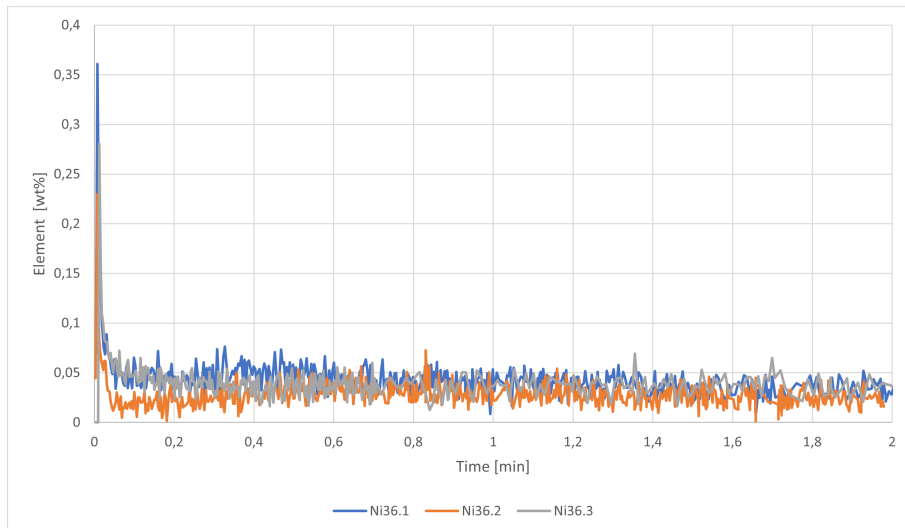


Figure 75: Sample of Ni after 360 min.

---

Figure 76 shows the data from the analysis of the Al-sample taken 18 hours into the trial. The sample was analysed three times for 3 minutes. The graph shows a stable signal between 0.01-0.05 wt% Ni, with peaks at the beginning of the graph.

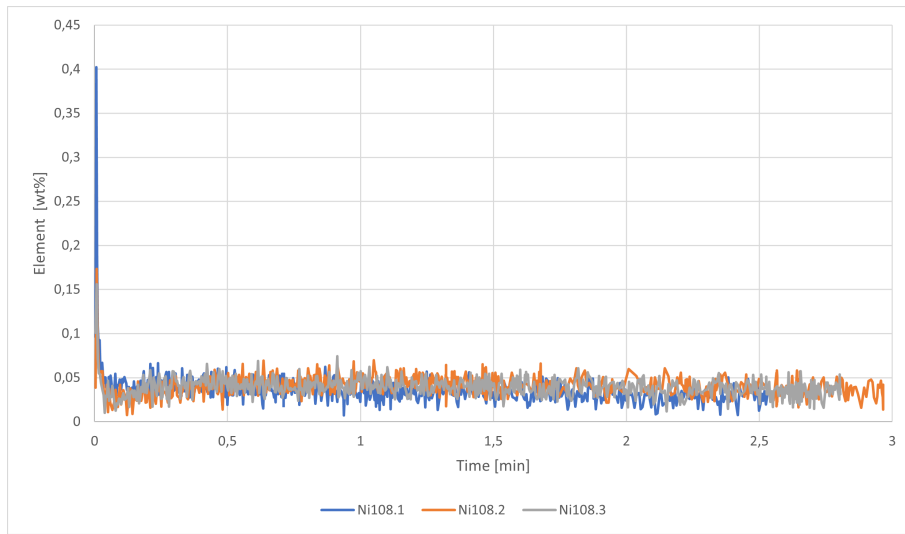


Figure 76: Sample of Ni after 1080 min.

Figure 77 shows the data from the analysis of the Al-sample taken after 20 hours. The sample was analysed three times for 2.5 minutes. The graph shows a stable signal between 0.01-0.05 wt% Ni, with peaks at 0 minutes.

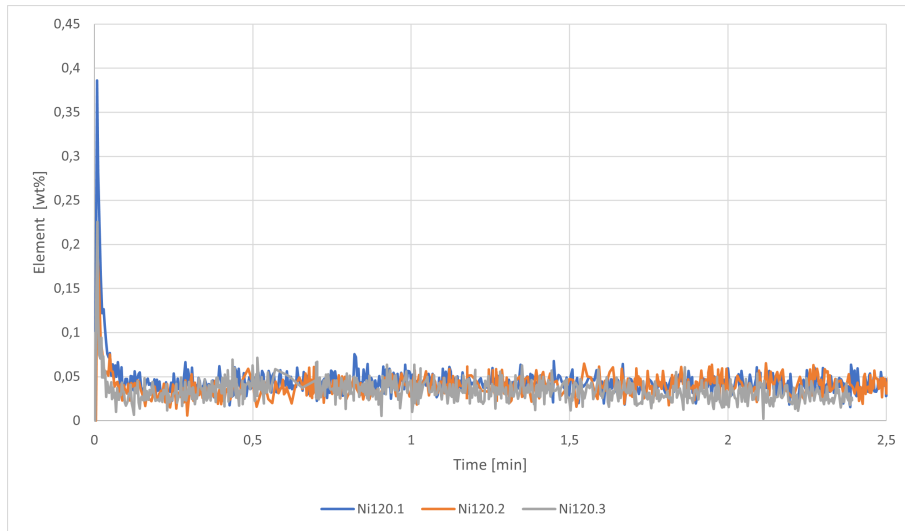


Figure 77: Sample of Ni after 1200 min.



---

#### 4.2.8 GD-OES-data from Ni-trial with AlSi7-alloy

Figure 78 shows the data from the sample taken at the start of the Ni-trial with the alloy. The sample was analysed three times for 3 minutes. The graph shows a signal the first 0.4 minutes of the analysis. The rest of the analysis have a signal of 0 wt% Ni, except for some Ni0.2-peaks.

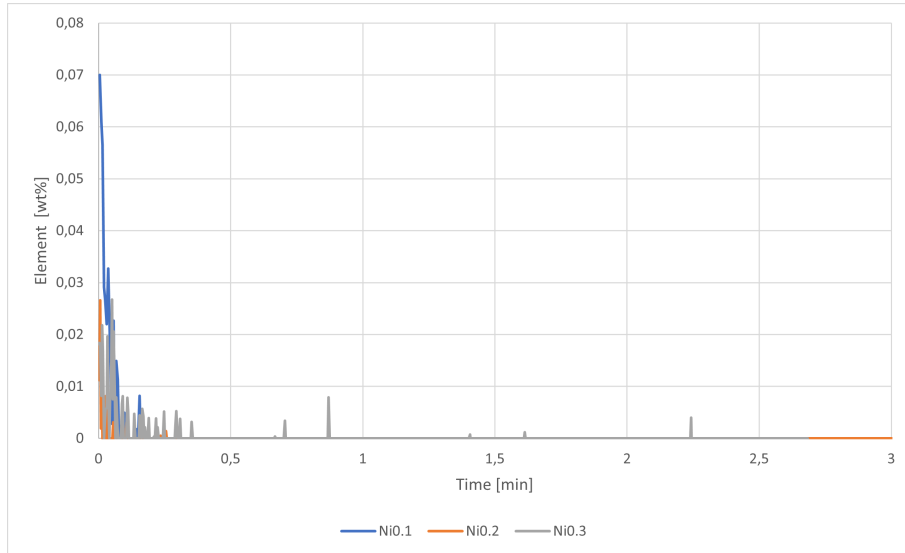


Figure 78: Reference AlSi7-sample before addition of Ni.

Figure 79 shows the data from the sample taken after 40 minutes. The sample was analysed one time for 5 minutes. The graph shows a decreasing signal, where the highest measured value was 0.07 wt% Ni and the lowest was 0 wt% Ni.

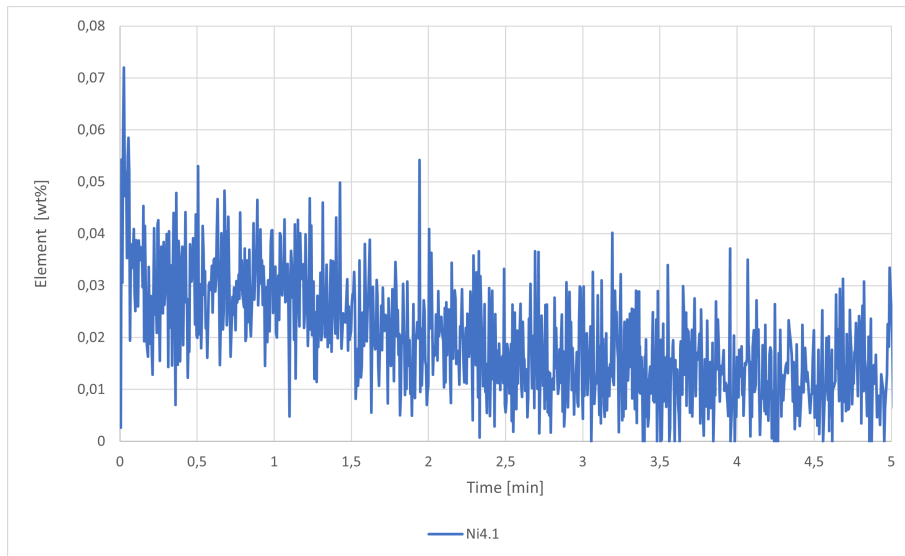


Figure 79: Sample of Ni after 40 min.

---

Figure 80 shows the data from the sample taken after 1 hour. The sample was analysed three times for 2.5 minutes. The graph shows a signal between 0-0.07 wt% Ni. Ni6.3 have the highest signal, followed by Ni6.1 and Ni6.2.

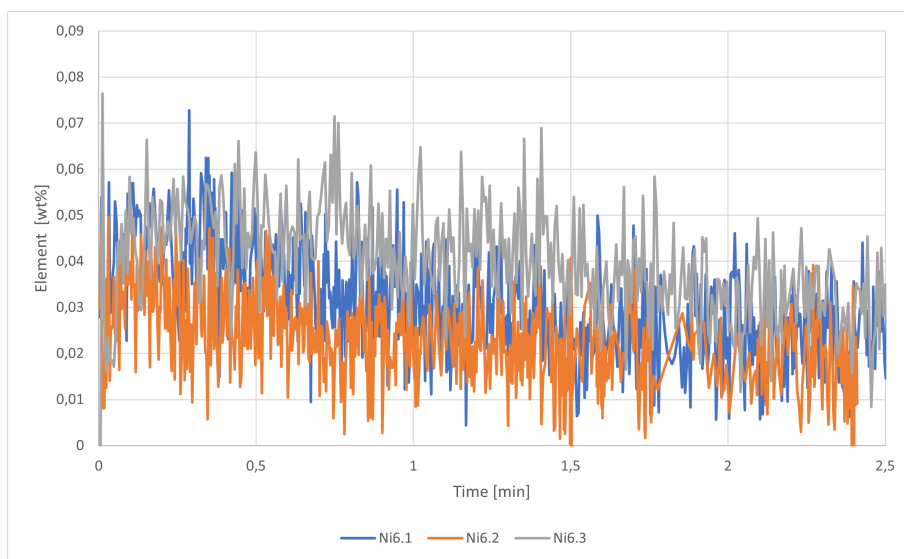


Figure 80: Sample of Ni after 60 min.

---

#### 4.2.9 GD-OES-data from 1h Sr-trial

Figure 81 shows the data from the analysis of the Al-sample taken at the start of the trial. The sample was analysed four times for 3.5 minutes. The graph is stable with signal between 0-0.003 wt% Sr, with peaks at 0 and at 1.5 minutes. Sr0.1 shows a higher signal in comparison to the other graphs.

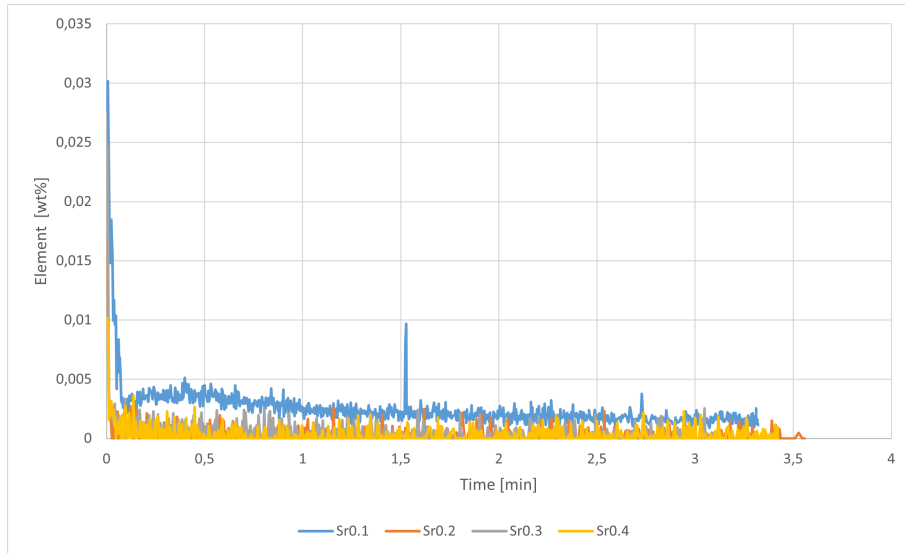


Figure 81: Reference Al-sample before addition of Sr.

Figure 82 shows the data from the sample taken at 10 minutes. The sample was analysed three times for about 1 minute. The graph marked as Sr1.1 gives higher signal (0.04-0.06 wt% Sr) than Sr1.2 and Sr1.3 (0-0.01 wt% Sr).

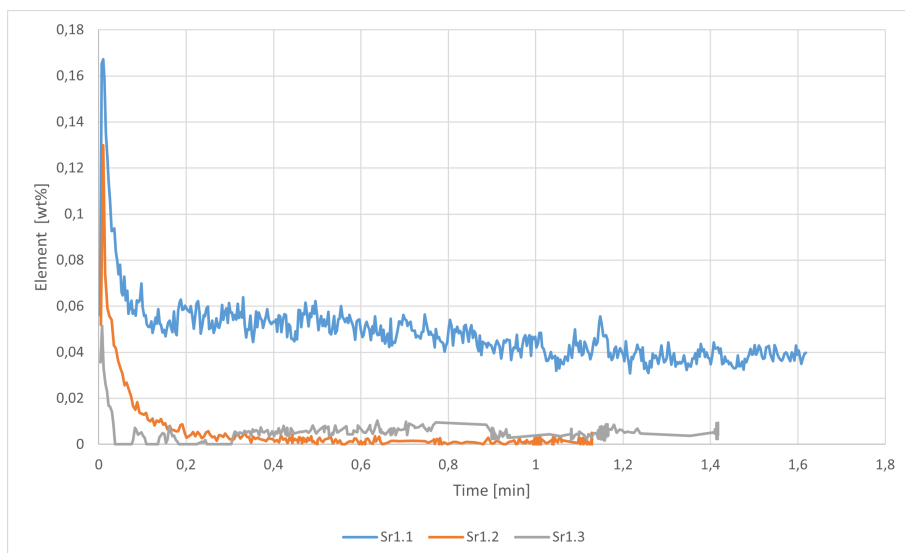


Figure 82: Sample of Sr after 10 min.

---

Figure 83 shows the data from the GD-OES-analysis of the Al-sample taken after 20 minutes. The sample was analysed four times for 4 minutes. The graphs increases from 0.005 wt% Sr at the beginning and stabilizes at 0.02-0.03 wt% Sr, except Sr2.4, which stabilizes around 0.015 wt% Sr.

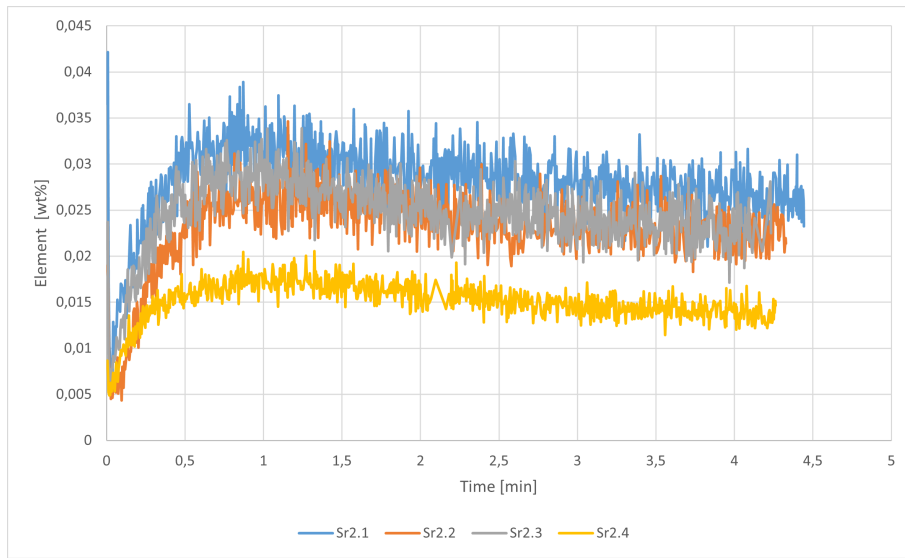


Figure 83: Sample of Sr after 20 min.

Figure 84 shows the data from the sample taken after 30 minutes. The sample was analysed four times for 3-4 minutes. The graph increases at the beginning of the graph and stabilizes at around 0.025 wt% Sr, except for Sr3.3, which stabilizes around 0.013 wt% Sr. Sr3.1 has a peak at 4 minutes.

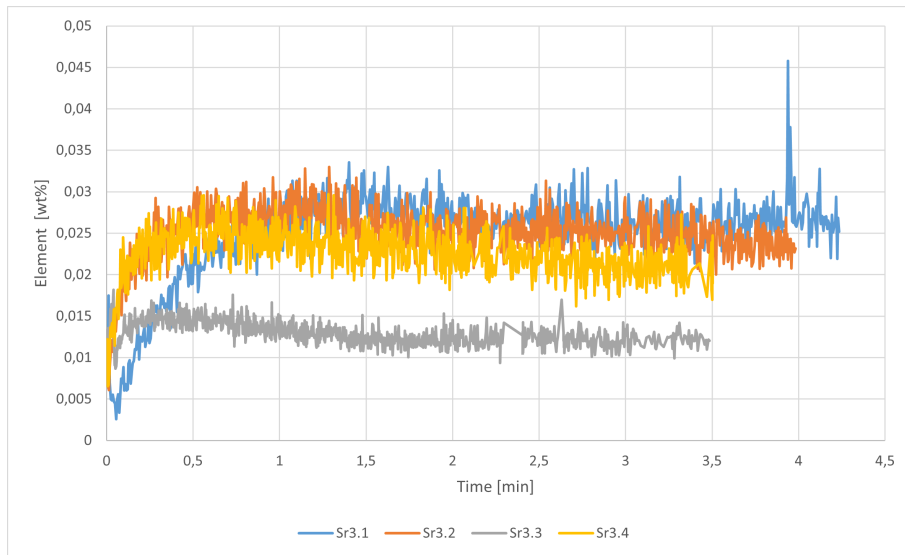


Figure 84: Sample of Sr after 30 min.

---

Figure 85 shows the GD-OES-data from the sample taken after 40 minutes. The sample was analysed four times for about 3 minutes. The graph increases in the beginning, decreases, and stabilizes at 0.02 wt% Sr. Sr3.1 shows a higher signal in comparison to the other graphs, while Sr4.4 shows a lower signal. Sr4.1 has a peak at 2.5 minutes.

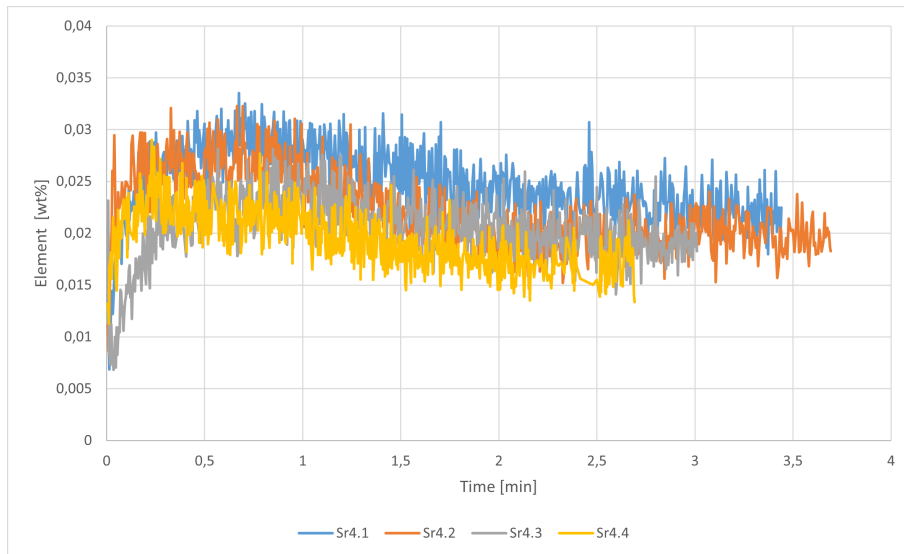


Figure 85: Sample of Sr after 40 min.

Figure 86 shows the data from the GD-OES-analysis of the Al-sample taken at 50 minutes. The sample was analysed four times for 3.5 minutes. The graph increases at the beginning of the graph and stabilizes after 1 minute. Sr5.4 gives the highest signal, followed by Sr5.1, Sr5.2 and lastly Sr5.3. The signals ranges from 0.01-0.025 wt% Sr.

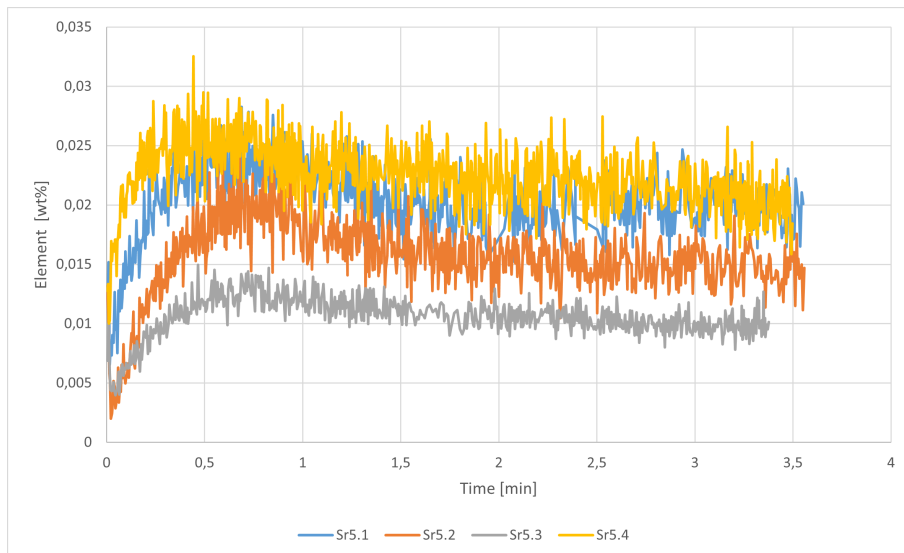


Figure 86: Sample of Sr after 50 min.

---

Figure 87 shows the data from the sample taken at the end of the trial. The sample was analysed four times for 3 minutes. The graph increases at the beginning of the analysis and stabilizes at around 0.015 wt% Sr. The graph has a peak at 0 minutes.

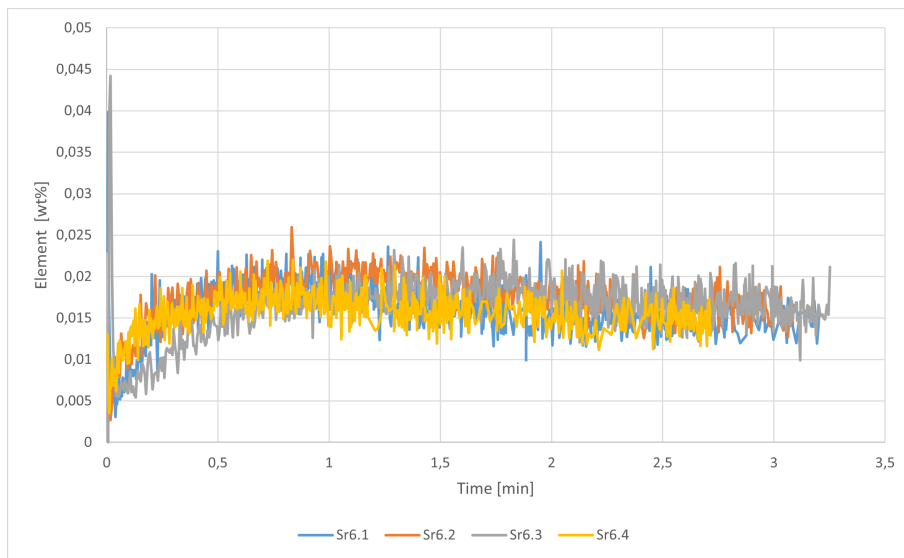


Figure 87: Sample of Sr after 60 min.

---

#### 4.2.10 GD-OES-data from 2h Sr-trial

Figure 88 shows the data from the analysis of the Al-sample taken at the start of the trial. The sample was analysed four times for 3 minutes. The graph shows a stable signal between 0-0.003 wt% Sr, with peaks at 0 minutes. Sr0.4 shows a higher signal in comparison to the other graphs.

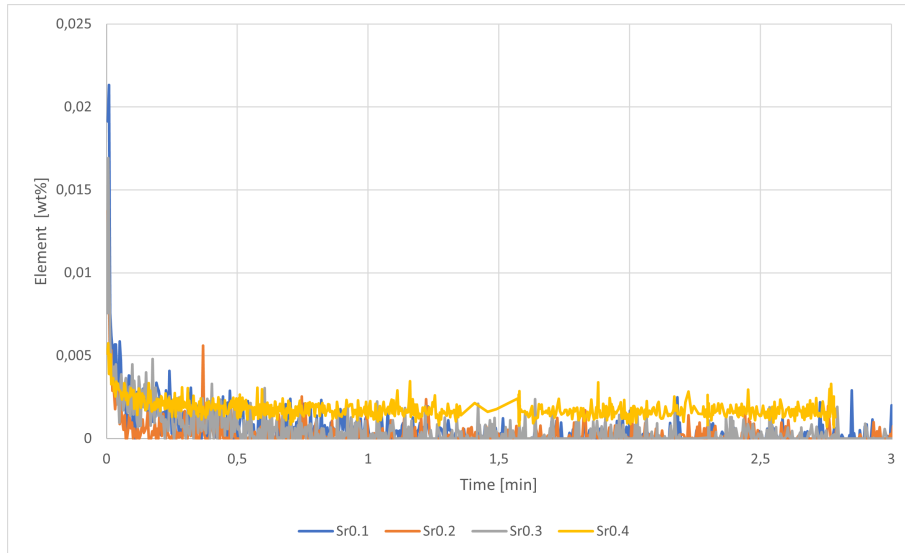


Figure 88: Reference Al-sample before addition of Sr.

Figure 89 shows the data from the Al-sample taken after 5 minutes. The sample was analysed four times for 3 minutes. The graph peaks at 0 minutes, and increases from 0.005 wt% Sr at 0.1 minutes, to 0.01-0.03 wt% Sr after 1 minute. Sr0.5.4 shows a lower signal in comparison to the other graphs.

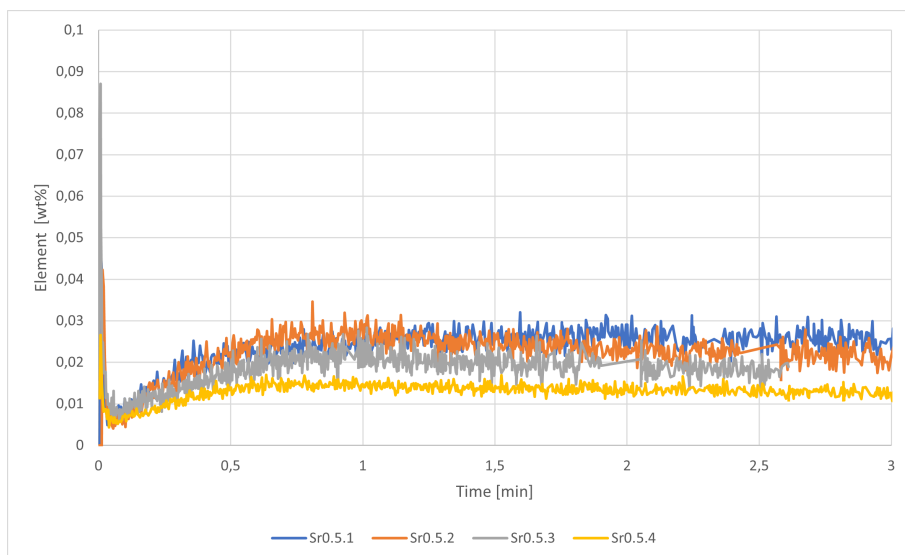


Figure 89: Sample of Sr after 5 min.

---

Figure 90 shows the data from the Al-sample taken at 10 minutes. The sample was analysed four times for 3 minutes. The graph peaks at 0 minutes, and increases from 0.005 wt% Sr at 0.1 minutes, to 0.01-0.03 wt% Sr after 1 minute. Sr1.2 shows a lower signal in comparison to the other graphs.

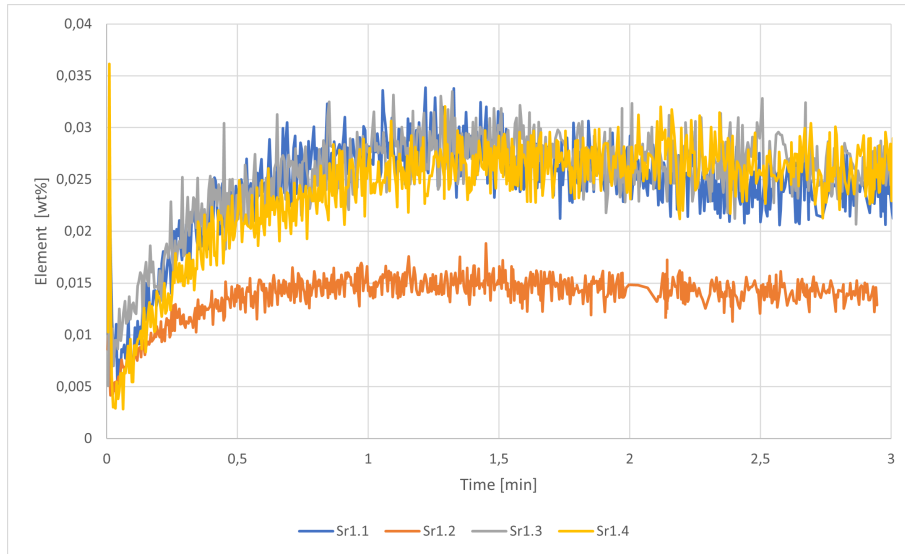


Figure 90: Sample of Sr after 10 min.

Figure 91 shows the data from the sample taken 20 minutes into the trial. The sample was analysed four times for 3 minutes. The graph peaks at 0 minutes, and increases from 0.002 wt% Sr at 0.1 minutes, to 0.015-0.03 wt% Sr after 1 minute.

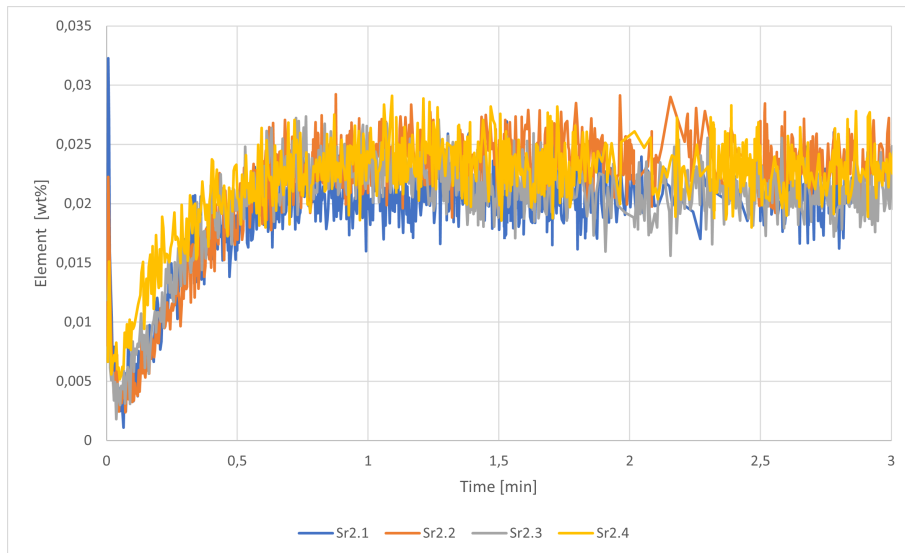


Figure 91: Sample of Sr after 20 min.



---

Figure 92 shows the data from the Al-sample taken at 40 minutes. The sample was analysed four times for 2.5 minutes. Sr4.1, Sr4.2 and Sr4.3 increases from 0.007 wt% Sr to 0.015-0.02 wt% Sr after 0.5 minutes. Sr4.1 have a peak at 0 minutes. Sr4.4 increases from a signal of 0 wt% Sr to 0.2 wt% Sr at 0 minutes, and shows a stable signal between 0.012-0.025 wt% Sr afterwards.

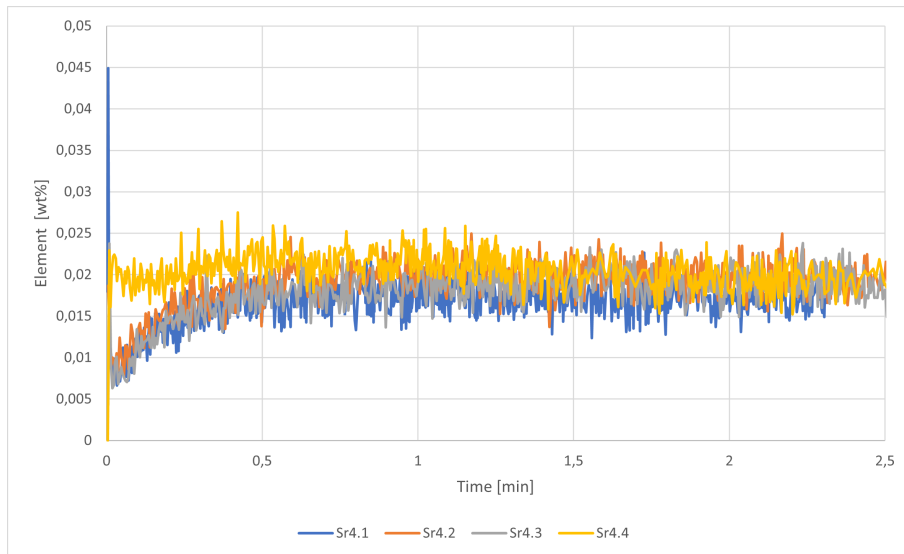


Figure 92: Sample of Sr after 40 min.

Figure 93 shows the data from the sample taken 1 hour into the trial. The sample was analysed four times for 2.5 minutes. Sr6.1, Sr6.3 and Sr6.4 peak at 0 minutes. Sr6.1, Sr6.2 and Sr6.4 increase from 0.005 wt% Sr at the beginning of the graph, to 0.01-0.02 wt% Sr after 0.5 minutes. Sr6.3 decreases, and stabilizes at values between 0.01-0.02.

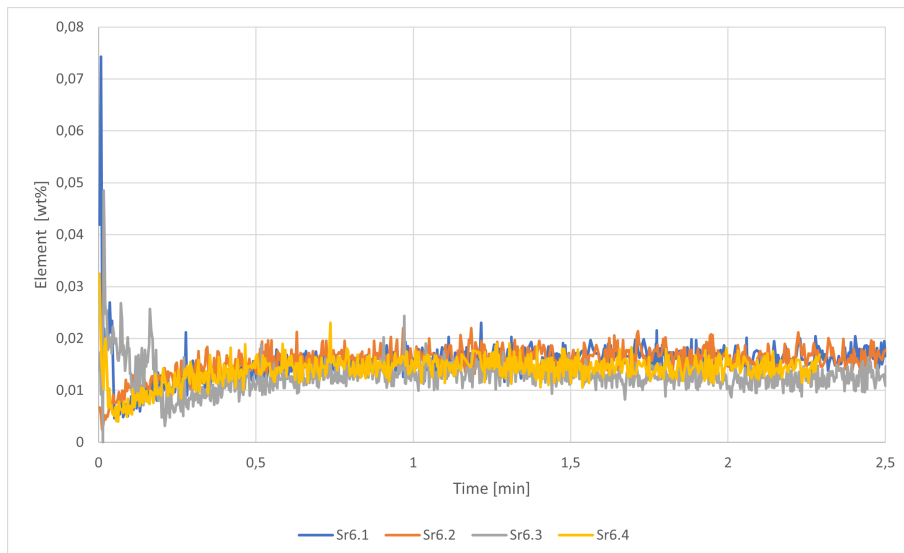


Figure 93: Sample of Sr after 60 min.

---

Figure 94 shows the data from the Al-sample taken at 80 minutes. The sample was analysed four times for 1.5 minutes. Sr8.1 and Sr8.2 have a peak at 0 minutes. The graphs show a signal between 0-0.02 wt% Sr. Sr8.4 have the highest signal, followed by Sr8.2, Sr8.1 and Sr8.3.

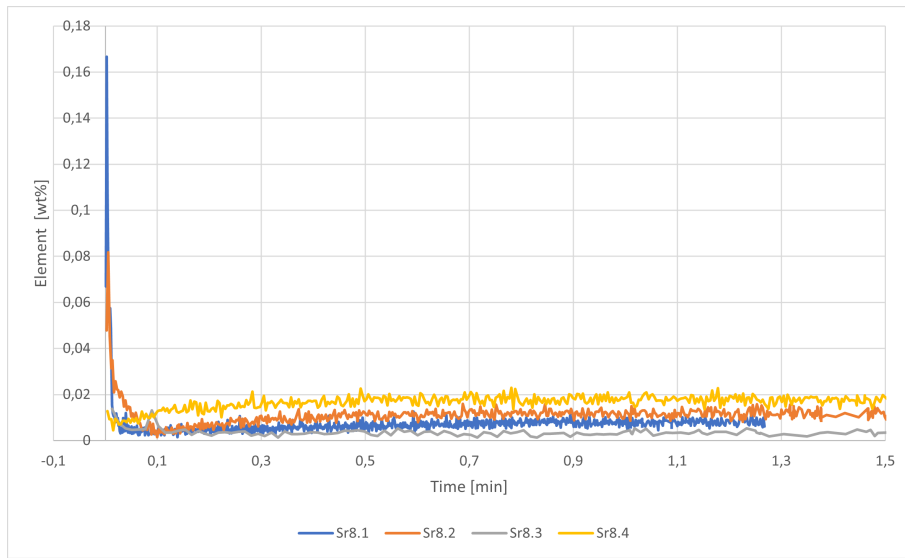


Figure 94: Sample of Sr after 80 min.

Figure 95 shows the data from the sample taken 100 minutes into the trial. The sample was analysed four times for 2 minutes. The graph peaks at 0 minutes, and increases from 0.002 wt% Sr, to 0.006-0.015 wt% Sr after 0.6 minutes.

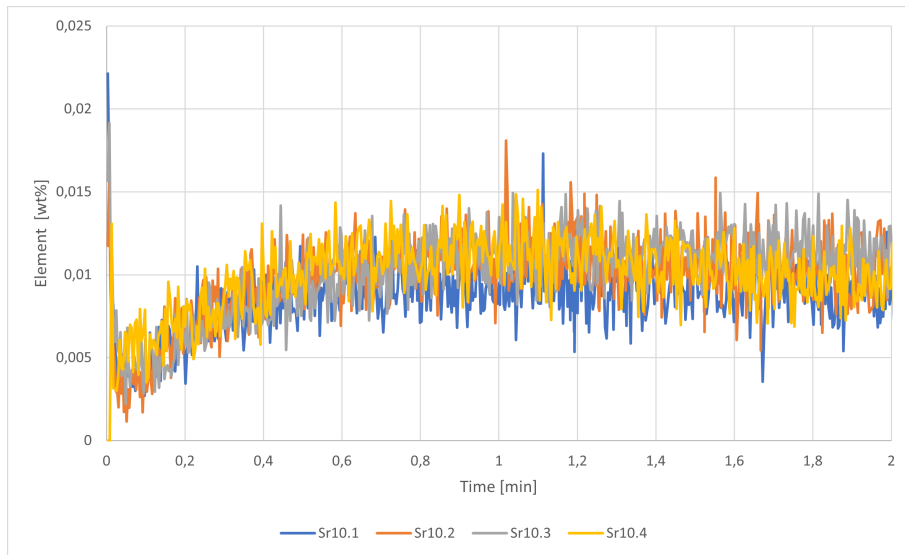


Figure 95: Sample of Sr after 100 min.

---

Figure 96 shows the data from the analysis of the Al-sample taken at the end of the trial. The sample was analysed four times for 3 minutes. The graph shows a stable signal between 0.005-0.01 wt% Sr, with peaks at 0 minutes.

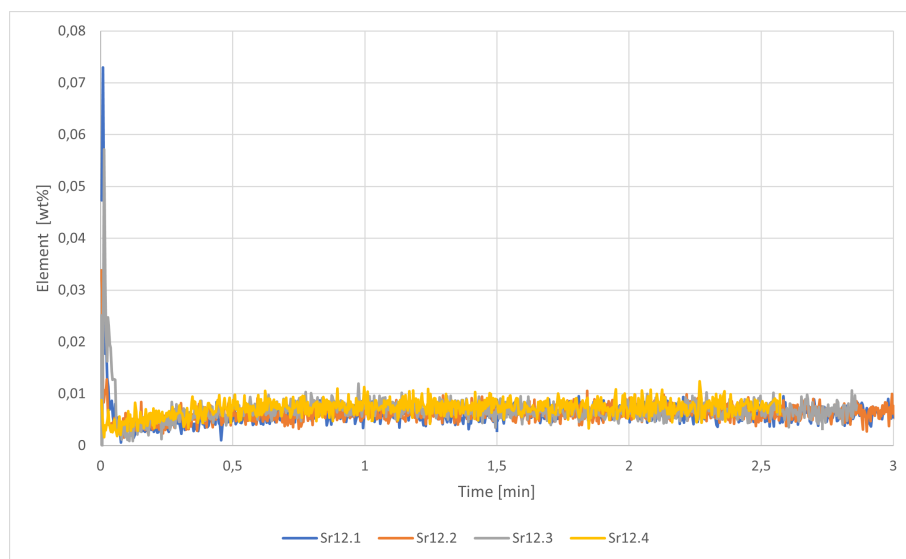


Figure 96: Sample of Sr after 120 min.

---

#### 4.2.11 GD-OES-data from 20h Sr-trial

Figure 97 shows the data from the analysis of the Al-sample taken at the start of the trial. The sample was analysed four times for 2.5 minutes. The graph shows a stable signal between 0-0.002 wt% Sr. Sr0.1 and Sr0.4 have a peak at 0 minutes.

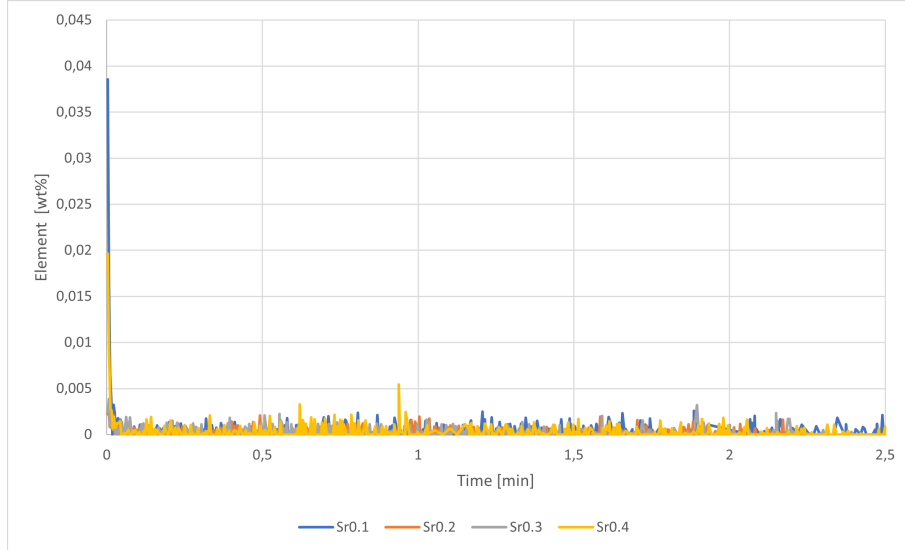


Figure 97: Reference Al-sample before addition of Sr.

Figure 98 shows the data from the analysis of the Al-sample taken after 10 minutes. The sample was analysed four times for 3 minutes. The graph increases from the beginning, to a stable signal between 0.015-0.025 wt% Sr after 0.5 minutes. Sr1.1 and Sr1.3 have a peak at 0 minutes.

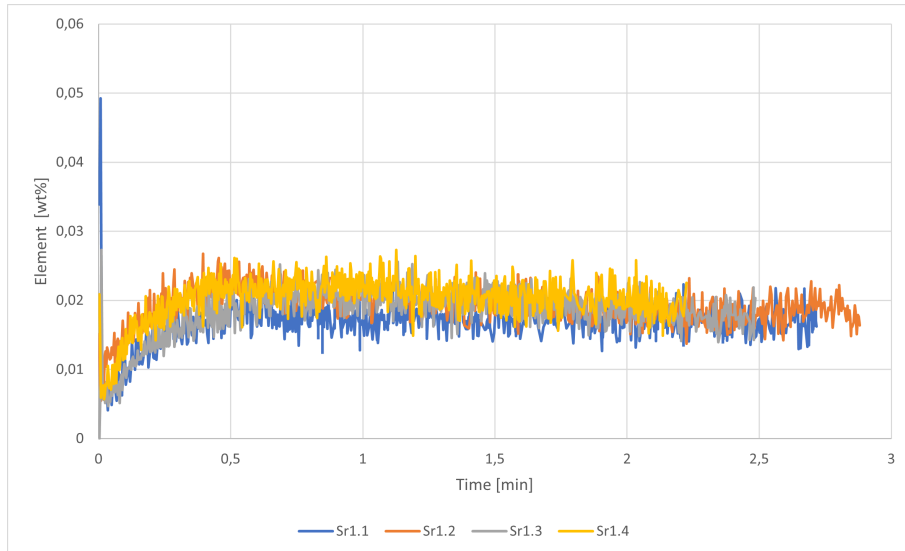


Figure 98: Sample of Sr after 10 min.

---

Figure 99 shows the data from the analysis of the Al-sample taken after 130 minutes. The sample was analysed four times for 2-3 minutes. The graph increases from the beginning, to a stable signal between 0.003-0.008 wt% Sr after 0.5 minutes. Sr13.1 and Sr13.2 have a peak at 0 minutes.

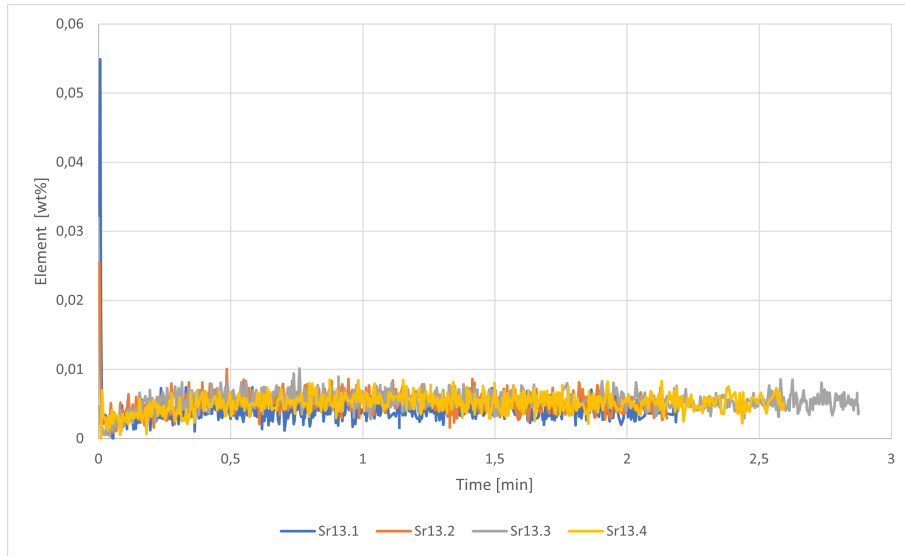


Figure 99: Sample of Sr after 130 min.

Figure 100 shows the data from the analysis of the Al-sample taken after 4 hours. The sample was analysed four times for 2 minutes. The graph shows a signal between 0-0.002 wt% Sr. The graphs have a peak at 0 minutes.

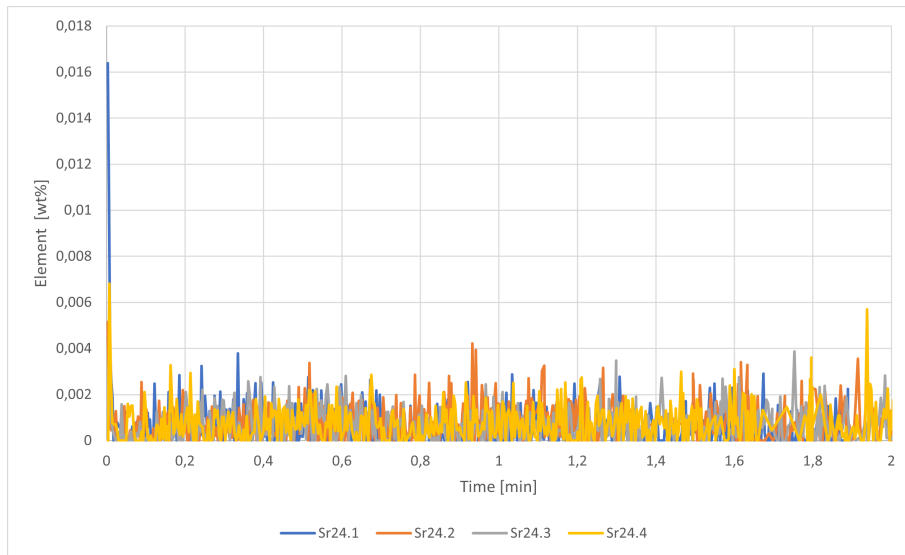


Figure 100: Sample of Sr after 240 min.

---

Figure 101 shows the data from the analysis of the Al-sample taken after 6 hours. The sample was analysed four times for 2 minutes. The graph shows a signal between 0-0.002 wt% Sr. The graphs have a peak at 0 minutes.

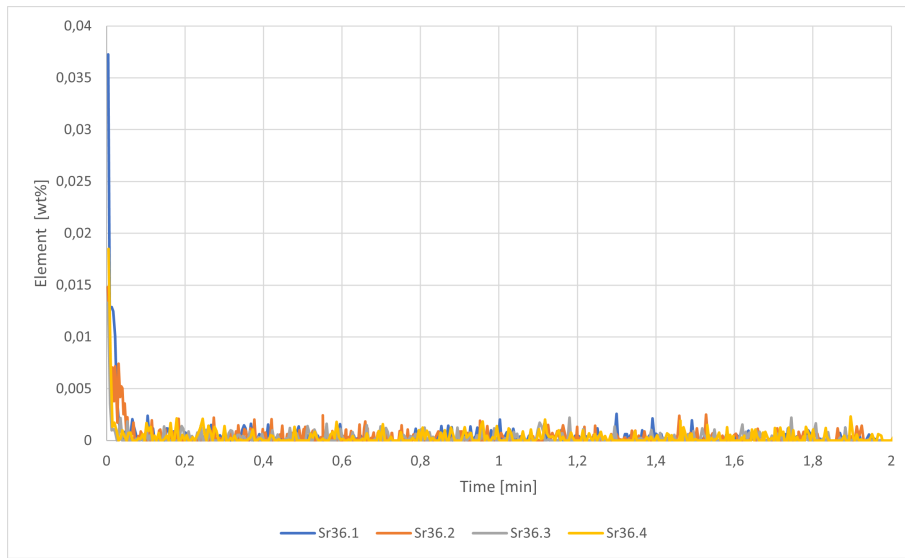


Figure 101: Sample of Sr after 360 min.

Figure 102 shows the data from the analysis of the Al-sample taken after 18 hours. The sample was analysed four times for 3 minutes. The graph shows a signal between 0-0.002 wt% Sr. Sr108.3 and Sr108.4 have a peak at 0 minutes.

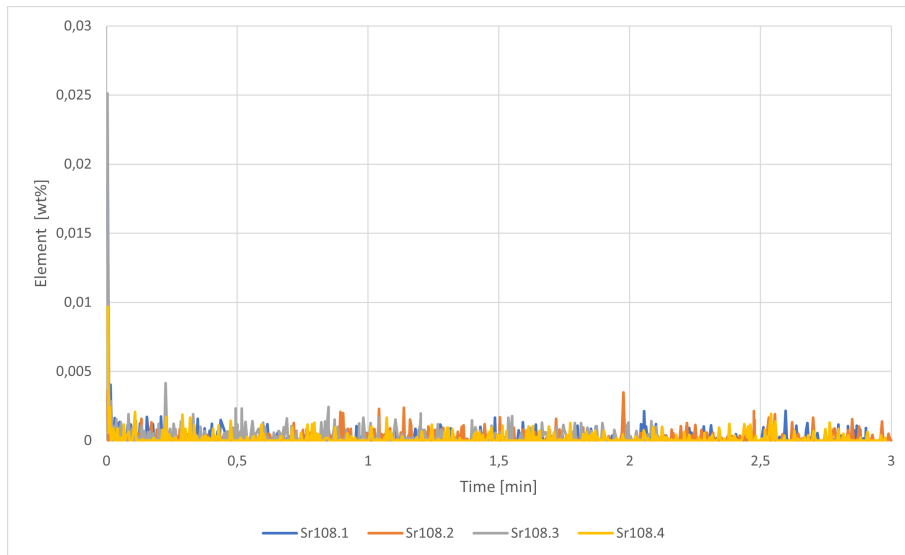


Figure 102: Sample of Sr after 1080 min.

---

Figure 103 shows the data from the analysis of the Al-sample taken after 20 hours. The sample was analysed four times for 3 minutes. The graph shows a signal between 0-0.002 wt% Sr, with peaks at 0 minutes.

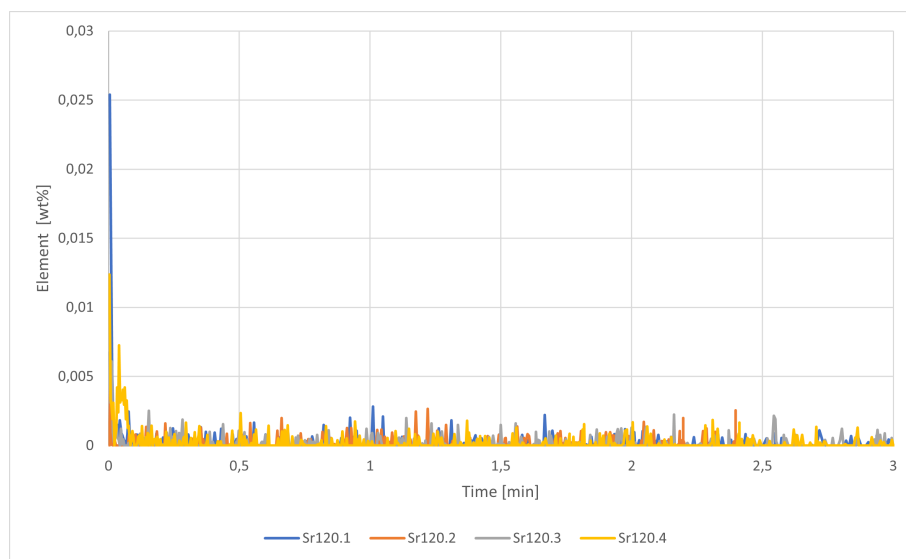


Figure 103: Sample of Sr after 1200 min.

---

#### 4.2.12 GD-OES-data from Sr-trial with AlSi7-alloy

Figure 104 shows the data from the analysis of the AlSi7-sample taken at the beginning of the trial. The sample was analysed three times for 3 minutes. The graph shows a signal between 0-0.002 wt% Sr. Sr0.1 have a peak at 0 minutes.

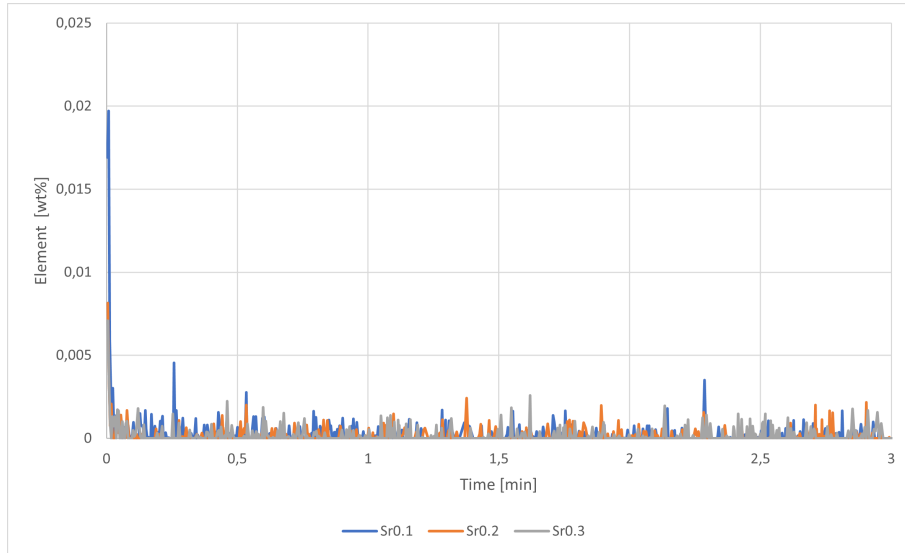


Figure 104: Reference AlSi7-sample before addition of Sr.

Figure 105 shows the data from the analysis of the AlSi7-sample taken at 40 minutes. The sample was analysed three times for 3 minutes. The graph shows an increasing signal from 0.002 wt% Sr, which stabilizes after 0.5 minutes between 0.015-0.025 wt% Sr.

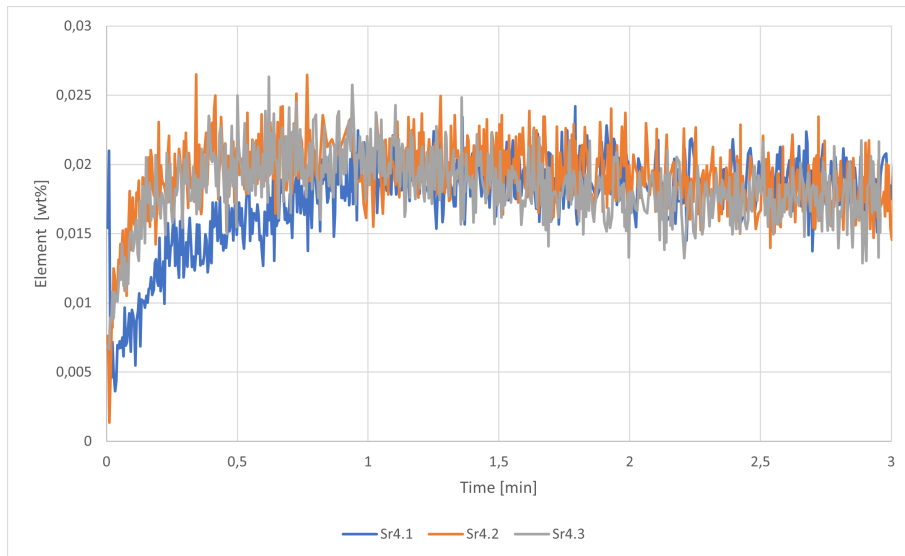


Figure 105: Sample of Sr after 40 min.



---

Figure 106 shows the data from the analysis of the AlSi7-sample taken after 2 hours. The sample was analysed three times for 2.5 minutes. Sr12.2 and Sr12.3 show an increasing signal from 0.003, which stabilizes after 0.5 minutes between 0.01-0.017 wt% Sr. Sr12.1 shows an increasing signal, which then decreases and stabilizes at the same level as Sr12.2 and Sr12.3.

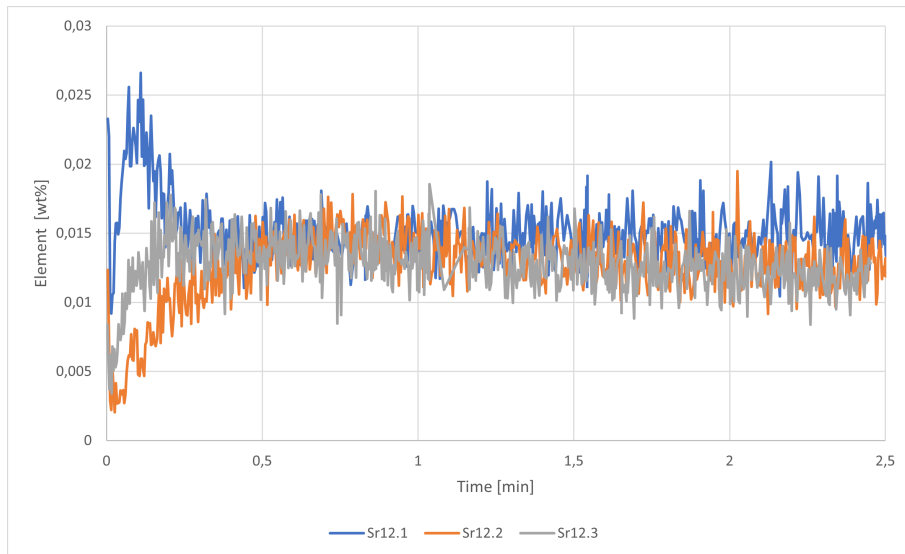


Figure 106: Sample of Sr after 120 min.

Figure 107 shows the data from the analysis of the AlSi7-sample taken at 4 hours. The sample was analysed three times for 3 minutes. The graph shows an increasing signal from 0.001 wt% Sr, which stabilizes after 0.5 minutes between 0.005-0.01 wt% Sr. Sr24.1 have a peak at 0 minutes.

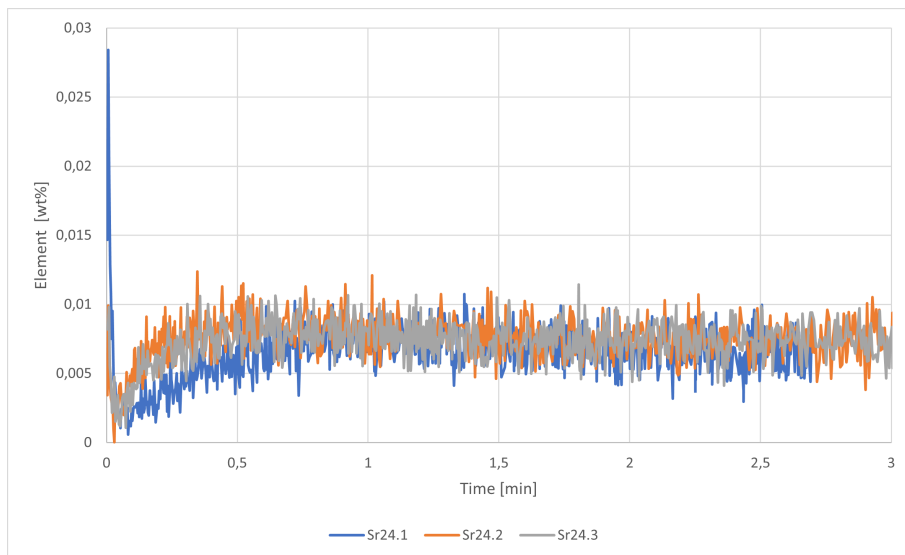


Figure 107: Sample of Sr after 240 min.

---

#### 4.2.13 GD-OES-data from 1h Bi-trial

Figure 108 shows the results from the analysis of the Bi-sample taken at 10 min. The sample was in total analysed four times for 2.5 min. The graph shows a signal between 0.05-0.5 wt% Bi, with peaks at 0.7, 1.2, 1.8 and 2.3 min. This analysis shows the lowest measured wt% to be 0.05 wt% Bi. These values are higher than expected and may be caused by a calibration issue. Expected results for wt% Bi would lay between an interval of 0-0.05 wt% Bi, as this would correspond to the added amount of Bi at the start of the trial.

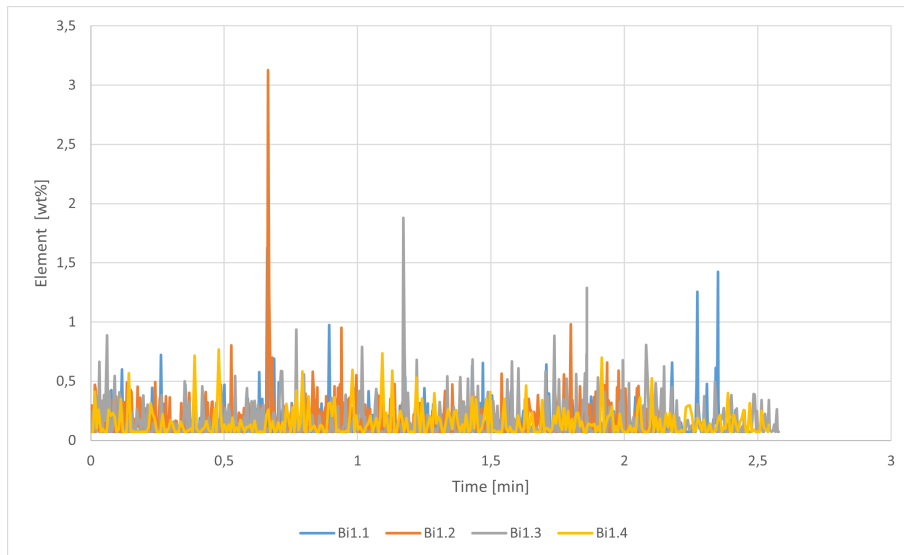


Figure 108: Sample of Bi after 10 min.

Figure 109 shows the results from the sample taken after 20 min. The sample was in total analysed four times for 2-2.5 min. The graph shows a signal between 0.05-0.4 wt% Bi, with a variety of peaks during the whole analysis. This analysis also shows the calibration issue concerning Bi.

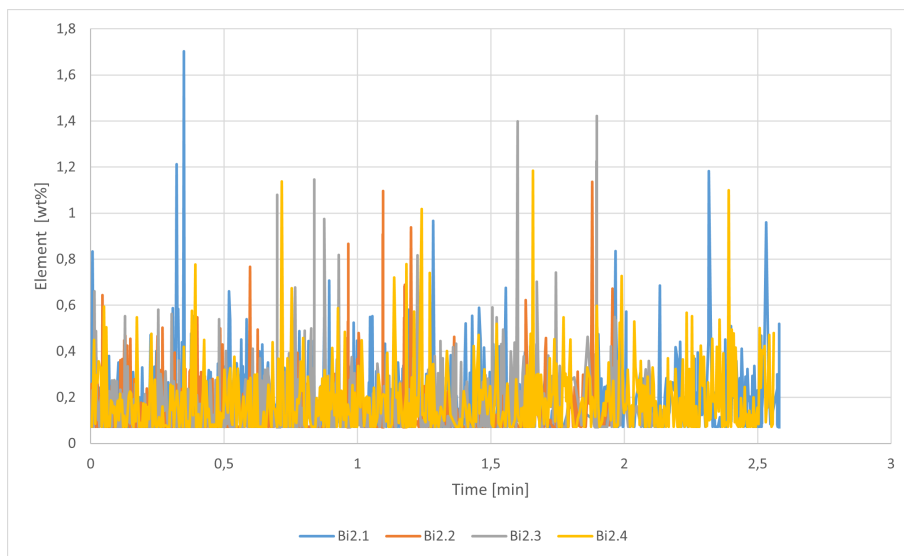


Figure 109: Sample of Bi after 20 min.

---

Figure 110 shows the results from the GD-OES-analysis of the Bismuth-sample taken after 30 min. The sample was analysed four times for 2.5-3 min. The graph shows a signal between 0.05-0.5 wt% Bi, with a variety of peaks from 0.1 to 1.9 min. The issue with GD-OES analysis of Bi is present for this sample as well.

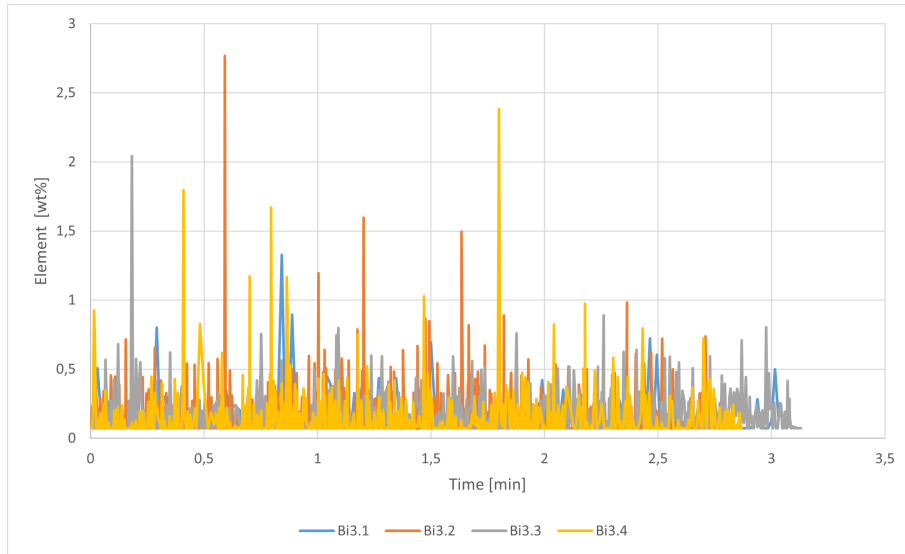


Figure 110: Sample of Bi after 30 min.

Figure 111 shows the results from the analysis of the sample taken after 40 min. The sample was in total analysed four times for 2.5-3.5 min. The graph shows a signal between 0-0.5 wt% Bi, with a variety of peaks during the whole analysis. Bi4.4 shows a signal of 0 through the analysis. This analysis is consistent with the other analyzes of Bi, and shows the calibration issue concerning Bi.

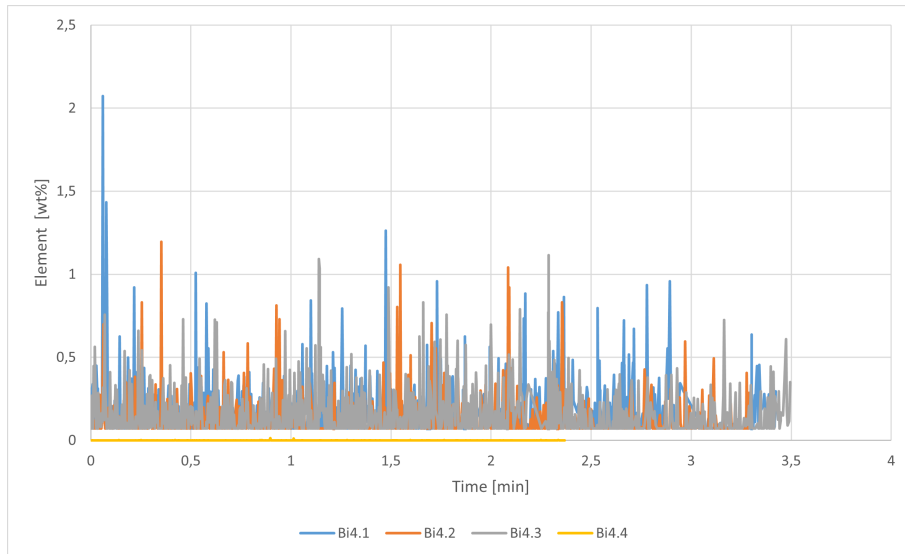


Figure 111: Sample of Bi after 40 min.

---

Figure 112 shows the results from the analysis of the sample taken at 50 minutes. The sample was in total analysed four times for 3 minutes. The graph shows a signal between 0.05-0.5 wt% Bi, furthering the calibration issue, with a variety of peaks during the whole analysis. The highest peak gave a signal of 2.6 at 1.4 minutes.

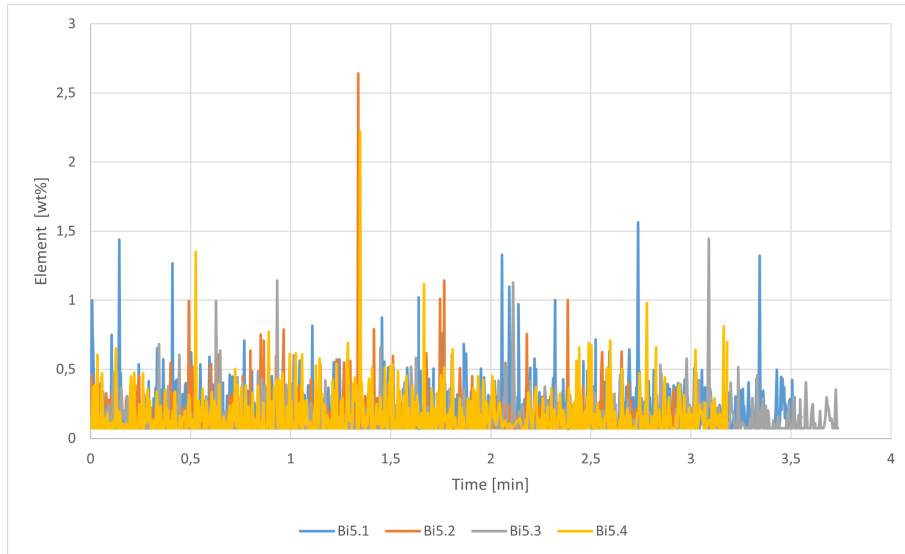


Figure 112: Sample of Bi after 50 min.

Figure 113 shows the results from the GD-OES-analysis of the Bismuth-sample taken at the end of the 1 hour trial. The sample was in total analysed five times for 1.5 to 3 minutes. The graph shows a signal between 0.05-0.4 wt% Bi for Bi6.3, Bi6.4 and Bi6.5, with a variety of peaks during the analysis. Bi6.1 and Bi6.2 has a signal of 0 through the analysis. This analysis also shows the calibration issue concerning Bi.

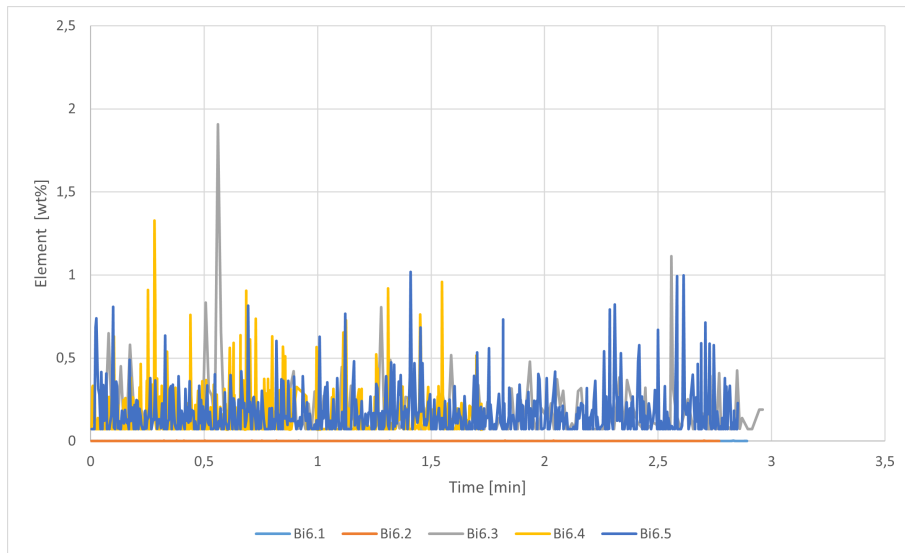


Figure 113: Sample of Bi after 60 min.

---

#### 4.2.14 GD-OES-data from 2h Bi-trial

Figure 114 shows the data from the sample of the 2h Bi-trial taken at 0 minutes. The graph give a signal from 0.8 wt% Bi and higher. The sample was analysed one time for 4 minutes.

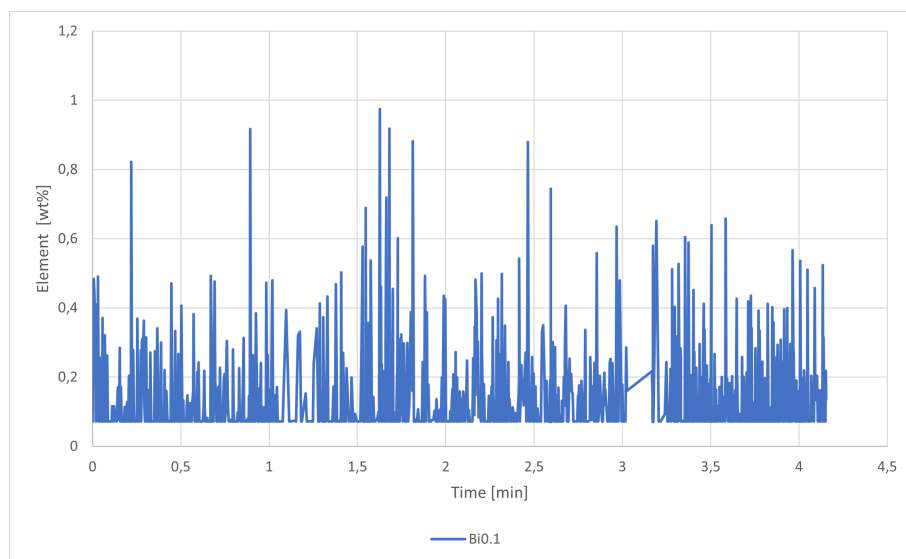


Figure 114: Reference Al-sample before addition of Bi.

Due to the continuation of the calibration issue, the samples containing bismuth were not analysed further with GD-OES.

---

### 4.3 Average measurements from GD-MS

Table 3 shows the result from the GD-MS analysis. The analysis was done on samples from the long (+20h) trials, and on samples from the Bi-trial with the AlSi7-alloy. As a consequence of high porosity of the vanadium-samples, the RSD-samples were not possible to be analysed by GD-MS.

Sample	Element [ppm]	Fe [wt%]
3Bi96	191.818	0.19
3Ni120	401.583	0.17
3Sr36	0.835	0.16
01Bi1	3.315	0.13
01Bi4	191.391	0.10
01Bi6	286.314	0.11

Table 3: Results from the GD-MS-analysis

The sample (3Bi96) analysed from the 20h Bi-trial, was the one taken 16h into the trial. The analysis of the 3Bi96-sample gave an average measurement of 191.818 ppm Bi and 0.19 wt% Fe. The trial was conducted with approximate 200 ppm alloying elements. Given accurate measurements of Bi from the GD-MS, This supports the assumption that Bi does not in molten aluminium.

The analysis from the 20h Ni-trial were done on the 3Ni120-sample, which was taken at the end of the trial. GD-MS measured the sample to have an average of 401.583 ppm Ni and 0.17 wt% Fe. The average measurement correlates with the respective results from the GD-OES analysis (Figure 77), where the graph showed an interval from 0.01-0.05 wt% Ni.

The strontium-sample (3Sr36), which was analysed by GD-MS, was taken 6h into the 20h-trial. The measurements from the analysis showed a sample containing an average of 0.835 ppm Sr and 0.16 wt% Fe. The GD-MS analysis is consistent with the GD-OES analysis of the same sample (Figure 101), where both shows a lower concentration of alloying element compared to the initial 200 ppm.

Three samples from the Bi-trial with AlSi7 were analysed by GD-MS:

1. The 10 minutes sample (01Bi1),
2. The 40 min. sample (01Bi4) and
3. The 1h sample (01Bi6).

The analysis of 01Bi1 gave an average of 3.315 ppm Bi and 0.13 wt% Fe, 01Bi4 gave an average of 191.391 ppm Bi and 0.10 wt% Fe, and 01Bi6 gave an average of 286.314 ppm Bi and 0.11 wt% Fe.

The GD-MS results showed an increase in the concentration of bismuth over time. This result was unexpected, and is possibly caused by the rate of solubility for bismuth in aluminium, though this have not been further tested. Another possibility for the increase of the bismuth over time, was a calibration issue regarding Bi in the GD-MS. The calibration issue with measuring Bi was also found for the GD-OES.

---

#### 4.4 Average measurements from ICP-OES

Table 4 shows the data received from Hösch Metallurgy of a various collection of samples.

Sample	Element [ppm]	Fe [ppm]	Ga [ppm]
3Bi0 Ref.	< 1	1383	115
3Bi0 Ref.	< 1	1317	115
1Bi6	< 1	1306	110
1Bi6	< 1	1343	120
3Bi120	135	1365	119
3Bi120	140	1399	122
3Bi2	139	1387	123
3Bi2	122	1347	121
1V2	175	1432	121
1V2	176	1466	124
3V132	241	1437	123
3V132	252	1588	121
2Ni1	245	1091	100
2Ni1	253	1159	100
3Ni108	221	1305	102
3Ni108	223	1199	111
3Sr1	118	1211	103
3Sr1	110	1159	106
3Sr108	2	1191	104
3Sr108	2	1291	108

Table 4: Results from the analysis of minor elements in pure Aluminium, by ICP-OES at Hösch Metallurgy, Germany.

The results from the ICP-OES indicate that there was no fading for bismuth on a 20-hour trial with commercial grade aluminium (3Bi2 and 3Bi120 samples), where the sample 3Bi2 has been taken 20 minutes after it was introduced to the molten aluminium, and the concentration has been in the same range as the concentration of bismuth in the sample taken 20 hours into the trial (3Bi120).

For the bismuth 1h trial, with commercial grade Al, it was clear that bismuth had not entered the system, and the concentration remained < 1 ppm for the sample taken 1 hour into the trial (1Bi6).

---

For the vanadium samples (1V2 and 3V132), both trials completed with commercial grade Al, it is apparent that vanadium's concentration in the system is stable, and did not decrease after 22 hours of the element being in the molten aluminium (3V132).

The nickel-Al-samples analysis did indicate that nickel's concentration was also stable, and does not show any signs of fading after 18 hours of being introduced to the molten aluminium (3Ni108).

The strontium addition to aluminium showed fading during the time of 18 hours (3Sr108). The concentration went from around 110 ppm after 10 minutes in the liquid Aluminium (3Sr1), to < 1 ppm after 18 hours of running trials (3Sr108). However, this data from ICP-OES does not provide an indicative time interval for when strontium fades out of the pure Al system, although indicating a general data frame to focus on.



---

## 4.5 Summary of the results

### 4.5.1 Vanadium

Figure 115 and Figure 116 show the regression-curve and box-plot of the 1h V-trial with the pure Al alloy. The regression-line in Figure 115 implies a slight indication of fading, even though a linear correlation seems unlikely in comparison to the box-plot of the same trial (Figure 116). Note that the y-axis ranges from 0.017-0.022 wt% V.

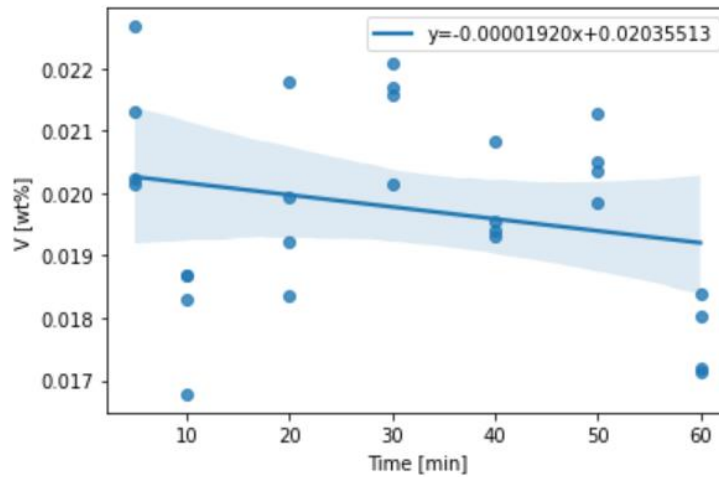


Figure 115: Regression analysis of the 1h trial of V.

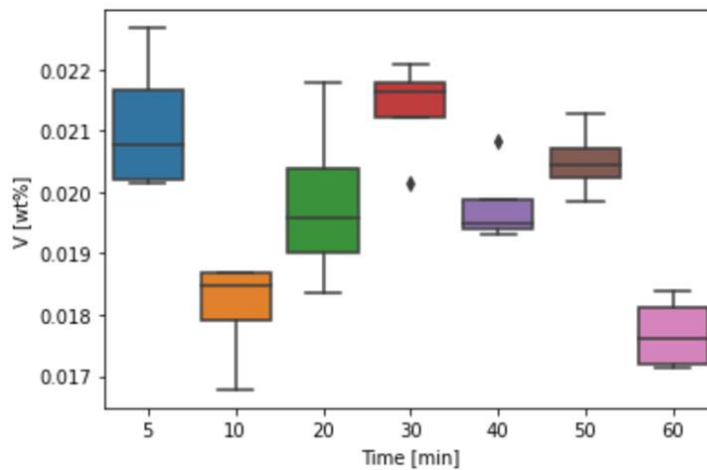


Figure 116: Box-plot of the 1h trial of V.

---

Figure 117 and Figure 118 show the regression-curve and box-plot of the 2h V-trial with the pure Al alloy. Both figures show an increase of vanadium over time. In comparison to the rest of the trial, an assumption is made that the vanadium in the 10 minute sample is not completely dissolved.

From the box-plot (Figure 118), the data-points at 60 and 100 minutes show a higher deviation compared to the remaining data-points. These two data-points may be part of the cause of the increase in vanadium over time.

The samples taken after 20 minutes and later show a wt% of 0.02 wt% V or higher. This suggest no fading of vanadium in aluminium.

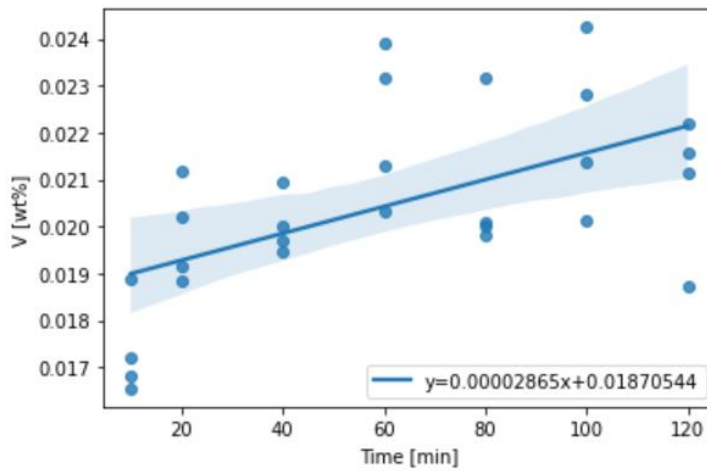


Figure 117: Regression analysis of the 2h trial of V.

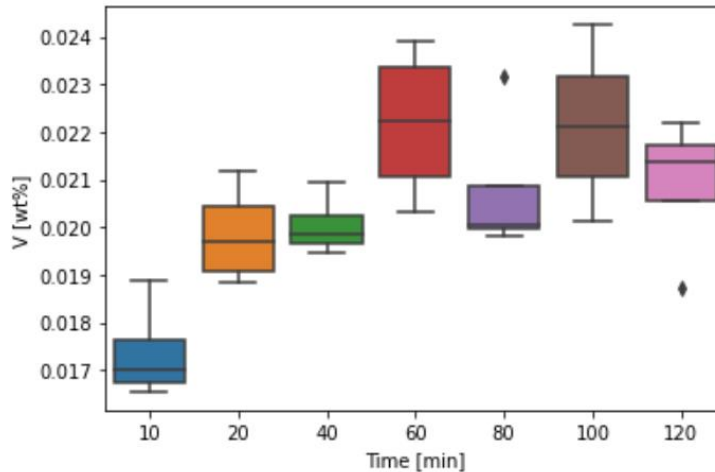


Figure 118: Box-plot of the 2h trial of V.

---

Figure 119 and Figure 120 show the regression-curve and box-plot of the 22h V-trial with the pure Al alloy. The plots give an indication of the increase of vanadium in the sample over time, though it should be noted that the y-axis have an interval from 0.0195 wt% to 0.0235 wt%. It would therefore be unlikely that the graph would continue to indicate increase of vanadium in the sample over time.

For the 22h-trial both plots show concentrations between 0.020-0.023 wt% V, which in comparison to the original 200 ppm V added, indicates no fading.

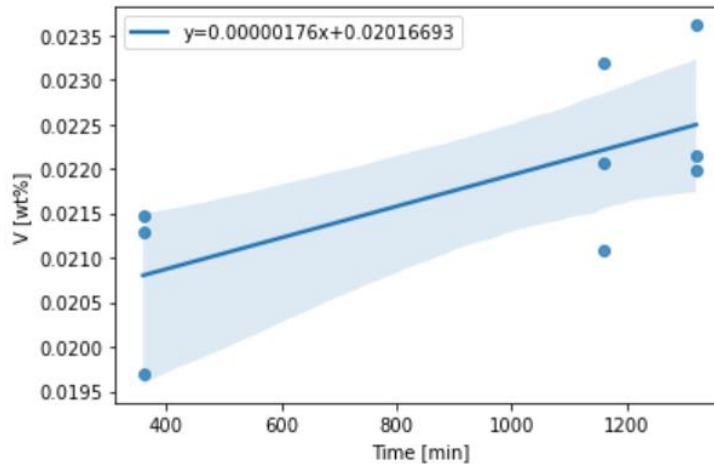


Figure 119: Regression analysis of the 20h trial of V.

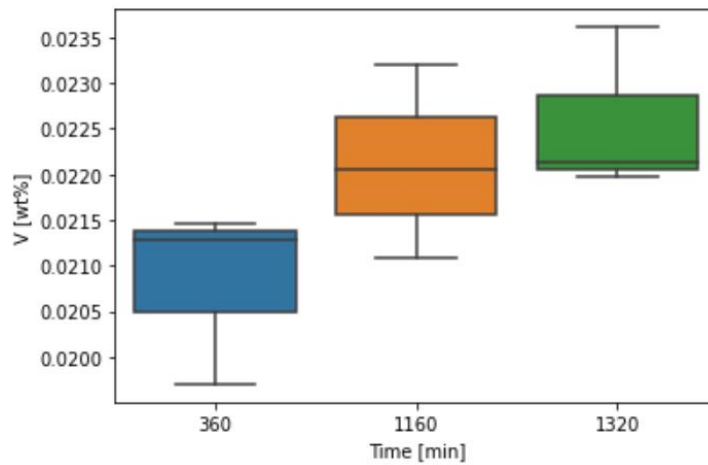


Figure 120: Box-plot of the 20h trial of V.

---

Figure 121 and Figure 122 show the regression-curve and box-plot of the V-trial with the AlSi7-alloy. The regression-curve shows an increase of the vanadium concentration over time, while the box-plot shows an increase from the first data-point to the data-points after.

The lower value for the 20 minute sample may be caused by the dissolution rate of the vanadium. The lower concentration in the 20 minute data-point, will impact the regression-curve by increasing the positive change in concentration over time. When looking at the data-points taken after the 20 min. sample, there is no trend suggesting fading. The 60 min. point shows a concentration of 0.019 wt% V, at the 120 min. point the concentration drops to 0.018 wt% V, while it increases back to 0.019 wt% V at the 240 min. point.

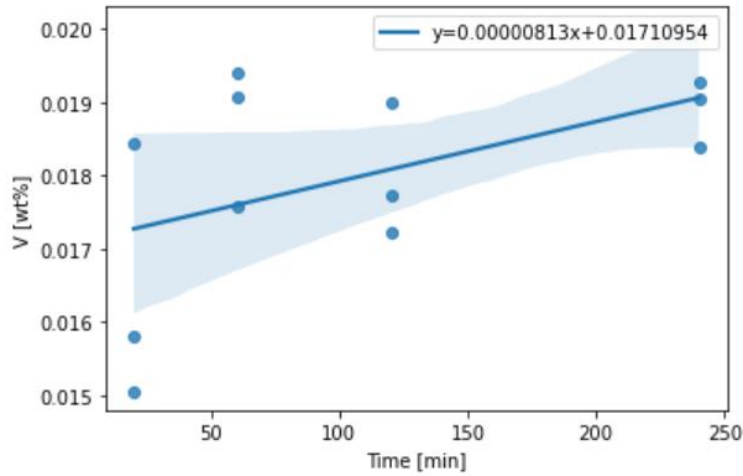


Figure 121: Regression analysis of the alloy-trial of V.

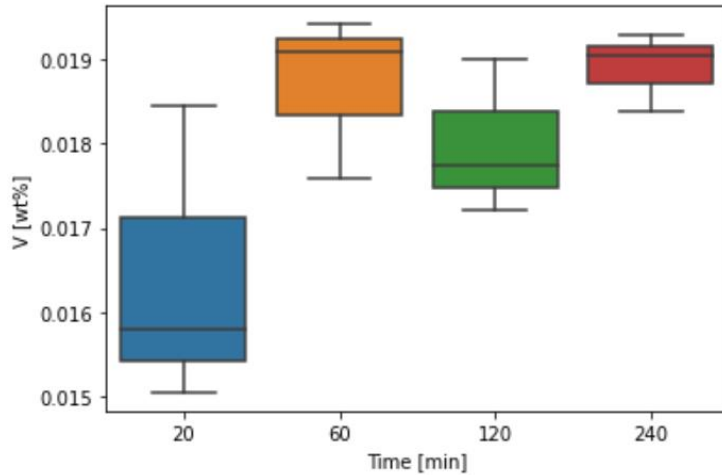


Figure 122: Box-plot of the alloy-trial of V.

---

#### 4.5.2 Nickel

Figure 123 and Figure 124 show, the regression-curve and box-plot of the 1Ni-trials with the pure Al alloy. The regression plot gives an indication of nickel maintaining a stable concentration over time. The trend-line equation show a slight decrease in concentration over time. However, it is most likely attributed to the standard deviation between points at each time interval.

The box plot for 1Ni trial indicate that the concentration was in the range from 200-250 ppm, or 0.020-0.025 wt%. The sample taken at 60 minutes show the biggest deviation, which can mean that some points analysed were at grain boundaries or in the grains.

Nevertheless, the 1 hour trial does not prove the absence of nickel fading from the system, but indicate relative stability of the element remaining in the liquid aluminium.

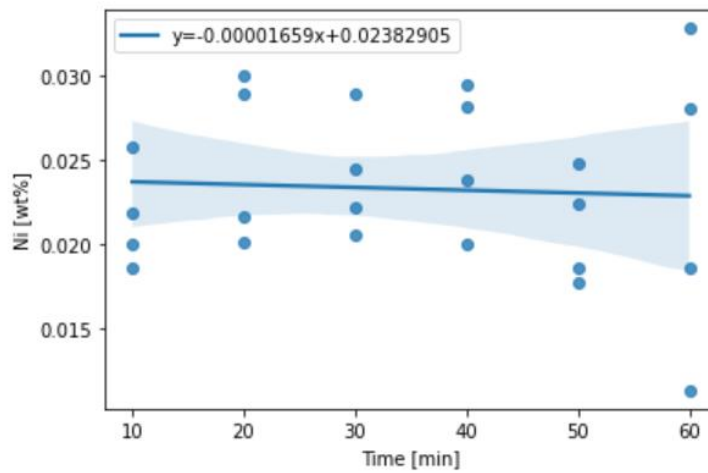


Figure 123: Regression analysis of the 1h trial of Ni.

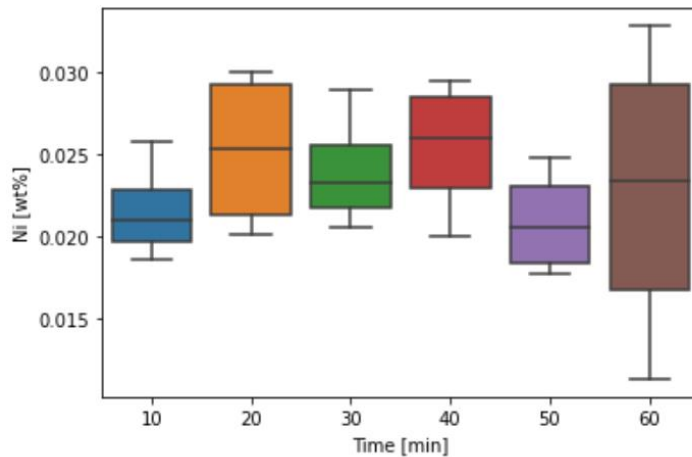


Figure 124: Box-plot of the 1h trial of Ni.

---

Figure 125 and Figure 126 show, the regression-curve and box-plot of the 2h Ni-trials with the pure Al alloy. The regression plot gives an indication of nickel's concentration decreasing over time to an extent. However, the box-plot shows that the values for Ni wt% are in the same range after a 20-min interval. The first two samples, at 10 and 20 minutes, respectively are within the same range as well.

The box plot for the 2h Ni-trial indicate that the concentration was in the range from 200-400 ppm, or 0.020-0.040 wt%, with some values off the chart. This could be explained by the grains and grain boundaries in the sample, as the metal is not uniform, concentration variation is possible and it can be expected that the concentration will vary to some extent.

The 2h trial provides a different result when comparing with the 1 hour trial. However, based on the box plot (figure 126), the concentration of nickel is stable, despite the initial drop.

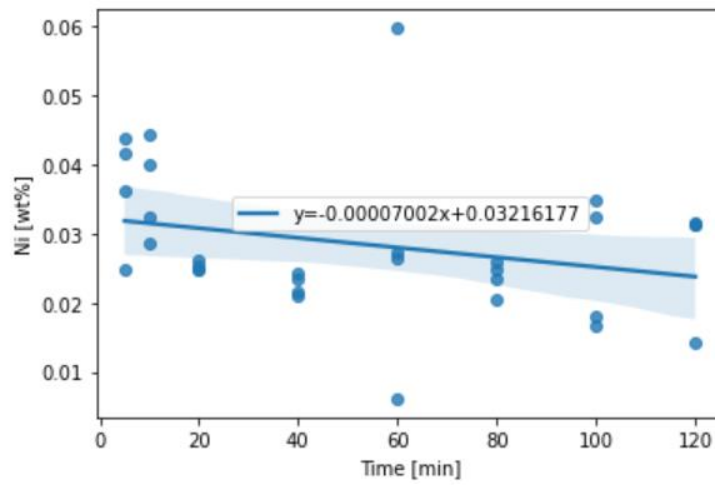


Figure 125: Regression analysis of the 2h trial of Ni.

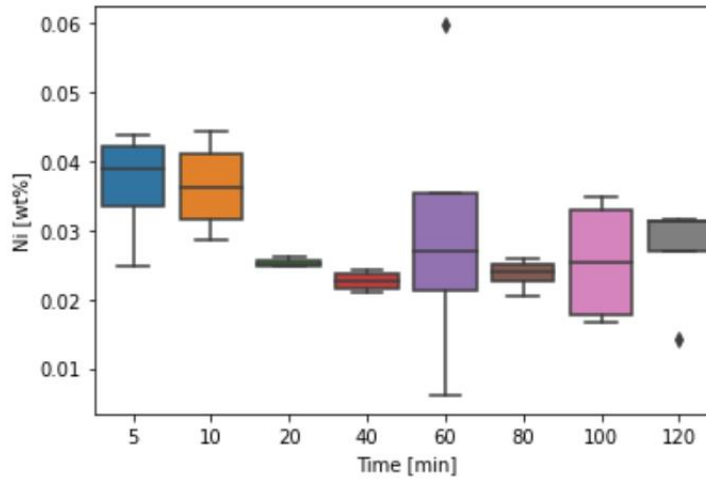


Figure 126: Box-plot of the 2h trial of Ni.

---

Figure 127 and Figure 128 show, the regression-curve and box-plot of the 20h Ni-trials with the pure Al alloy. The regression plot gives an indication of nickel's concentration increasing over time to an extent. The box plot indicates that the nickel wt% is in the same range, and is stable to an extent.

The box plot for the 20h Ni-trial indicate that the concentration was in the range from 310-400 ppm, or 0.031-0.040 wt%, with some values off the chart. However, as seen on the box-plot, it is within the error-bar range for the sample, and does not affect the general trend for the regression line.

The 20 hour trial is limited, due to the limited amount of samples analysed, however it can be used to conclude that nickel is stable in the molten aluminium, and is remaining in the melt after 20 hours since being introduced to the system.

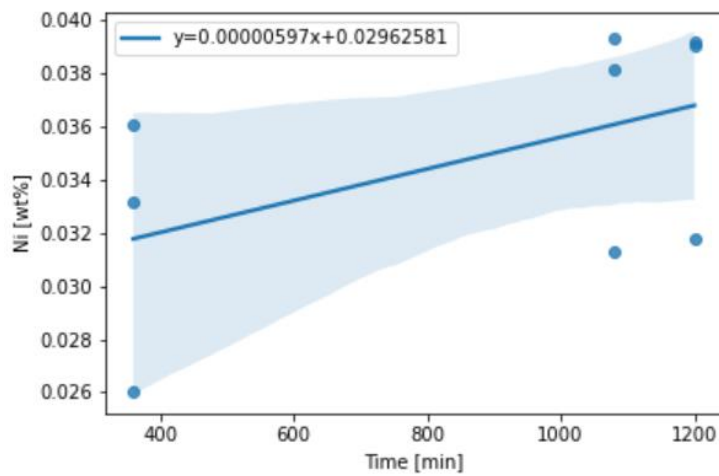


Figure 127: Regression analysis of the 20h trial of Ni.

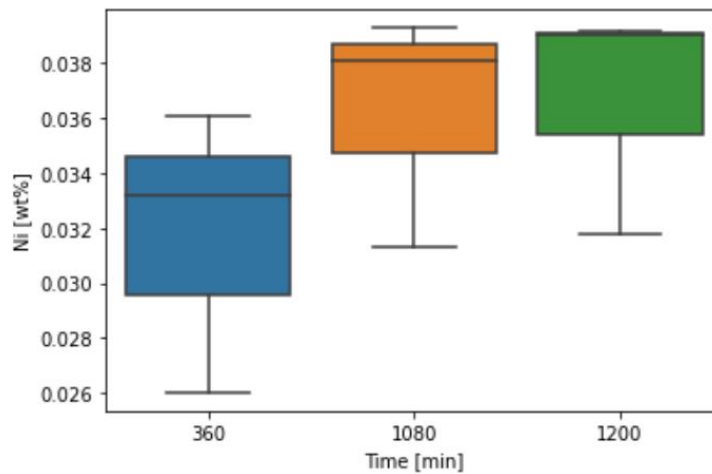


Figure 128: Box-plot of the 20h trial of Ni.

---

Figure 129 and Figure 130 show, the regression-curve and box-plot of the nickel trials on the AlSi7 alloys. Both plots do not provide sufficient information, as there were only two samples analysed. However, there is an indication of nickel being present in the concentration, theoretically calculated at 60 min. mark, which suggest that nickel remains stable in the melt, even with a higher Si-concentration. The regression plot gives an indication of nickel's concentration increasing over time to an extent. This can be due to the fact that only one point has been analysed on the sample taken at 40 minutes.

The box plot for alloy-Ni-trial indicate that the concentration was in the range from 140-280 ppm, or 0.014-0.028 wt%. Lower concentration at the 40 minute mark may indicate incomplete dissolution of Nickel at that time. However, more trials are needed to observe the dissolution rate of nickel in the alloy.

Although the alloy-nickel trial is limited, it can be used to conclude that nickel is stable in the molten alloy AlSi7 for the first hour.

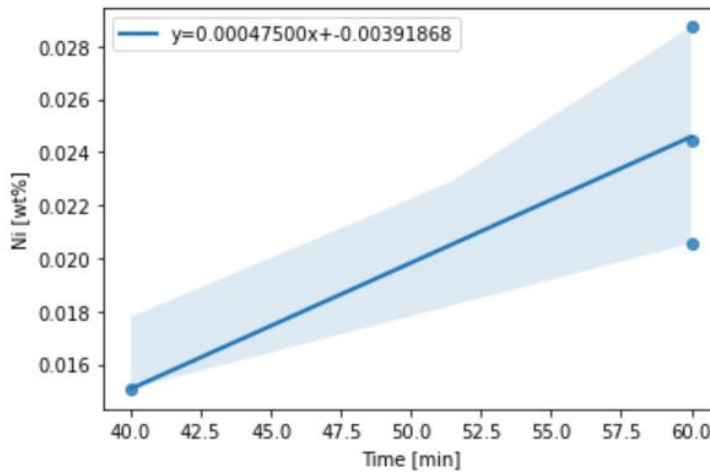


Figure 129: Regression analysis of the alloy-trial of Ni.

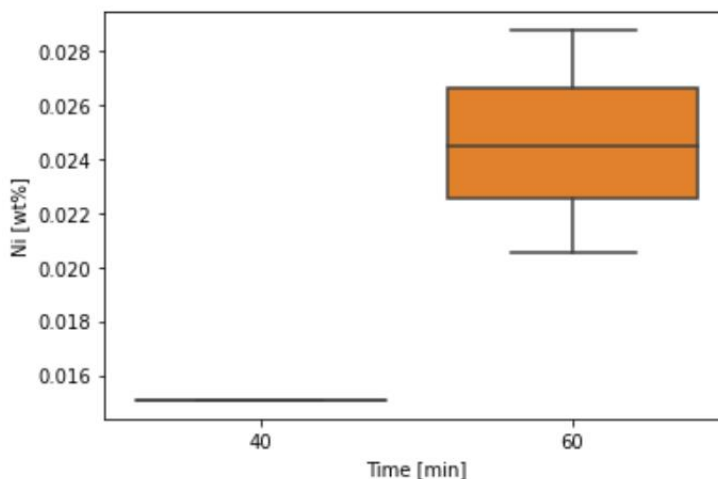


Figure 130: Box-plot of the alloy-trial of Ni.



---

### 4.5.3 Strontium

Figure 131 and Figure 132 show, the regression-curve and box-plot of the 1h Sr-trials with the pure Al alloy. Both plots visualise fading of strontium in aluminium. At the 10 min. data-point the sample shows an average concentration of 0.027 wt% Sr, while the sample taken at 1h has dropped to an average concentration of 0.016 wt% Sr.

The data-set from the 1h trial, show a considerable deviation in the data-points, where the outliers are marked in a diamond shape. The 1h-trial is therefore not enough to give a conclusive indication of fading, but implies a suggestion of this occurring.

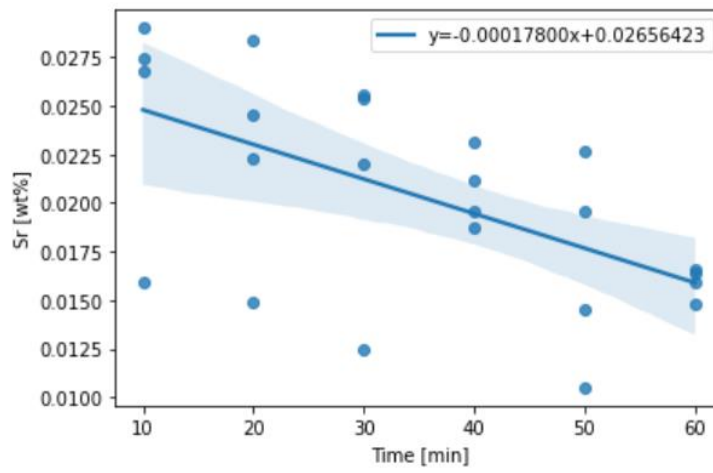


Figure 131: Regression analysis of the 1h trial of Sr.

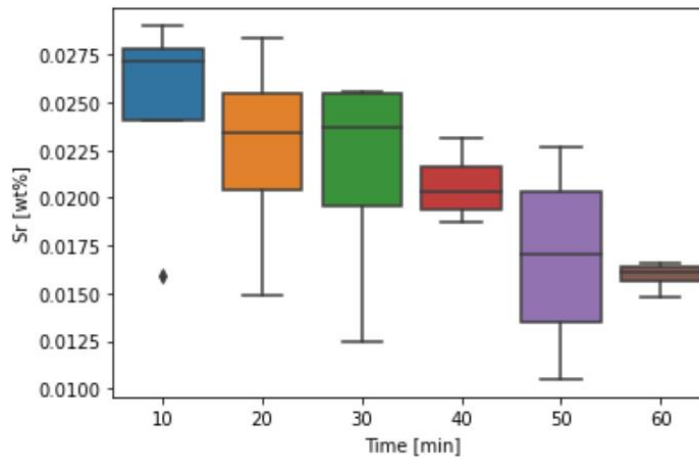


Figure 132: Box-plot of the 1h trial of Sr.

---

Figure 133 and Figure 134 show, the regression-curve and box-plot of the 2h Sr-trials with the pure Al alloy. In addition to the 1h trial, both the box-plot and the regression-curve indicates fading of strontium. The measured concentrations in the trial have its highest value at 0.025 wt% Sr and its lowest at 0.007 wt% Sr.

The sample at 5 min. have a lower concentration in comparison to the data-point at 10 min., which probably is due to the dissolution rate of strontium in aluminum.

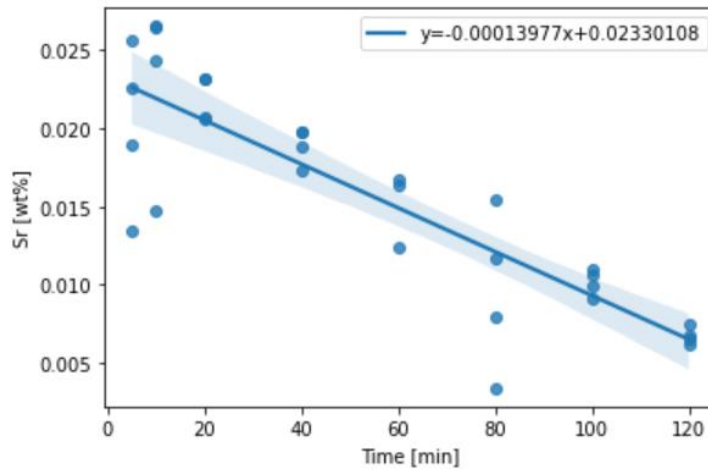


Figure 133: Regression analysis of the 2h trial of Sr.

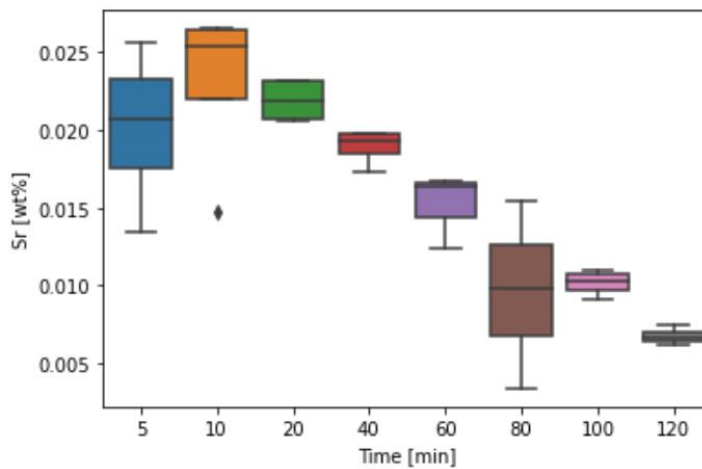


Figure 134: Box-plot of the 2h trial of Sr.

---

Figure 135 and Figure 136 show, the regression-curve and box-plot of the 20h Sr-trials with the pure Al alloy. For the box-plot the concentration begins at 0.019 wt% Sr, and decreases to approx. 0 wt% Sr, i.e. strontium fades entirely.

Figure 135 shows a linear regression curve. The fading do not behave linearly, but decreases exponential as visualised in the box-plot (Figure 136). The regression-curve is therefore imprecise, but sufficient to give quick indication of the rate of fading. The regression-curve show fading with a slope of  $-8.65 \cdot 10^{-6}$  wt% Sr.

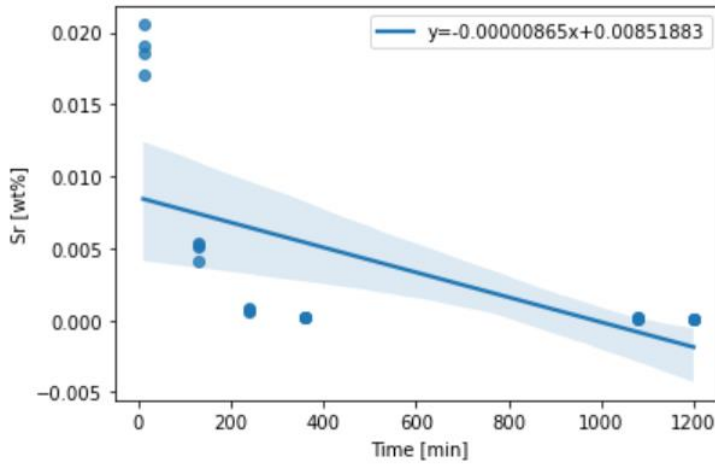


Figure 135: Regression analysis of the 20h trial of Sr.

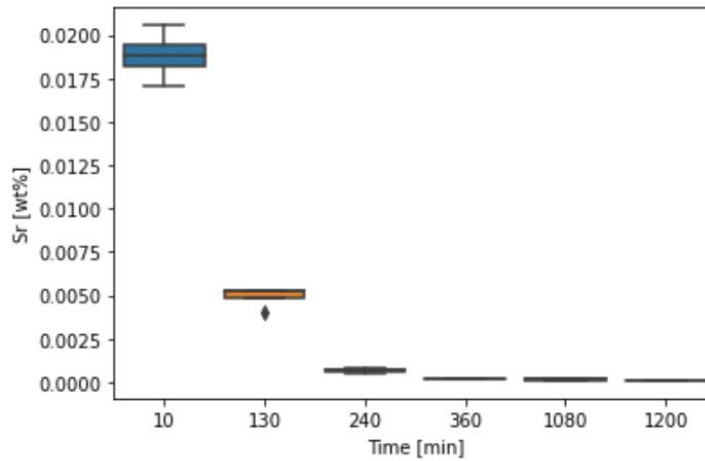


Figure 136: Box-plot of the 20h trial of Sr.

---

Figure 137 and Figure 138 show, the regression-curve and box-plot of the Sr-trial with the AlSi7-alloy. Both the box-plot and the regression-curve show signs of fading, as the Sr-trials with industrial Al also have concluded.

The 40 min. data-point show an average concentration of 0.018 wt% Sr, which then drops to 0.008 wt% Sr at 4h. The regression-curve show fading with a slope of  $-5.45 \cdot 10^{-5}$  wt% Sr. In comparison to the slope from the 20h Sr-trial ( $-8.65 \cdot 10^{-6}$  wt% Sr) the fading happens faster for the alloy than the industrial Al. This may be the cause of interactions between the strontium and silicon in the melt, though this have not been further investigated.

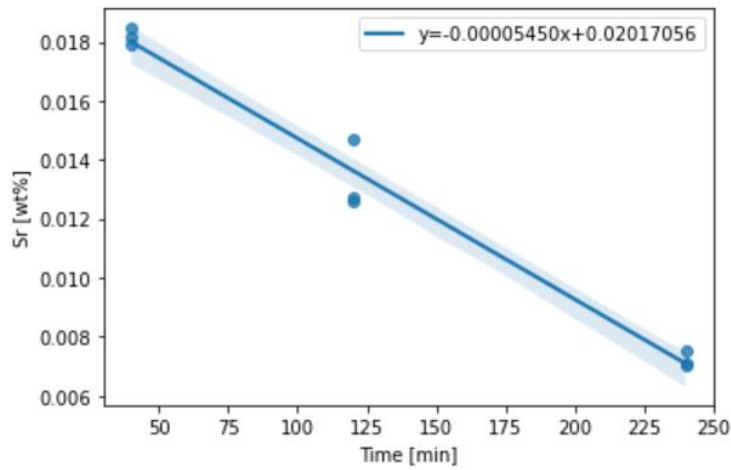


Figure 137: Regression analysis of the alloy-trial of Sr.

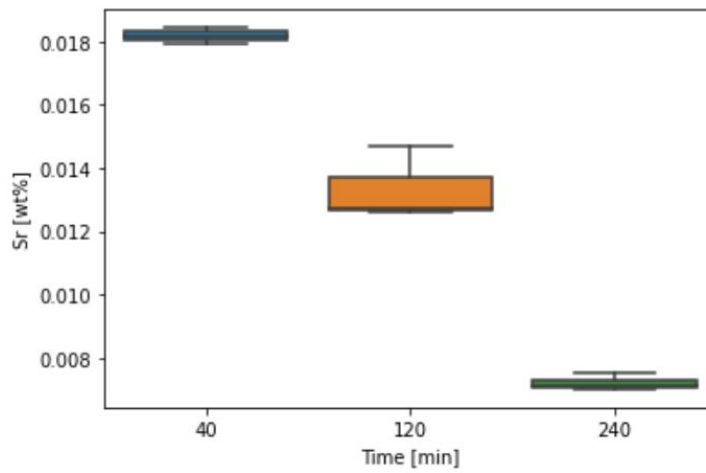


Figure 138: Box-plot of the alloy-trial of Sr.

---

#### 4.5.4 Bismuth

Bismuth has proven to be a difficult element to analyse, when using the primary analysis instrument: GD-OES. GD-OES requires a precise and accurate calibration in order to provide precise results. However, the calibration for bismuth has proven to be accurate only at higher concentrations. It can be seen on the raw GD-OES data plots shown on figures 108 to 114. The concentration of Bi in the samples is over 0.1 wt% in most cases, and no Bi present in some cases. However, the concentrations of Bi introduced to the liquid aluminium were much lower, as the analysis of the behavior of the elements was done on ppm scale. The results gotten on ICP-OES and GD-MS prove that the concentrations were much lower than indicated by GD-OES (Table 4 and Table 3).

Based on the GD-MS average measurements, shown in table 3, bismuth was present in the third trial with industrial aluminium at 16 hours, which indicates that bismuth is stable in the molten aluminium. However, the concentration of bismuth at 20 hours is recorded to be lower, based on the ICP-OES results (table 4, sample 3Bi120). This can either be influenced by the different analysis method, or it can serve as an indication of fading.

For the alloy-Bi trial (table 3, samples 01Bi1, 01Bi4 and 01Bi4), it is seen that the concentration of bismuth at 10 minutes was low, which indicates that the element was likely not dissolved in the molten alloy, however, it rises to 191 ppm after 40 minutes of first being introduced, and eventually rises up to 286 ppm after an hour. The rise in the bismuth concentration over an hour may indicate a slow dissolution rate. However, it is very unlikely, as the bismuth melting point is much lower than the melting point of the AlSi7 alloy, thus Bi is expected to dissolve fast.

Overall, bismuth-trials have yielded results that were not expected, based on its known interactions, according to the phase diagram shown on Figure 11. Thus, the results remain inconclusive for now, as the data provided by the analysis method varies, and has a small selection of samples to provide a definite result.

---

## 5 Conclusion

This work showed the initiation of the fundamental field of fading of elements in aluminium and its alloys. It covered the identification of methodology, such as the impact of melting, preparation and processing of the alloys. It discussed and validated different analysis methods, such as the GD and the ICP with OES and MS, and generated a starting point for future data creation.

The following conclusions were drawn:

1. V and traces of V in Al and its alloys:

Vanadium has shown no significant signs of fading in neither, commercial grade Al, nor in the alloy. However, it showed that the concentration of V increased in some cases over time. It can be explained by a slow dissolution rate due to a much higher melting point than Al. Vanadium has also proven to interact with the coating used, which made the melt adhere to the tongs and crucible, which has been difficult to remove.

2. Ni and traces of Ni in Al and its alloys:

Nickel has shown no signs of major fading in neither commercial grade aluminium, nor in the alloy (AlSi7). It remains stable in concentrations from 200-400 ppm. The concentration of Ni provided by GD-OES analysis is different that that provided by ICP-OES, which may indicate a poor calibration for the element.

3. Sr and traces of Sr in Al and its alloys:

Sr is the only element out of the four studied elements that shows the signs of fading. It fades in both, pure commercial aluminium and AlSi7. In commercial grade Al, strontium was faded to the concentration of < 1 ppm, after 6 hours. It is showing the sings of fading at the same rate in the alloy.

4. Bi and traces of Bi in Al and its alloys:

Identification of bismuth has been proven difficult, and the results are inconclusive. However, the data that has been gathers suggest that bismuth is stable in the molten aluminium over a period of 20 hours, at concentration of 140 ppm.

---

## 5. General conclusions:

Overall, the results of this work have been consistent with the initial findings by dr. Ohm, and yielded a more in-depth look into the behavior of the elements in a melt over different time-periods. The elements appear to behave similarly in pure aluminium and AlSi7. However, more trials are required to observe the elements' behavior in aluminium alloys of different compositions. Elements appeared to have no issue getting into the liquid metal. There might have been minor contaminating of the melt linked to the tongs as well as the crucibles; however, the application of the coating to both instruments minimized the risk of it.

It is worth noting that the trials with Bi do not provide sufficient amount of data to draw any considerable conclusions, as the primary analytical method (GD-OES) has not been calibrated to a satisfactory degree, and the other analytical tools have not been available to analyse all the samples to yield a similar box plot and regression graph. However, the results gotten strongly suggest that Bismuth is stable in the melt.

---

## 6 Future Work

As this study has been a baseline investigation, further parametric studies could be conducted to explore the influence of alloying elements on solubility of the elements of focus, but also more complex systems as fading in alloy system situations. This would give a better insight in the effects of long term recycling of aluminium and alloys.

This work has majorly focused on the simple interactions of the elements of interest and aluminium, however, the trials have been done using pure Al and alloys, rather than scraps, as it happens in the recycling. For the future work, the trials can be done with the recycling scrap, in order to observe the element interactions not only with Al, but with other possible contamination that may be present in the recycling process. The addition of primary Al may also be of interest, and have an effect on the elements under study.

A field trial comparing lab scale to industrial scale fading would be a considerable future research project to give further insight in this field of study. Increasing or decreasing the concentrations of the elements added can also be a substantial research project, as it might give an insight over possible changes in the element's behavior under different conditions.



---

## References

- [1] The Aluminum Association. *Infinitely Recyclable*. <https://www.aluminum.org/Recycling> (cit. on pp. 1, 2).
- [2] J. Davies. *GLOBAL ALUMINIUM CYCLE 2019*. <https://alucycle.international-aluminium.org/public-access/#global>. 2021 (cit. on p. 1).
- [3] N. Ding; F. Gao; Z. Wang; G. Xianzheng. ‘Comparative analysis of primary aluminum and recycled aluminum on energy consumption and greenhouse gas emission’. In: *Zhongguo Youse Jinshu Xuebao/Chinese Journal of Nonferrous Metals* (2012) (cit. on p. 1).
- [4] O. Ignatenko; A. van Schaik; M.A. Reuter. ‘Exergy as a tool for evaluation of the resource efficiency of recycling systems’. In: *Minerals Engineering* (2007) (cit. on p. 1).
- [5] D. Paraskevas; K. Kellens; W. Dewulf; J. R. Duflou. ‘Environmental modelling of aluminium recycling: a Life Cycle Assessment tool for sustainable metal management’. In: *Journal of Cleaner Production* (2015) (cit. on p. 1).
- [6] et. al. K. Nakajima. ‘Thermodynamic Analysis of Contamination by Alloying Elements in Aluminum Recycling’. In: *Environmental Science & Technology* (2010) (cit. on p. 1).
- [7] Castro et. al. ‘A thermodynamic approach to the compatibility of materials combinations for recycling’. In: *Resources, Conservation and Recycling* (2004) (cit. on p. 1).
- [8] V. K. Soo et. al. ‘Sustainable aluminium recycling of end-of-life products: A joining techniques perspective’. In: *Journal of Cleaner Production* (2018) (cit. on p. 2).
- [9] Roger Lumley. *Fundamentals of aluminium metallurgy: Production, processing and applications*. Woodhead Publishing Limited, 2011 (cit. on p. 3).
- [10] L.F.Mondolfo. *Aluminium Alloys: Structure and Properties*. Butter Worths, 1976 (cit. on pp. 3, 4).
- [11] George E. Totten; D. Scott MacKenzie. *Handbook of Aluminium, Volume 1: Physical Metallurgy and Processes*. Marcel Dekker, Inc., 2003 (cit. on pp. 3, 4).
- [12] Snorre Farner. *Remelting of Aluminium by Continuous Submersion of Rolled Scrap*. [https://www.researchgate.net/publication/277863872\\_Remelting\\_of\\_Aluminium\\_by\\_Continuous\\_Submersion\\_of\\_Rolled\\_Scrap/figures?lo=1](https://www.researchgate.net/publication/277863872_Remelting_of_Aluminium_by_Continuous_Submersion_of_Rolled_Scrap/figures?lo=1) (cit. on p. 3).
- [13] J. Gilbert Kaufman. *Understanding Wrought and Cast Aluminium Alloys Designations*. <https://materialsdata.nist.gov/bitstream/handle/11115/185/Understanding%20Wrought%20and%20Cast%20Al%20Alloy%20Designations.pdf>. 2000 (cit. on p. 5).
- [14] J. Campbell. *Castings-The New Metallurgy of Cast Metal*. Butterworth-Heinemann, 2003 (cit. on p. 6).
- [15] T. Lipiński. ‘Modification of the Hypo-Eutectic Al-Si Alloys with an Exothermic Modifier’. In: *Archives of Metallurgy and Materials* (2013) (cit. on p. 6).
- [16] P. Atkins et. al. *Physical Chemistry*. Oxford, 2018 (cit. on p. 7).
- [17] *User manual: GD-Profiler 2*. 2010 (cit. on pp. 9–11).
- [18] T. Nelis and R. Payling. *Glow Discharge Optical Emission Spectroscopy: A Practical Guide*. The Royal Society of Chemistry, 2003 (cit. on pp. 9, 10).
- [19] *AstruM Glow Discharge Mass Spectrometer, System Manual, Issue 1.1.1* (cit. on pp. 12, 13).

- 
- [20] *AstruM Glow Discharge Mass Spectrometer, Getting Started Guide, Issue 1.3* (cit. on pp. 12, 13).
- [21] *Principle of ICP Optical Emission Spectrometry (ICP-OES)*. <https://www.hitachi-hightech.com/global/products/science/tech/ana/icp/descriptions/icp-oes.html> (cit. on p. 14).

---

## A H/P-phrases for BN-coating

<b>BN Lubriccoat-Blue ZV</b>	
H320	Causes eye irritation.
H332	Harmful if inhaled.
H335	May cause respiratory irritation.
P261	Avoid breathing dust/fume/gas/mist/vapours/spray.
P264	Wash hands thoroughly after handling.
P271	Use only outdoors or in well-ventilated area.
P304+P340	IF INHALED: Remove victim to fresh air and keep at rest in a position comfortable for breathing.
P312	Call a POISON CENTER or doctor/physician if you feel unwell.
P305+P351+P338	IF IN EYES: Rinse cautiously with water for several minutes. Remove contact lenses, if present and easy to do. Continue Rinsing.
P337+P313	If eye irritation persist: Get medical advice/attention.
P403+P233	Store in a well-ventilated place. Keep container tightly closed.
P405	Store locked up.
P501	Dispose of contents/container in accordance with local/regional/national/international regulations.

Table 5: H/P-phrases for softcoat.

<b>BN Hardcoat</b>	
H319	Causes serious eye irritation.
H332	Harmful if inhaled.
H335	May cause respiratory irritation.
P261	Avoid breathing dust/fume/gas/mist/vapours/spray.
P264	Wash hands thoroughly after handling.
P271	Use only outdoors or in well-ventilated area.
P280	Wear eye protection/face protection.
P304+P340	IF INHALED: Remove victim to fresh air and keep at rest in a position comfortable for breathing.
P305+P351+P338	IF IN EYES: Rinse cautiously with water for several minutes. Remove contact lenses, if present and easy to do. Continue Rinsing.
P312	Call a POISON CENTER or doctor/physician if you feel unwell.
P337+P313	If eye irritation persists: Get medical advice/attention.
P403+P233	Store in a well-ventilated place. Keep container tightly closed.
P405	Store locked up.
P501	Dispose of contents/container in accordance with local/regional/national/international regulations.

Table 6: H/P-phrases for hardcoat.

